CORRELATION OF OPERATING CAPACITY OF STRONG ACID CATION EXCHANGE RESIN

By

ANUPAMA BALACHANDRAN

Bachelor of Science

Sri Venkateswara College of Engineering
University of Madras
Chennai, India

2001

Submitted to the Faculty of the
Graduate College of the
Oklahoma State University
in partial fulfillment of
the requirements for
the Degree of
MASTER OF SCIENCE
December 2005

CORRELATION OF OPERATING CAPACITY OF STRONG ACID CATION EXCHANGE RESIN

Thesis Approved:

Gary L. Foutch

Thesis Adviser
R. Russell Rhinehart

Khaled A.M. Gasem

A. Gordon Emslie

Dean of the Graduate College

AKNOWLEDGEMENTS

I am greatly thankful to a number of people who have provided me the guidance and support that I needed to complete my masters study. I would like to sincerely thank my advisor Dr. Gary L. Foutch for having given me the opportunity to work with him. His able guidance and support throughout the course of the project has been crucial in completing this thesis. He has been very patient with me. I would like to thank Dr. R. Russell Rhinehart for serving on my committee; his valuable input toward my thesis is gratefully appreciated. I am thankful to Dr. Khaled A. M. Gasem for serving on my committee and providing constant support and encouragement throughout my stay here at OSU.

I would especially like to thank my family for their love and encouragement; they have always been there for me. I would like to thank Asma and Sarosh for their concern, support and help all along the way. Thanks to Samuel and Srini for all the helpful discussions in relation to my work. Thanks to Priya, Aparna, Rahul and others for making my experience at OSU so enjoyable. Last but not least, I would like to thank Genny, Eileen, Sam, and Carolyn for their assistance.

TABLE OF CONTENTS

LIST OF TABLES

Table Page

LIST OF FIGURES

Figure Page

NOMENCLATURE

e	Number of equivalents	
c	Concentration of solution	eq/l
v	Volume of solution consumed in cycle	l
R	Radius of a resin particle	L
C	Concentration of ion	eq/l
r_c	Radius of the unreacted core	L
N	Total number of ions	
t	Contact time between the resin and the brine solution	T
S_{ex}	Surface area of the exterior of a resin particle	L^2
K	Mass transfer coefficient	L/T
V	Volume of a resin particle	L^3
F	Flow rate	ml/min
X	Fraction of unreacted sites on the resin particle	
D	Axial dispersion coefficient	L^2/T
z	Length of the column	L
V_z	Interstitial velocity	L/T
D_e	Effective diffusion coefficient	L/T

Greek Symbols

ρ	Molar density of resin particle in the regeneration phase	M/L^3
τ	time taken for complete conversion of one resin particle	T
ε	bed porosity	

Subscripts

Na	Sodium
Ca	Calcium
l	Liquid phase
p	Particle

CHAPTER 1

OVERVIEW OF WATER TREATMENT

1.1 Introduction

Water is one of our world's greatest natural resources. Humans consume thousands of gallons of water everyday for domestic, industrial and commercial applications. However, many applications, especially industrial, require water of high purity which is not readily available. Natural water sources such as ground water contain varying amounts of dissolved salts and other electrolytes which have been leached out of the soil and rocks through and over which the water has percolated. The most common natural water impurities include calcium (Ca^{2+}) and magnesium (Mg^{2+}) ions, dissolved organics, hydrogen sulfide, and iron.

Several problems, including scale formation have been associated with the presence of calcium and magnesium ions in water. Often referred to as hardness, these calcium and magnesium cations (positively charged ions) react with other anions (negatively charged ions) such as bicarbonates, sulfates, chlorides and nitrates to form insoluble salts. Hardness of water is usually defined as the sum of calcium and magnesium ions present in water and is expressed in units of grains per gallon or equivalents per liter. Severe salt deposition problems are found in boilers and other heat exchange equipment. Deposits formed as hard scale act as an insulation preventing efficient heat transfer and cause energy losses due to inefficient heating and equipment

failures due to overheating of metal parts (Applebaum, 1968). A boiler fed with hard water produces poor quality steam containing impurities, which further foul steam-using equipment such as turbines, thereby decreasing their efficiency. Corrosion of metal containers, heaters, boilers and piping may result as a result of hardness in water. Advantages of using softened water (from which cationic impurities have been removed) include reduced energy consumption and lower equipment maintenance and replacement costs. Hence the cost-effective softening of water (removal of Ca^{2+} and Mg^{2+}) is of paramount importance to most industrial and domestic applications.

1.2 Current Approaches to Water Softening

The hardness of water is principally due to the presence of calcium and magnesium ions, so much so that these cations themselves are referred to as "the hardness". Iron, manganese and acidity are present in most raw waters but in such small quantities that they are neglected in hardness considerations.

The factors considered in the choice of a water softening process include the raw water composition, the end use and desired quality of the soft water, the ways and costs of disposing the waste streams, ecological problems associated with the process in general, versatility of the process and its adaptability to different processing scales (Jonathan, 1992). A detailed list of methods to remove ionic, non-ionic and gaseous impurities is presented by Applebaum (1968). The commonly employed methods for cation removal are (a) lime-soda process, (b) precipitation, (c) nanofiltration and (d) ion exchange, each of which is explained in detail below.

1.2.1 Lime-Soda Process: The lime-soda process involves precipitation of Ca^{2+} and Mg^{2+} ions with lime and soda ash. The lime reacts with bicarbonate hardness to precipitate calcium carbonate and magnesium hydroxide. The soda ash reacts with the non-carbonate hardness to form the same insoluble products. These precipitates are allowed to settle out and the water is usually clarified by filtration.

1.2.2 Reverse Osmosis: Reverse Osmosis is a purification process where a pressure is applied to force water through a differentially permeable membrane. This membrane allows water to pass but retains most of the dissolved salts and all the suspended solids. To avoid blocking the pores of the membrane, most suspended salts need to be removed by prior filtration.

1.2.3 Nanofiltration: Nanofiltration is a pressure driven process where monovalent ions are allowed to pass through a membrane but highly charged, multivalent ions and low molecular weight organics are retained (Applebaum, 1968). The major difference between nanofiltration and reverse osmosis is that membranes used in nanofiltration have larger pores. Membrane filtration is considered to be an advanced treatment process as it retains most ions including manganese and iron present in ground water.

1.2.4 Ion Exchange*:* Water for domestic use can be softened using a Strong Acid Cation (SAC) resin to eliminate the calcium and magnesium ions present. The exchange resin replaces sodium ions for calcium, magnesium and other heavy metal ions in water thus softening it. The exhausted resin is replenished using sodium chloride as regenerant A cation exchange resin bead consists of the sulfonate (SO_3^-) group permanently attached to a water porous matrix of polystyrene. The matrix of the bead does not participate in the reaction. To maintain electrical equilibrium within the bead there must be sufficient

positive metal ions to balance the negative sulfonate ions. For electronic neutrality the monovalent Na^{+} ion needs just one sulfonate ion; whereas, two sulfonate groups are needed to neutralize one Ca^{2+} group. It is only when electrical balance is maintained in the bead and the water that the calcium and sodium ions may freely interchange between the water and the interior of the bead. When the resin beads become completely exhausted, they are regenerated by passing a concentrated solution of sodium chloride or an acid through the column.

1.3 Comparison of Methods

A detailed review of hardness in water with reasons and methods to soften it are discussed in detail elsewhere (Fox , 1979) and a brief review of the most widely used techniques has been presented above. Lime softening and sodium ion exchange were compared with respect to cost, sludge disposal, volume of waste water, effectiveness and the control that can be exercised during the process. The lime-soda process generates a lot of sludge which is expensive to handle and dispose. The comparison between lime softening and nanofiltration for groundwater treatment in Florida has been extensively described by Bergman (1995). A cost comparison showed that the plant operation and maintenance costs for lime softening were lower than that for membrane softening, but the relative difference in costs decreased with larger facilities. Lime softening is still currently used due to tradition (Van Bruggen, 2002) but other alternative processes produce better water quality in comparison.

Reverse osmosis is one of the best methods in terms of product water quality but is extremely slow or requires high surface area. This process is extremely uneconomical as the capital and membrane replacement costs are high.

Nanofiltration is useful when there is a need for reduction in hardness, alkalinity and residual carbon dioxide. Though removing hardness was the primary objective of nanofiltration, removing dissolved organics has also become an essential part of this process. Application of nanofiltration in drinking water industry for removal of pollutants from surface and ground waters are discussed by Bruggen et al. (2002). Nanofiltration has the additional advantage of removing color and turbidity from groundwater. Other favorable advantages for nanofiltration are process flexibility, smaller land requirements, and the absence of sludge disposal. New developments have resulted in improving the performance characteristics of the membranes; including lower operating pressure requirements, which increases the efficiency of the system and reduces the overall plant construction, operation and maintenance costs.

Comparison between ion exchange and nanofiltration for softening of industrial water has been reported by Canepa et al. (1996). These processes were compared from the perspective of both the economics and the quality of water produced. A resin-based plant is slightly cheaper than the membrane-based plant. In the membrane process, waste water generally complies with the standards for sewage processing and can be discharged without further treatment. On the other hand, backwash water from the resin-based plant contains chlorides in high concentrations and hence cannot be directly discharged.

The sodium-zeolite process was the first ion exchange process. It was very successful and had a number of advantages over other softening processes. The exchange

reaction was simple and did not need chemical addition. There were no precipitates formed and consequently no concern of sludge disposal. The softening was complete to the extent of achieving ‘zero-hardness’ water. Lastly, the operation and maintenance costs were low. Since then, there have been a lot of advancements in ion exchange technology that led to separate cation and anion exchangers in an attempt to achieve complete demineralization.

The process of ion exchange is widely used for water purification, as it ensures good water quality and regular operation at relatively low costs (Canepa, 1996). Though problems exist with disposal of waste water high in calcium chloride and higher costs as a result of greater volume of water needed to clean the bed, this process is used extensively because of its many advantages. Ion exchange reactions can be easily controlled and automated whereas lime softening needs continuous vigilance by an operator (Bergman, 1995).

This study deals with the ion exchange process and provides a tool for optimizing the softening process and improving the system efficiency. Strong Acid Cation (SAC) resins were chosen as they are the most commonly used exchangers for hardness removal. SAC resins help achieve complete hardness removal as they have high selectivity for calcium and magnesium. This type of exchanger has good physical and oxidation stabilities.

1.4 System Efficiency

The key considerations in improving the efficiency of an ion-exchange system are quality of the product water, the overall cost involved in the process and the cost of brine in particular. Monitoring deionizer efficiency can help reduce chemical and labor costs, extend the useful life of the resin and improve the quality of water.

A good ion exchange monitoring system enables an operator to establish a service history which serves as a tool for troubleshooting and detecting resin fouling and mechanical failures before they can become severe. Effects of loss in capacity in deionizers are cumulative; and, if not corrected in time, even lead to a shut down of the whole plant. With regards to the importance of understanding capacity loss it has been rightly said “Without means for monitoring capacity remaining, it is much like running a car with a broken fuel gauge” (Gray, year unknown).

1.4.1 Monitoring Resin Exhaustion

Exhausted resin begins to leak hardness into the effluent soft water. It is advantageous to predict when the onset of exhaustion allow coming off line and regenerating beforehand (Gray, year unknown). Predicting resin exhaustion can also help avoid running to completion during an inadequately staffed shift. It can also reduce overtime labor and chemical costs by maintaining a reliable operation schedule. Knowledge of resin performance will allow longer service runs and save costs of premature regeneration. Premature regeneration also results in costs associated with usage of expensive acid and wastes useful system capacity.

A common method of detecting end of a run is by direct conductivity measurement at the column outlet. The disadvantage of this method is that the exhaustion is detected after the breakthrough as there is no prior warning. The process downstream begins to get contaminated at the same time that the measurement detects it. Common methods to predict resin exhaustion are based upon monitoring the number of gallons treated per cycle, which does not take into account the feed water composition. Monitoring resin bed working capacity takes into account the variations in feed water composition, incomplete regeneration, loss of resin, fouling, and any mechanical problems associated with the system. Another advantage of graphing working capacity is an indication of system deterioration which shows up as sudden loss in working capacity if any mechanical problem occurs even though the deionizer unit is working just fine. Even a subtle decrease in performance can be observed so that corrective action can be taken before the problem becomes worse.

1.5 Rationale

PEDI (Portable Exchange Deionization) plants collect resin tanks from different customers and regenerate the used resins at a central facility. It is important to know how well the resin would perform when put back to service. The PEDI dealers usually rely on relatively imprecise methods to do their job. They rely on performance projection programs which are available from the resin manufacturer. These product data are available at different regeneration levels, but these numbers correspond to resin that has been regenerated only once and the predictions might not hold true for regenerated resin of all ages. When the resin is first put to service the results can be impressive. However

regenerated cation resins are converted to only about 90% of their original capacity. Moreover, a manufacturer typically reports broad ranges for operating capacities which envelope data to avoid liability for insufficient efficiency. Information from product data sheet cannot be used for any application as they are usually approximate estimations of run lengths at best (Desilva, 2001). Therefore a detailed study of resin performance is necessitated for better representation of resin performance.

Even with the performance monitoring systems in place there is no tool to help optimize the process to increase efficiency. Higher capacities obtained from a process mean larger volumes of water can be treated. However, higher capacities also mean regenerating the bed with a stronger concentration of brine which increases the cost. The question that still remains is whether the savings on the regeneration of chemicals justifies the resulting lower capacities and consequently lower volumes of water treated.

After the bed has been put to service, operators have to decide whether to replace or regenerate the existing bed. Regenerating the bed at higher levels are thrice as expensive as regenerating them at lower levels (Gottlieb, 1991). The issue of whether the resulting cash inflow and reduced chemical consumption justify the capital involved in replacing the resin remains.

These are the areas where predictive technology is especially useful. Mathematical models that predict the brine requirement or capacity utilized for a given concentration of hard water assist the operator in decision making which could be used as a tool to optimize the system efficiency.

1.6 Objectives

The objectives of this study were (a) to evaluate experimentally the capacity of SAC resins and (b) to develop mathematical models to predict and optimize the ion-exchange system performance. To attain these objectives several tasks were established and include:

1) Conduct experiments to evaluate the capacity of SAC resins in both the (a) service and (b) regeneration cycles

2) Develop a model to predict the capacity of the resin as a function of bed volume and quantity of hard water treated

3) Develop a model to predict the brine volume required for regeneration as a function of regeneration level and resin bed volume.

Successful completion of these tasks would provide water treatment operators with the necessary tools to improve the efficiency of deionization systems and optimize their operations.

1.7 Organization of Thesis

This chapter has introduced the need for water softening, basic ion exchange process and explicitly stated the objectives of this work. In Chapter 2 is a review of technical aspects related to ion exchange and water softening. Chapter 3 details with the experimental procedure involved in measuring the capacity of SAC resin, the calibration procedure and the calibration curves are discussed. The breakthrough curves obtained for sodium and calcium ions at different regeneration levels are discussed in detail in Chapter 4. Data reduction and correlation techniques are discussed in Chapter 5 and conclusions

and recommendations are presented in Chapter 6. Uncertainties from experimental measurement are presented in Appendix A. This section discusses errors due to solution preparation, flow measurement, volume measurement and capacity evaluation. All calibration data at different regeneration levels are presented in Appendix B. Appendix C consists of experimental breakthrough curves for sodium and calcium ions at different regeneration levels. Appendix D consists of data involved in obtaining the mathematical correlations.

CHAPTER 2

LITERATURE REVIEW

2.1 Introduction

The ion exchange process for water softening was first used in 1905 (Owens, 1995). As demands for high quality water increased, a number of efficient methods to carry out the traditional softening process were developed. Improvements were made by adapting the properties of the ion exchange resins, developing special processes to reduce operating costs and optimizing the process. Improvements in ion exchange resins were brought about by improving their selectivity, kinetics and physical properties. A review of topics related to water softening and ion exchange is given below.

2.2 Regeneration Efficiency

A review of methods to increase the efficiency of regeneration has been described by Keller. Fine mesh resins that have a smaller bead diameter than standard resins increase efficiency as greater surface area makes the exchange of hardness onto the resin more efficient. Laboratory testing has shown that fine mesh resins have approximately 10 % more capacity than standard resins (Keller, year unknown). Countercurrent regeneration consumes half the rinse volume as compared to co-current regeneration particularly at low regeneration levels (Sanks, 1967). Depending on the water chemistry, the use of weak acid exchanger before the strong acid exchanger is the more effective and

probably the most practical method for increasing the capacity and the exchange efficiency (Mommaerts, year unknown).

McMahon (1992) designed an improved process for regenerating the ion exchange resin in a water softening system aided by an agitator positioned in the exterior of the tank. This process reduces the amount of water and salt required for regeneration of the resin substantially.

Sanks (1967) studied methods to improve the efficiency of cation exchange. Counter-current regeneration, low levels of regeneration, storage and reuse of waste regenerant have increased the efficiency of the cation exchange process. The use of a weak acid exchanger in combination with a strong acid exchanger in a separate reactor or the use of the two types of resins in layers one above the other within the same reactor also increases the exchange efficiency.

2.3 Capacity of SAC Resins

For major areas of application, the manufacturer of standard ion-exchange materials publishes performance data. Data from different sources are presented in this section. Table 2.1 shows the softening capacity and salt regeneration efficiency for different regeneration levels for NaCl as a regenerant. The softening capacity or capacity of a resin is defined as the number of ionic groups per unit volume of ion exchanger that is available for the softening operation. Salt regeneration efficiency is the ratio of regeneration level and breakthrough capacity. Breakthrough capacity is the capacity of the bed at the time when the breakthrough occurs. Breakthrough capacity is a fraction of the total available capacity of the bed after regeneration.

Table 2.2 shows operating capacities for different regeneration systems at different regeneration levels. Capacity data for three different regenerants in both counter-current and co-current operations are presented. The performance data for Duolite C- 20 cation resin (Duolite International, Inc.) is presented in Table 2.3.

Table 2.1: Operating capacity for sulphonic acid cation exchange resin; (Rohm & Haas, 1960)

Regeneration Level	Softening Capacity	Salt regeneration Efficiency
Kgr ($CaCO_3$)/cu. ft.	lb NaCl/cu. ft.	lb NaCl /Kgr
5	15.4	0.32
10	24.0	0.41
15	29.4	0.51
20	32.3	0.62
25	34.2	0.73
30	35.4	0.85

Table 2.2: Operating capacity for sulphonic acid cation exchange resin; (Dow, 2004)

Regeneration	Regeneration Level		Typical Operating Capacity	
System	g/l	lb/cu.ft	eq/l	Kgr/cu.ft
Co-Current				
HCl	80-120	5-7.5	0.8-1.2	17.5-26
H_2SO_4	150-200	9.5-12.5	0.5-0.8	11-17.5
NaOH	80-120	5-7.5	0.4-0.6	8.5-13
Counter-Current				
HCl	40-55	2.5-3.5	0.8-1.2	17.5-26
H_2SO_4	60-80	3.75-5	0.5-0.8	11-17.5
NaOH	30-45	2-2.8	0.4-0.6	8.5-13

Table 2.3: Expected capacities for different regeneration levels for Duolite C-20 cation resin

Regeneration level lb NaCl /Cu.ft. resin	Capacity Kgr/cu. ft.	Regeneration efficiency lb NaCl /Kgr, Average
4	16-18	0.24
5	19-21	0.25
6	21-23	0.27
8	24-26	0.32
10	26-28	0.37
12	28-30	0.41
15	30-32	0.48
20	32-34	0.60
50	36-38	1.35

Tables 2.2 and 2.3 show broad ranges for capacity and regeneration levels. The most important factor which determines the capacity of a resin is the regeneration level employed. Low regeneration levels are the most efficient in terms of cost savings. Increasing the regeneration level increases the capacity of the resin, but beyond a particular level, a point of diminishing returns is reached.

The performance data shown in Table 2.3 are based upon experiments performed in their laboratory with a bed depth of 28 inches. For maximum efficiency of regenerating cation exchange resins, the flow rate of brine should be less than approximately 8 ml/min (Duolite International, Inc.). Higher flowrates tend to result in lower capacities. For intermittent use flow rates of 10 gpm/cu.ft. can be tolerated (Duolite International, Inc.). Capacity is affected by the composition of hard water. In the water softening process, calcium and magnesium ions in the water exchange for sodium in the resin. Sodium is usually present in influent water and the sodium to hardness ratio in waters is less than one. If this ratio is increased, considerable decrease in the capacity can be expected.

CHAPTER 3

EXPERIMENTAL - SETUP AND METHOD

3.1 Introduction

A series of experiments generated performance data for strong acid cation exchange resins in order to meet the objectives mentioned in Chapter 1. Dowex Monosphere 650C-H resins were used in all the experiments. These experiments measured the operating capacity of a strong acid cation resin at different regeneration levels. For each regeneration level, the operating capacities were measured in the service as well as the regeneration cycles.

3.2 Experimental Setup

The experiment measures the capacity of cation exchange resin placed inside a glass column. Figure 3.1 shows the laboratory schematic. The equipment includes a feed solution storage tank, centrifugal pump, a cation exchange glass column, flow meter and an effluent storage tank. The feed enters the column from an overhead tank and after exchange, the effluent passes through a pump, a flow meter and finally to an effluent storage tank. The conductivity is detected at the point where the effluent exits the flowmeter. All measurements were made at room temperature ($25 \pm 2^{o}C$). The individual components of the setup are described in detail in the following section.

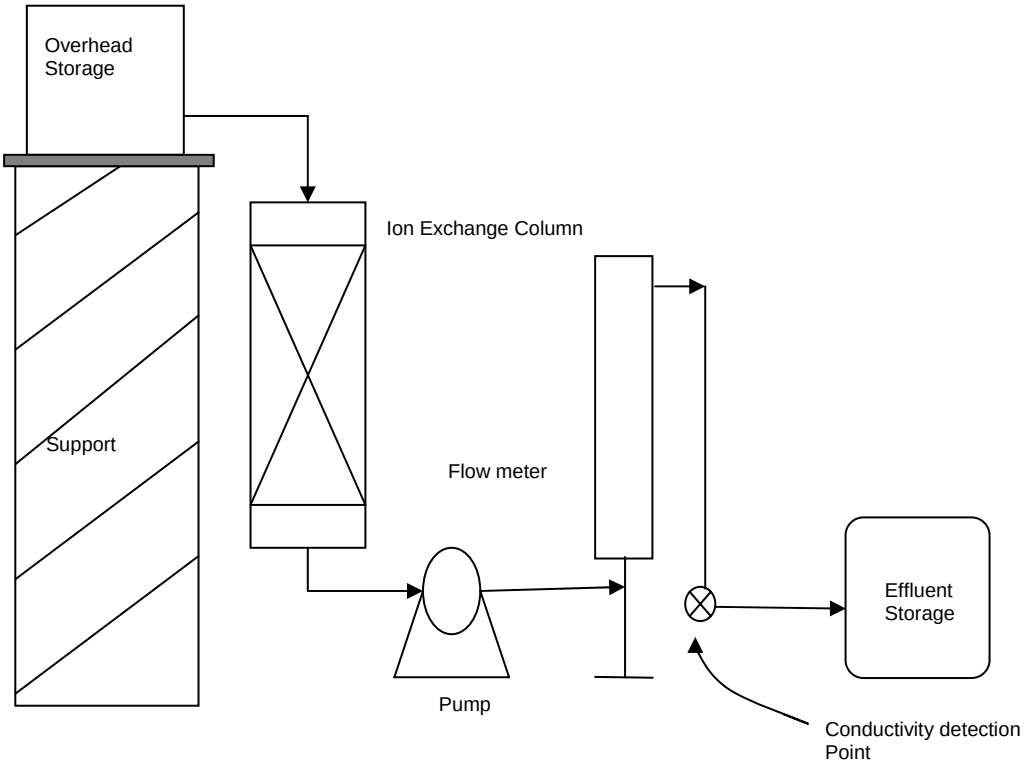

Figure 3.1: Experimental Setup

3.2.1 Feed Solution: The feed solution storage tank consisted of a glass carboy with a spigot. Feed was distributed throughout the system using a centrifugal pump. The pump was primed before operation. This was done by filling the pump and the piping system with water deionized water and ensuring there were no air bubbles present in the distribution system.

To minimize frictional resistance throughout the apparatus, minimal piping and bends were used. A corrosion resistant vinyl hose, used to transport the feed and effluent throughout the system, could endure the pressure of the pump operation. The inner diameter of the tube was 3/8 inch and the wall thickness was 1/8 inch.

3.2.2 Ion Exchange Column: The ion exchange column was designed specifically for the experiment and built by the glass shop, department of chemistry at OSU (Oklahoma State University). The column was made of Pyrex with an inside diameter of 1 inch and height of 20 inches above the fritted glass disk. The porous disk sealed into the bottom of the column, ensuring uniform flow distribution also supported the resin bed. The column was fitted with an opening at the top which served as an inlet to load the wet resin. A valve at the bottom was used to regulate flow of liquid through the column.

3.2.3 Flow Meter: A flow meter (Gilmont Instruments, Inc.) indicated the flow rate of the fluid. A correlated flow table accompanied the flow meter, with the flow rate in ml/min corresponding to the reading on the scale of the meter. The table was correlated for both water and air as fluids and stainless steel and glass as float material. This flow table was used to directly read the flow rate in units of ml/min.

3.2.4 Effluent Storage: The effluent from the system was collected continuously in a tank and its concentration was measured at regular intervals using a conductivity meter (Hach).

3.2.5 Ion-Exchange Resins: Dowex Monosphere 650 (H) Cation Exchange Resin was used in the study. Unfouled resins used were used in all experiments. The product information from the manufacturer is given below (Monosphere) in Table 3.1.

Table 3.1: Properties of the wet resin and bed characteristics

Product Type:	Strong acid Cation
Matrix:	Styrene-Divinyl Benzene gel
Functional group:	Sulphonic acid
Water retention capacity:	46-51 %
Mean Particle size:	650±50 μm
Particle density:	1.22 g/ml
Bed height:	6.00cm
Bed diameter:	2.54 cm

3.2.6 Conductivity Meter: A conductivity meter (Sension 5, Hach) was used to detect the ion concentration in the effluent. The conductivity range of the meter was 0-199.9 mS/cm. The meter operates in a temperature range of -10 to 105 ^{o} C. The meter was calibrated with a standard calibrating solution (1000±10 μS/cm).The conductivity probe was cleaned with deionized water and then rinsed with the standard. A glass container taller than the working part of the cell and few inches greater in diameter was selected. This container was cleaned, dried and filled with a small amount of calibrating standard used to clean the container thoroughly. The container was filled with fresh calibrating standard to a depth of at least 2 inches greater than the height of the working part of the cell. The cell was then immersed in the calibrating standard .The solution was stirred with the cell as the conductivity reading was adjusted in the instrument.

3.2.6.1 Theory of operation: Conductivity is the ability of a material to conduct current. The ions in a solution will move to the oppositely charged electrode when an electric

charge is applied to the solution, thus conducting current. Ion movement is also affected by the solvent properties and the physical properties of the ion. Conductivity is measured when a cell (probe) is placed in an electrolytic solution. A cell consists of two electrodes of a specific size, spaced at a known distance. The conductivity of the liquid is the ratio of current to voltage between electrodes. Its value changes if the electrodes are placed closer or further from each other. In theory, a conductivity measuring cell consists of two 1-cm square electrode surfaces 1 cm apart. The cell constant (K) is determined by the cell length (L) and cross sectional area (A), (K=L/A). The theoretical cell just described has a cell constant of K=1.0/cm. The cell constant is a factor which reflects a particular cell's physical configuration; it must be multiplied by the observed conductance to obtain the actual conductivity reading in µS/cm.

3.3 Experimental Method

A strong acid cation exchange resin was examined over a range of co-current regenerant conditions. Sodium chloride solution was used as the regenerant. The test water was made from deionized water (0.5 µS/cm) to which a calculated amount of calcium chloride was added. There was no other divalent ion present at detectible concentrations (>0.5 µS/cm). The bed was softened in the sodium form and regenerated in the calcium form. Before the experiments were conducted, calibration curves were plotted for all regeneration levels. The calibration plot establishes the relationship between the two units of conductivity (mS/cm) and concentration (equivalents/liter).

3.3.1 Calibration

A calibration was performed for all the regeneration levels individually and the calibration curves plotted. It was performed with two salts, sodium chloride and calcium chloride. Calibration is based on the fact that cations (Na^+ and Ca^{2+}) have different conductivities in solutions of identical strengths. The concentration of sodium chloride varied from 0% to 100%, as that of calcium chloride varied from 100% to 0% on an equivalent basis. When the concentrations vary on an equivalent basis, the concentration of Cl^- does not change and change in conductivity is due to change in cation concentration.

The calculations involved in calibration (regeneration level of 80 g/l) are described below. 1 liter of brine contains 80 g of NaCl. The equivalent weight of NaCl is 58.5g. The strength of this solution is 80/58.5 =1.3675N. The equivalent weight of $CaCl_2.2H_2O$ = 73.5g. The weight of $CaCl_2.2H_2O$ solution that would make up a solution of the same strength is therefore, 1.3675 * 73.5 = 100.51g. The end point of the calibration curve is known namely, 80g/l and 100.51 g/l. The points in between are percentages of concentrations of the pure components. All of the calibration data is presented in the results section. The appropriate amount of salt was weighed and added to a 250 ml beaker.

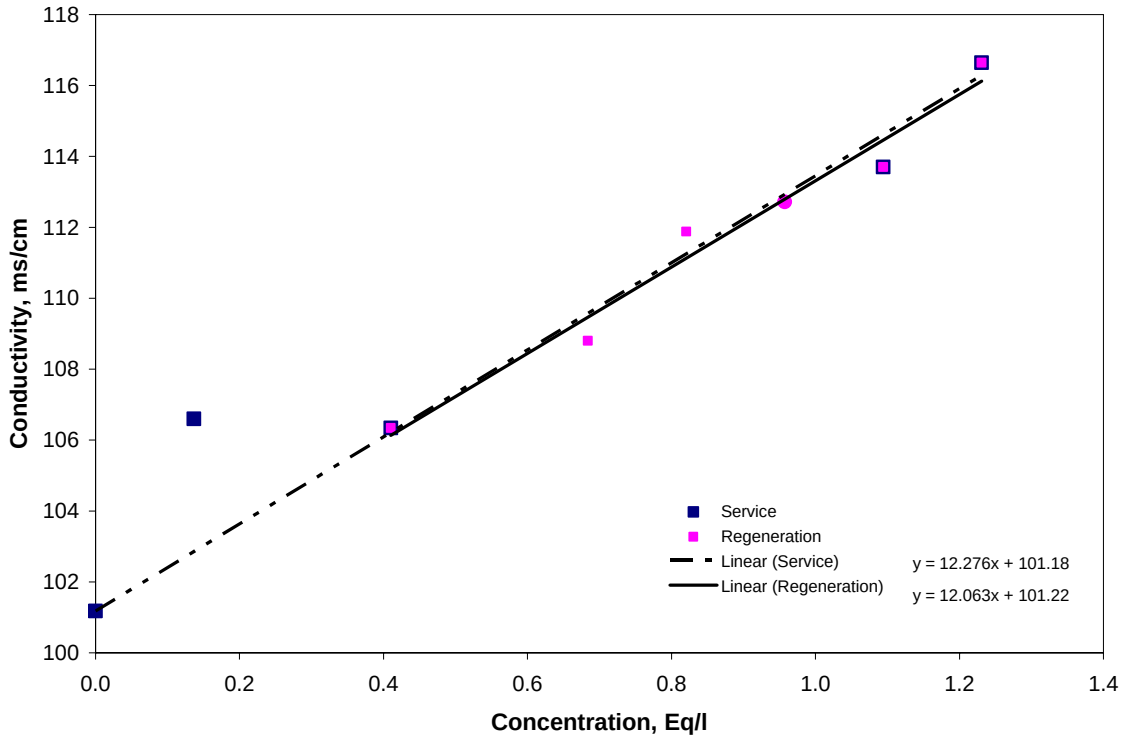

Figure 3.2: **Calibration curve, Regeneration level of 80g/l**

Deionized water was added to make up 100 ml of solution. The solution was stirred magnetically and the conductivity of the solution was recorded. The calibration curve for a regeneration level of 80 g/l of brine is Figure 3.2.

Figure 3.2 shows two separate trendlines fitted for the two cycles of operation. The solid line represents the regeneration cycle and the dotted line represents the service cycle. The corresponding linear equations are also mentioned in the plot. The calibration was repeated thrice and the errors reported.

The calibration plot consists of two trendlines; one for the region of concentration where the service cycle operates and the other for the region where the regeneration cycle operates. Typically, the service cycle operates near the lower concentration region, is

represented by the dashed line on the plot. The regeneration cycle operated near the region of higher concentration, is represented by the solid line on the plot. The scale of concentration increases as a percentage of sodium chloride and correspondingly, decreases as a percentage of calcium chloride. The first and last points in the plot indicate the concentration of the pure salts.

3.3.2 Experimental Method

A modified version of the ASTM procedure, D 1782 (Standard Test Method for the Operating Performance of Particulate Cation-Exchange Materials) was adopted, as described below.

3.3.2.1 Feed Preparation: Deionized water was used in the preparation of feed. The strength of deionized water was 0.50 µS/cm. Four liters of brine (4% regeneration level) was prepared, i.e., 40 g NaCl /liter of solution. The corresponding amount of $CaCl_2 \cdot 2H_2O$ required that would have the same strength as 4% NaCl is 50.25g/liter of solution. For every liter of deionized water, 50.25g of $CaCl_2 \cdot 2H_2O$ was added. Four liters of test water was prepared. For other regeneration levels, solutions of test water and brine were prepared by adding the appropriate amount of salt.

3.3.2.2 Experimental Procedure

The column was half filled with water and sufficient sample was added to give a bed height of 5.0 centimeters above the top of the support. The volume of this sample was 0.057 liters. To avoid drying, a layer of liquid was maintained above the top of the bed at all times.

The entire column was filled with test water to ensure uniform contact of the solution with the resin. The pump was switched on and the test water was allowed to pass through the bed. According to the ASTM procedure, a flow rate of approximately 100 ml/min was maintained throughout the service run. The effluent was collected in a container and the concentration was measured at regular intervals with a conductivity meter. The effluent concentration was recorded in mS/cm at regular time intervals. The run was stopped when the effluent concentration reached that of the feed concentration. The time taken for an entire run as well as the total volume required for one cycle was noted. After the service run, the entire apparatus was cleaned with deionized water followed by rinsing with brine. Rinsing with brine ensures that the entire apparatus carries solution at feed concentration eliminating too many rinse spikes or dips which in turn makes it easier to monitor the experiment. The entire column was filled with brine to ensure uniform contact with the resin. A flow rate of approximately 13 ml/min was maintained throughout the run. A lower flow rate was maintained here to ensure a longer contact time. A lower flowrate also helps to monitor the breakthrough. A detailed explanation of the breakthrough concept is given in Chapter 4. The effluent concentration was measured and recorded as mentioned earlier in the service run. All experiments were carried out at room temperature 25$\pm$2 ^{o}C. Experimental data is discussed in Chapter 4 and all sets of data are presented in Appendix C

The equation that governs the exchange reaction is as follows

$$2R-Na+CaCl_2 \rightleftharpoons R_2-Ca+2NaCl \qquad (3.1)$$

This is a reversible reaction. The resin has more affinity for calcium than sodium, due to which the forward reaction is more favorable than the reverse reaction. For this reason, when regenerating the exhausted resin with brine solution, a high concentration of brine was used to maintain the driving force for the exchange reaction.

Since the resin is never in the H^+ form, there is no acid (HCl) in the effluent. Therefore there is no change in pH and the point where the effluent conductivity reaches the feed conductivity was used to signal the end point.

Equation (3.1) shows that for every two ions of chloride that enters; there is an equivalent number leaving i.e. there is no chloride exchange. Hence, any increase or decrease in the conductivity observed is due to the calcium that is forced out in the regeneration cycle or the sodium in the service cycle.

CHAPTER 4

RESULTS AND DISCUSSION

4.1 Introduction

In this section, the results obtained from experiments conducted to measure operating capacity are presented. Breakthrough curves for Na^+ and Ca^{2+} ions at different regeneration levels are discussed. The complete set of data is presented in Appendix C. The following section describes how the breakthrough curves were generated. Five different regenerant levels for both the service and the regeneration cycles were studied. The entire set of ten trials was repeated to test for reproducibility. The softening cycles were carried out at an average flowrate of 96.2 ml/min the regeneration cycles were carried out at an average flowrate of 13.6 ml/min.

4.2 Breakthrough Curves

The calibration procedure was discussed in the previous section. The calibration plots are presented in Appendix B. The errors in calibration are also presented. The calibration curve yielded two linear approximations corresponding to the service and the regeneration cycles. The resulting equation was programmed as a macro in Excel to convert experimental conductivity readings to concentration (equivalents/liter). A breakthrough curve was obtained by plotting effluent concentration versus volume of

solution (liters) consumed. Explanation for ion exchange in columns and a description of breakthrough curves follows:

When calcium chloride solution is passed through the cation exchange resin in the sodium form, it comes in contact over and over again with layers of resin particles which are still in Na^+ form. This is equivalent to the solution going automatically through a series of batch equilibrations. Thus all Ca^{2+} ions in solution are eventually replaced with Na^+ ions before the solution appears in the effluent.

When the solution is first fed to the column, it will exchange all its Ca^{2+} ions for Na^+ ions in a relatively narrow zone at the top of the bed. The solution, now containing NaCl now passes through the lower part of the column without further change in composition. As the feed is continued, the top layers of the bed are constantly exposed to fresh calcium chloride solution. Eventually, they are completely converted to the Ca^{2+} form, and lose their efficiency and become exhausted. The zone in which the ion exchange occurs is thus displaced downstream. In due course, this zone reaches the bottom of the column. This is the breakthrough of Ca^{2+} ion. This is the point when Ca^{2+} ions first appear in the effluent. The operation is discontinued at or before this breakthrough and the column is regenerated with a solution of NaCl. Continuation beyond breakthrough results in complete displacement of Na^+ by Ca^{2+} in the column. Thereafter, the whole bed is in equilibrium with the feed (calcium chloride solution), which then passes through without change in composition.

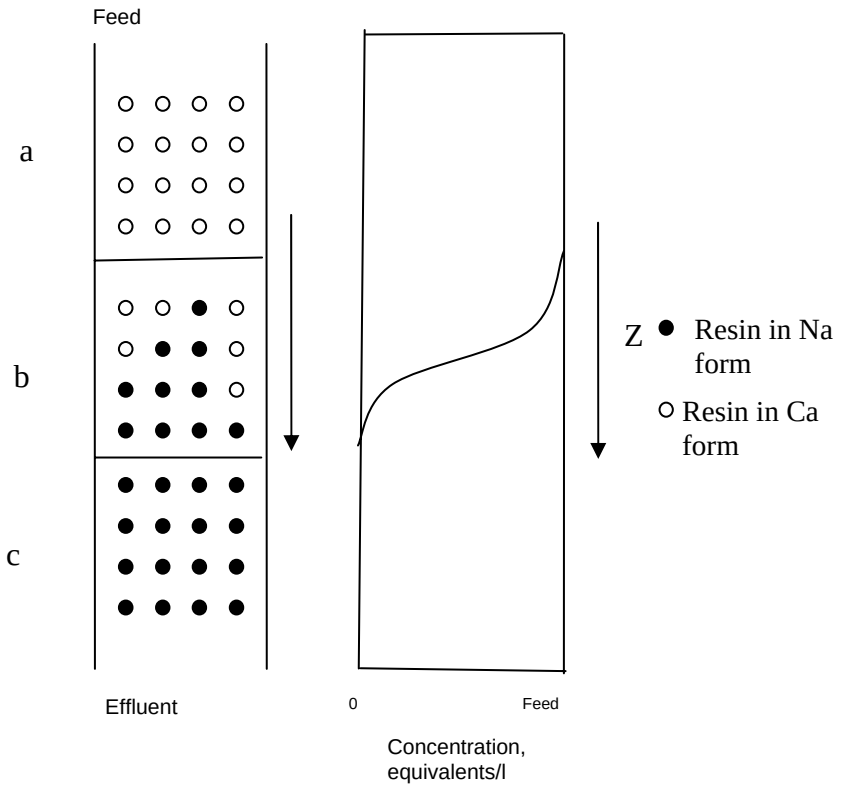

Figure 4.1: Performance of an ion exchange column (schematic). The exhausted zone, the ion-exchange zone and the still unconverted zone are marked a,b,c; the axial concentration profile of the counter ion from feed is shown on the right

Figure 4.1 represents a column initially in Na^+ form where the uppermost layers of the bed are completely exhausted; the subsequent layers are progressively getting exhausted and the bottom-most layers that are still in the Na^+ form. This phenomenon is illustrated by an axial concentration profile showing the breakthrough of Ca^{2+} ions.

At breakthrough, the bottom layers of the bed are not yet completely converted to calcium form. The breakthrough capacity is the number of calcium ions taken up prior to breakthrough. This is obviously less than the over-all ion-exchange capacity of the column. The over-all capacity of the bed is given by the volume capacity of the ion-exchanger and the size of the bed. The breakthrough capacity of a resin depends on the operating conditions, the ionic form of the resin, the composition of the solution with

which the resin has contacted and is a meaningless figure unless these are specified. The ratio of the breakthrough capacity to the total capacity is defined as the *degree of column utilization*.

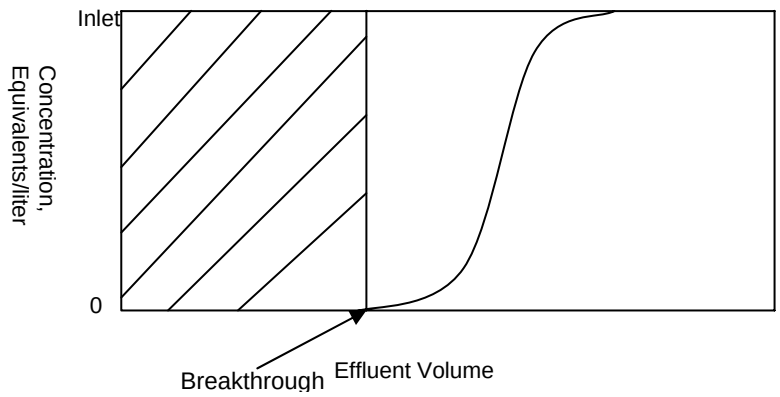

Figure 4.2: Breakthrough curve of counter ion from the feed

The degree of utilization is high when the breakthrough is sharp. The shaded portion of breakthrough curve shown in Figure 4.2 corresponds to the breakthrough capacity and the over-all capacity corresponds to the entire area to the left of the curve. The breakthrough is sharp when the preference of the ion-exchanger is for the ion from the solution. The shape of the curve also depends upon the kinetics effects. Imperfect interface mass transfer may reduce the sharpness of the curve and broaden the ion-exchange zone.

Figures 4.3 and 4.4 are breakthrough curves for the service cycle for a regeneration level of 40 g/l. A spike may be observed sometimes at the beginning of the cycle. This is a rinse spike, and is due to the feed solution already present in the pipe between the outlet of the ion exchange column and the effluent point where the conductivity meter is placed. There is a lapse of time before the sodium ions from the reaction can be measured. The spike is due to the sudden discharge of sodium ions from

the system. With time, the sodium in the effluent is slowly replaced with calcium (from the feed). Equilibrium is said to be attained when there are no more sodium ions left to be discharged from the system and the effluent concentration reaches that of feed. The area under the curve is measured from between the highest point in the spike and the point where it levels off.

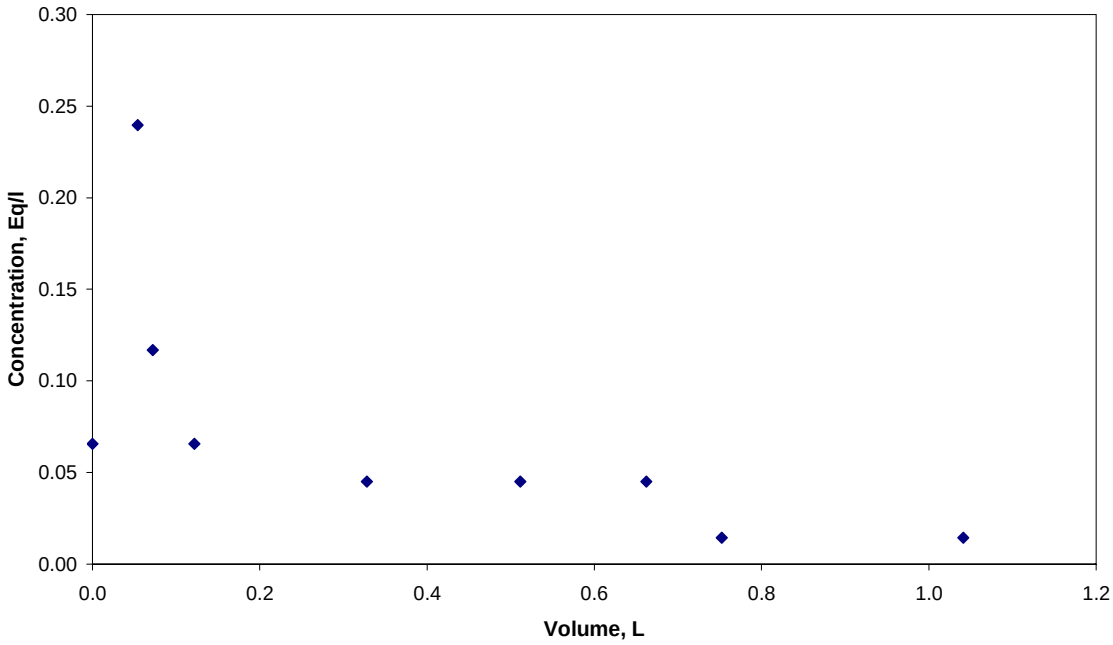

Figure 4.3: Breakthrough curve for Ca^{2+} at regeneration level of 40 g/L (run1)

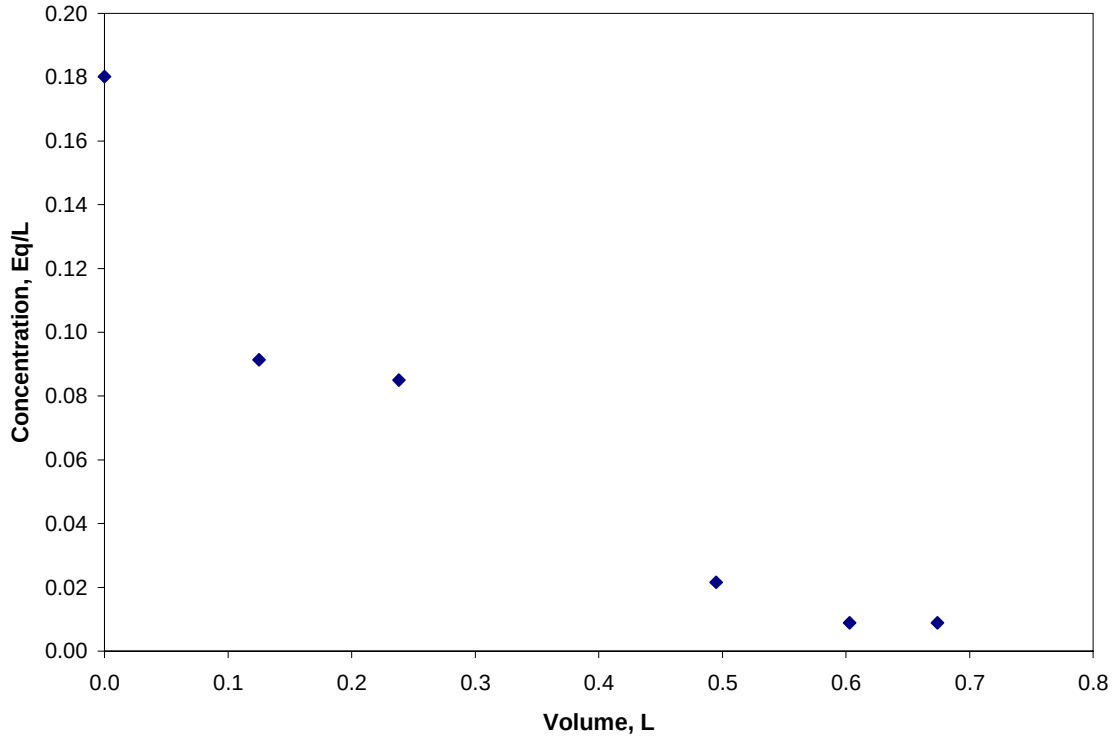

Figure 4.4: Breakthrough curve for Ca^{2+} at regeneration level of 40g/L, run 2

4.3 Computing Total Equivalents in Resin Bed

The total equivalents in resin bed can be computed using the breakthrough curves. Figure 4.3 shows the breakthrough curve for Na^{+} ion. The area under the curve between the points 0.05 and 1.05 on the horizontal axis in Figure 4.3 is the total number of equivalents for the bed volume of 0.057 liters. This area was found numerically, using the *trapz* function in MATLAB. This function approximates the area below the curve by dividing it into a number of trapezoidal sections of width ΔV, as shown in Figure 4.5 and adding the area of all the individual trapezoids.

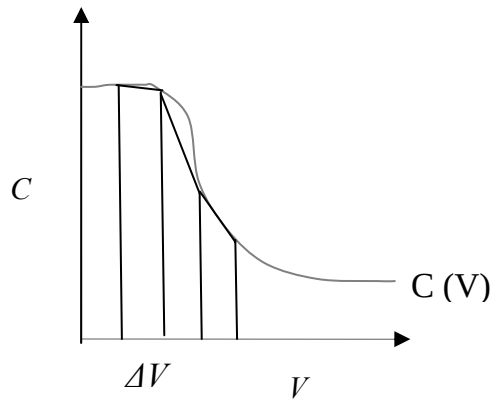

Figure 4.5: Determination of area below curve using trapezoidal rule

The total number of equivalents as evaluated from the trapezoidal rule is

$$e = \left(\frac{c_1 + c_2}{2}\right) \cdot (v_2 - v_1) + \left(\frac{c_2 + c_3}{2}\right) \cdot (v_3 - v_2) + \ldots \quad (4.1)$$

where $c_1, c_2, c_3, \ldots$ are the concentrations in eq/l corresponding to volumes $v_1, v_2, v_3, \ldots$and

$$\Delta v = v_2 - v_v = v_3 - v_2 \quad (4.2)$$

Figures 4.6 and 4.7 are breakthrough curves for calcium ion for the same regeneration level of 40 g/l. In this cycle, a dip can be observed in the curves. The dip is because of the brine already present in the pipe between the outlet of the ion exchange column and the point where the conductivity meter is placed. There is a lapse of time before the calcium ions from the reaction can be measured. When there is a sudden discharge of calcium ions from the effluent, the curve hits a low. With time, the calcium ions from the bed are replaced with the sodium ions from feed and the curve eventually reaches the concentration of feed. The curve levels off here. The area under the curve was calculated between the lowest point in the dip and the point where it levels off.

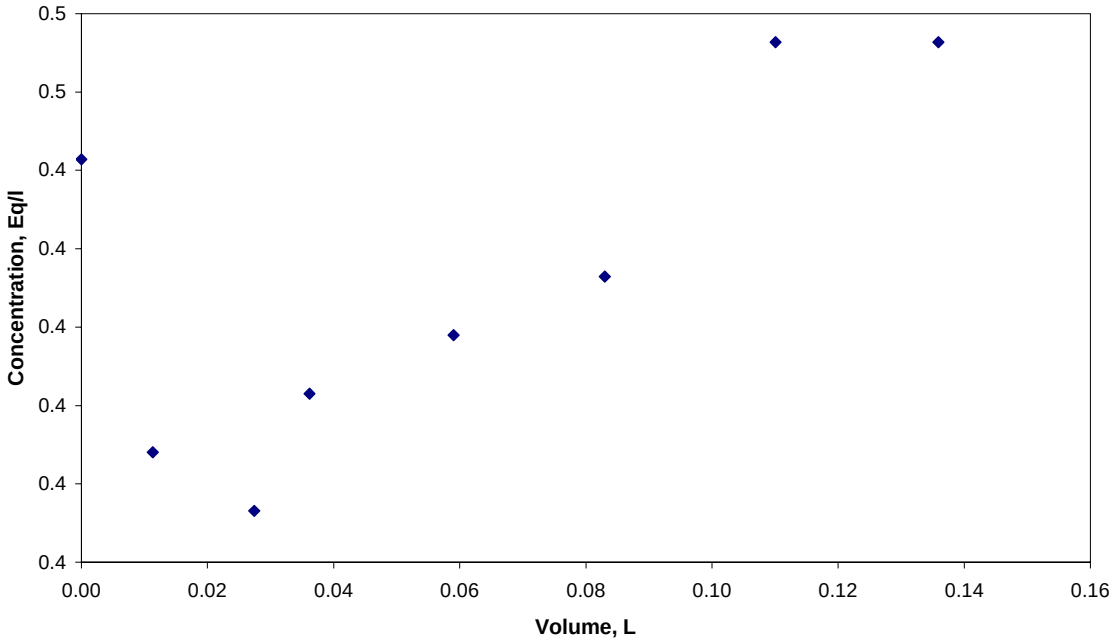

Figure 4.6: Breakthrough curve for Na^+ at regeneration level of 40g/L (run 1)

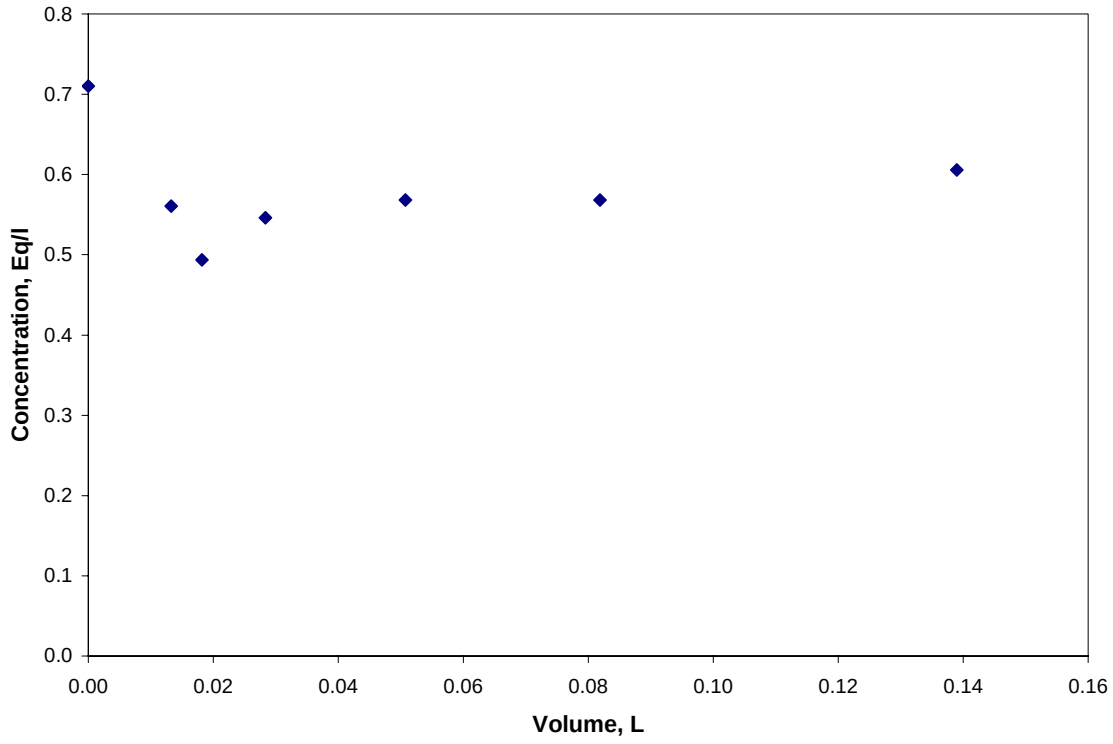

Figure 4.7: Breakthrough curve for Na^+ at regeneration level of 40g/L (run 2)

These curves indicate the volume of solution consumed per cycle. The area below the curve would indicate the capacity of the resin sample (total number of equivalents). This is the area of integration used in Equation (4.1). When this capacity is converted to represent one liter of bed, the operating capacity in units of eq/l is obtained.

The capacity presented in this study is the volume capacity and it refers to the exchange capacity of the bed under operating conditions. The capacity is dependent upon the water content of the resin and the degree of crosslinking.

4.4 Comparison of capacity

The total exchange capacity for the resin as stated in the manufacturer's literature is 2.0 eq/l. The capacity at the same regeneration level for the SAC resin was recorded to be 0.4 – 0.6 eq/l in literature (Product Information-Dowex Monosphere 650 (H)). The capacity of the SAC resin when regenerated with brine at a concentration of 80 g/l was experimentally determined to be 1.5 eq/l, which falls in the range of acceptable values and is less than the theoretical maximum. This difference in capacity does not come as a surprise as the values from product information sheets was expected to be lower than the true value.

CHAPTER 5

CORRELATION OF EXPERIMENTAL DATA

5.1 Introduction

In this section, experimental data from the laboratory are scaled up to represent full-scale performance. The accuracy of the predictions has also been documented (Appendix A). A mathematical model to predict the regenerant volume as a function of regeneration level and bed volume for SAC resin was constructed. Capacity projections as a function of volume of water treated and its concentration have been established. This kind of plot is useful to an operator of a deionizer unit. A plot which evaluates the bed volume as a function of capacity of the bed and the concentration of water was constructed to aid the design engineer to build deionizer units of appropriate size depending on the requirement.

Before proceeding to regress data into a mathematical model, the ion-exchange reaction needs to be studied. To study the kinetics of the reaction, the shrinking core model (SCM) was considered. The SCM was studied as it is said to be the best simple representation for the majority of reacting fluid-solid systems (Levenspiel, 1999). The only exceptions to SCM being slow reaction of a gas with a very porous solid, as in some catalyzed reactions and reactions where solid is converted by the action of heat, without needing contact with gas, as in reactions involved in bread baking (Levenspiel, 1999).

5.2 Shrinking Core Model (SCM)

The shrinking core model assumes that the reaction occurs first at the surface of the particle and as the outer layers of the particle begin to get consumed by reaction, the amount of material being consumed is constantly shrinking. The inert material left behind after reaction is referred to as "ash." An examination of the cross section of partly reacted solid particles reveals that at any time, there is an unreacted core surrounded by a layer of ash, as shown in Figure 5.1.

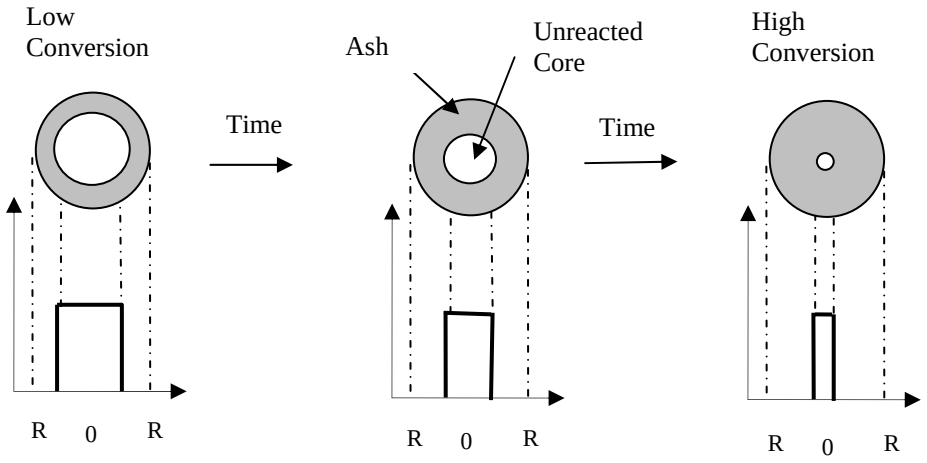

Figure 5.1: Shrinking-core model; reaction proceeds at a narrow front which moves into the solid particle (Levenspiel 1999)

This model however can be applied only to the regeneration phase. The resin in calcium form is visualized as solid particles consisting of Ca^{2+} ions that are available for exchange. The already reacted sites on the resin particle are referred to as "ash". Five steps occurring in succession during the regeneration of resin are visualized;

Step 1. Diffusion of Na^{+} ions into the surface of the resin particle

Step 2. Penetration and diffusion of Na^+ ions through the layer of ash to the surface of the unreacted core

Step 3. Exchange of Ca^+ ions for Na^+ ions by the resin

Step 4. Diffusion of Ca^+ ions through the ash back to the exterior surface of the resin

Step 5. Diffusion of Ca^+ ions through the fluid film into the body of the fluid

The step with the highest resistance is rate controlling. In fully ionized systems, the rate-determining step of ion exchange is the diffusion of the mobile ions.

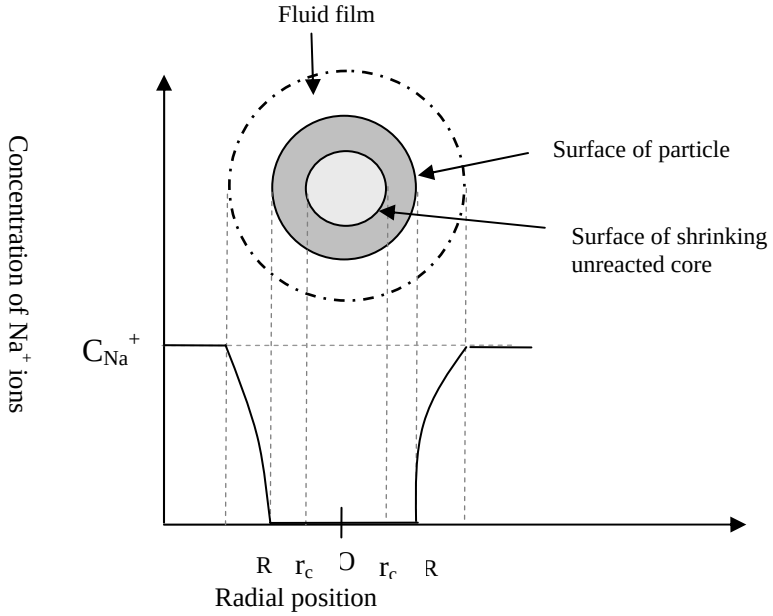

Figure 5.2: Concentration profile of a reacting particle exhibiting film-controlled diffusion (Levenspiel 1999)

The exchange reaction between the resin particle and brine solution is represented by the following equation

$$b\,R_2Ca + NaCl \leftrightarrow b\,CaCl_2 + RNa \qquad (5.1)$$

Let S_{ex} be surface area of one resin particle

N_{Na^+} - Number of Na^+ ions

N_{Ca^+} - Number of Ca^+ ions

C_{Na^+} - Bulk concentration of Na^+ ions

$$dN_{Ca2+} = bdN_{Na^+} \tag{5.2}$$

When the resistance of the liquid film controls, the concentration profile for Na^+ ions is as shown in the Figure 5.2.

The rate of change of calcium ion concentration per particle can be written as

$$\frac{-1}{S_{ex}}\frac{dN_{Ca^{2+}}}{dt} = \frac{-1}{4\pi R^2}\frac{dN_{Ca^{2+}}}{dt} \tag{5.3}$$

$$= bK_g C_{Na^+} \quad \text{(Constant)} \tag{5.4}$$

Where K_g is the mass transfer co-efficient between fluid and particle, R is the radius of the particle and C_{Na^+} is constant.

If $\rho_{Ca^{2+}}$ is the molar density of Ca^{2+} ions and $V_{p,}$ the volume of a particle, the amount of Ca^{2+} ions is $\rho_{Ca^{2+}} V_p$

The decrease in volume or radius of unreacted core $r_{c,}$ accompanying the disappearance of $dN_{Ca^{2+}}$ moles of solid reactant, is given by

$$-dN_{Ca2+} = -bdN_{Na^+} = -\rho_{Ca^{2+}} V_p$$

$$= -\rho_{Ca^{2+}} d(\frac{4}{3}\pi r_c^{\,3})$$

$$= -4\pi\rho_{Ca^{2+}} r_c^{\,3} dr_c \tag{5.5}$$

Replacing Equation (5.5) in (5.4) gives the rate of reaction in terms of the shrinking radius of the unreacted core,

$$\frac{-1}{S_{ex}}\frac{dN_{Ca^{2+}}}{dt} = -\frac{\rho_{Ca^{2+}} r_c^{\,2} dr_c}{R^2 dt} = bK_g C_{Na^+} \tag{5.6}$$

Rearranging and integrating,

$$-\frac{\rho_{Ca^{2+}}}{R^2}\int_R^{r_c} r_c^{\,2} dr_c = bK_g C_{Na^+}\int_0^t dt \tag{5.7}$$

$$t = \frac{\rho_{Ca^{2+}} R}{3bK_g C_{Na^+}}\left[1-\left(\frac{r_c}{R}\right)^3\right] \tag{5.8}$$

The above equation describes how the particle shrinks over time, due to reaction where *t* represents the contact time between the brine and the resin particle. And hence, *t* can be replaced with $\frac{Volume\ (V)\ of\ liquid\ consumed}{Flowrate\,(F_l)}$

$$V = \frac{\rho_{Ca^{2+}} RF_l}{3bK_g C_{Na^+}}\left[1-\left(\frac{r_c}{R}\right)^3\right] \tag{5.9}$$

Equation (5.9) implies that the volume of brine required is inversely related to the concentration of Na^+ ions in the solution (C_{Na^+}).

If $X_{Ca^{2+}}$ is the fraction of Ca^{2+} ions that has reacted

$$1 - X_{Ca^{2+}} = \left(\frac{Volume\ of\ unreacted\ core}{Total\,volume\,of\ particle}\right) = \frac{\frac{4}{3}\pi r_c^{\,3}}{\frac{4}{3}\pi R^3} = \left(\frac{r_c}{R}\right)^3 \tag{5.10}$$

If τ is the time taken for complete conversion,

$$\tau = \frac{\rho_{Ca^{2+}} R}{3bK_g C_{Na^+}} \tag{5.11}$$

$$\frac{t}{\tau} = 1 - \left(\frac{r_c}{R}\right)^3 = X_{Ca^{2+}}$$

Again, by replacing *t*, the above equation can be rewritten as $\frac{V}{\tau F_l} = X_{Ca^{2+}}$ (5.12)

Equation (5.12) explains that volume of brine required is directly related to the concentration of calcium ions present in the resin during regeneration. Equation (5.9) and Equation (5.12) describe the correlation between the three variables; the volume of brine consumed, the concentration of sodium ions in the surrounding liquid and the concentration of calcium ions in the resin. This correlation for a single particle is representative of the entire bed of resin. In other words, a linear relationship between the volume of brine consumed, bed volume and regeneration level exists, where the brine consumption is directly related to the volume of the resin bed in calcium form and inversely related to the concentration of sodium ion in the brine.

5.3 Ion Exchange Model

A model based on mass transfer can be used to describe the ion exchange reaction. Consider a solution of calcium chloride flowing through a column of length *z*. This solution is subjected to intermixing and is described by an axial dispersion coefficient *D*. No short circuiting or by-passing are assumed to be present. The mass transfer from the mobile phase to the surface of the bead is described by a film mass transfer coefficient *K*. The mass transfer within the bead and to the exchange site is a

diffusive process and is described by an effective diffusion coefficient D_e. To describe the concentration change of adsorbate with time in the liquid phase, the following equation can be derived by performing a material balance over a differential volume of the column.

$$\frac{\partial C_l}{\partial t} = D\frac{\partial^2 C_l}{\partial z^2} - v_z\frac{\partial C_l}{\partial z} - K.a.\frac{(1-e)}{e}(C_l - C_p) \qquad (5.13)$$

C_l is the concentration of calcium ions in the liquid phase and e is the porosity of the resin. The left hand side of the equation describes the accumulation of adsorbate in the mobile phase. On the right hand side, the first term describes the change in concentration with time caused by dispersion. The second term describes the convective flow through the column where v is the interstitial velocity of the flow. The last term represents the uptake of calcium ions by the beads. It describes the mass transferred from the mobile phase to the surface of the particle whose concentration is given by C_p.

The following boundary conditions for the inlet and the outlet of the column have been used (Dankwerts, 1951)

$$\frac{\partial C_{inlet}}{\partial l} = \frac{v}{D}\cdot(C_{inlet} - C_o)$$

and

$$\frac{\partial C_{outlet}}{\partial l} = 0$$

The concentration of Ca^{2+} on the particle surface, C_p is assumed to be in equilibrium with its liquid concentration C_l , Diffusion into the particle can be expressed as $\frac{\partial C_P}{\partial t} = D_e\nabla^2 C_P$ (5.7)

One of the effects that has to be taken into consideration, when modeling the performance of the column is the shrinking core assumption. The concentration profile within the particle varies along the length of the reactor. The reactor can be considered to be divided into a number of sections of different particle concentrations; one partial differential equation describing each section. The larger the sections considered, the more accurate the model.

A complete model is obtained when the partial differential equations are solved to obtain a concentration profile as described by Figure 5.3.

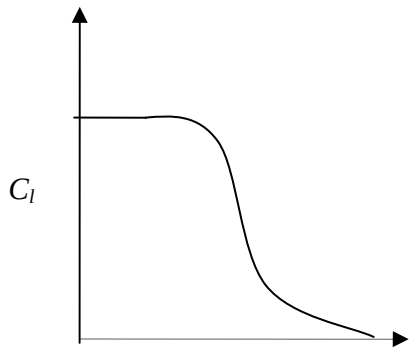

Figure 5.3: Concentration of Ca^{2+} ions along the length of the reactor

These partial differential equations cannot be solved analytically. An advanced numerical method like the finite difference method for partial differential equations has to be used.

5. 4 Computing Regenerant Volume

The regenerant volume consumed when the bed is regenerated at different concentrations of brine is tabulated in Table 5.1. At higher regeneration levels less rinse volume is required for the same volume of bed. This trend is observed for all sets of data. The number of exchange sites in the resin bed is fixed. Higher regeneration levels imply

more ions available for ion exchange in a given volume of solution. The film surrounding the resin particle is thicker encouraging the build up of a concentration gradient thus increasing the diffusion rates.

Table 5.1: Regenerant volume required as a function of regeneration level

S.No	Regeneration level, g/l	Volume Consumed, L	
		Regeneration run 1	Regeneration run 2
1	40	0.140	0.140
2	50	0.130	0.130
3	60	0.140	0.110
4	70	0.10	0.10
5	80	0.08	0.08

The rinse volumes required for different bed volumes ranging from 100-800 l are extended from experimental data and presented in Appendix D.

5.4.1 Correlation of Regenerant Volume

For different bed volumes ranging from 100 l to 800 l, the amount of brine consumed was plotted as a function of regeneration level. Figures 5.4 to 5.10 show the relationship between these variables. In practice, this plot can be used to determine the rinse volume required given the regeneration level and bed volume to be treated. The uncertainties from experimental measurements are also mentioned in the plot. There is an error of 5% associated with this prediction, based on uncertainties calculated from experimental measurements.

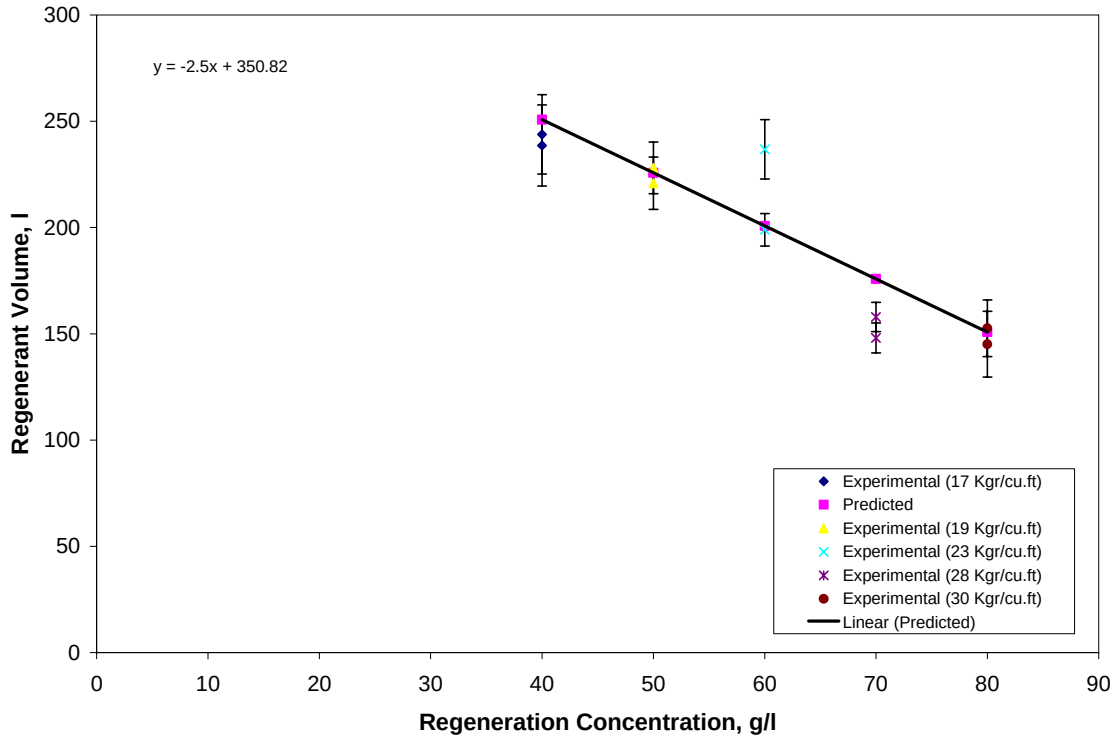

Figure 5.4: Regenerant volume prediction, Bed volume: 100 l

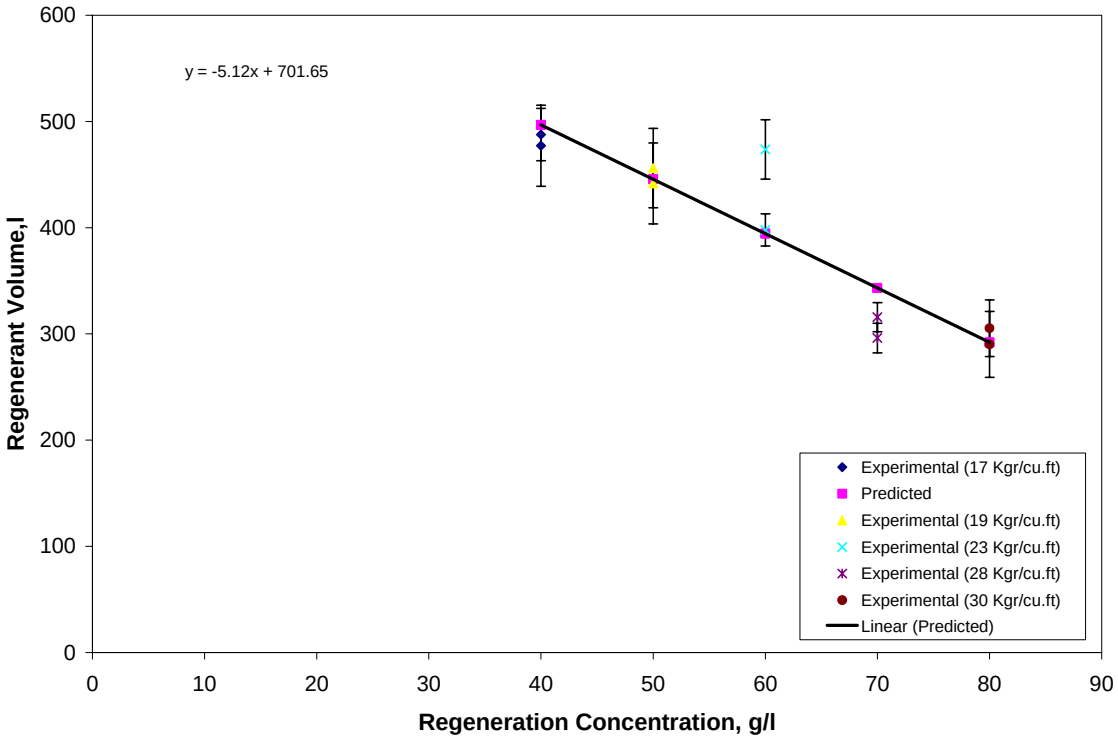

Figure 5.5: Regenerant volume prediction, Bed volume: 200 l

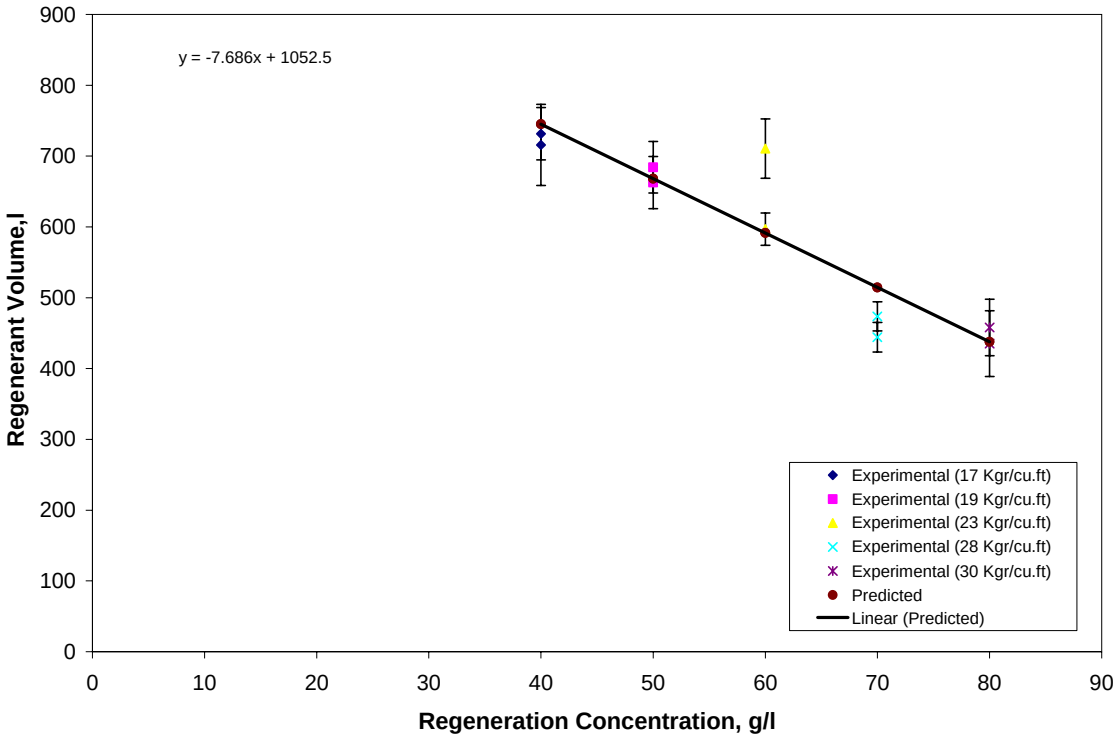

Figure 5.6: Regenerant volume prediction, Bed volume: 300 l

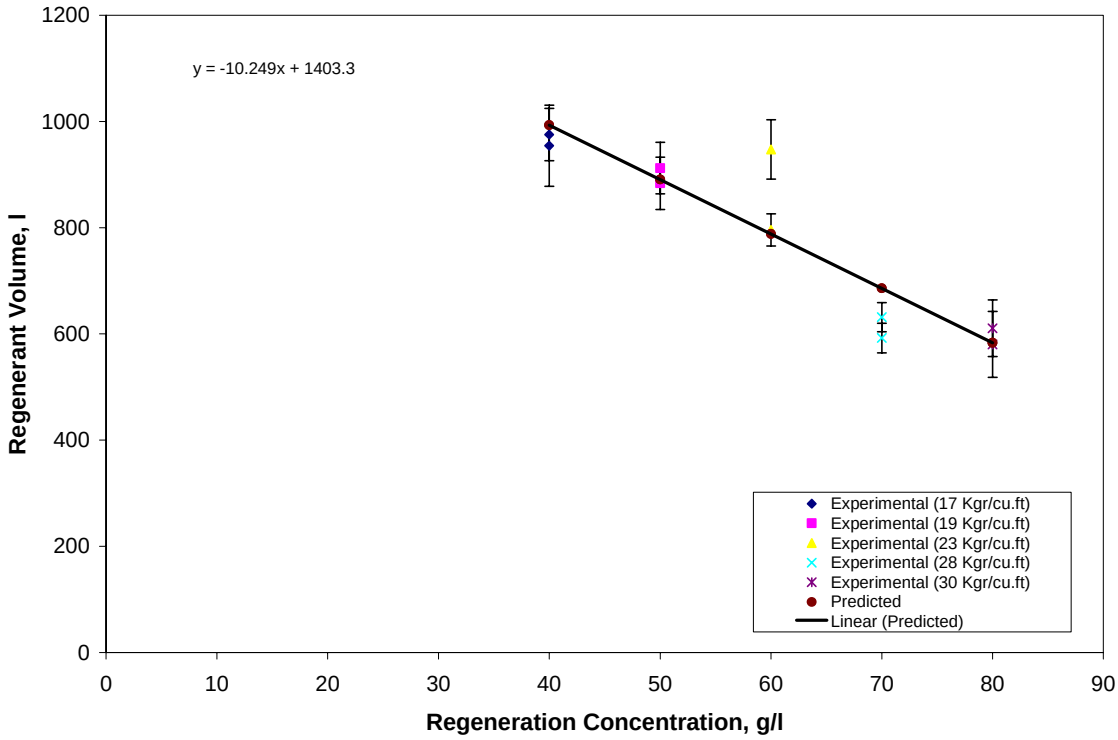

Figure 5.7: Regenerant volume prediction, Bed volume: 400 l

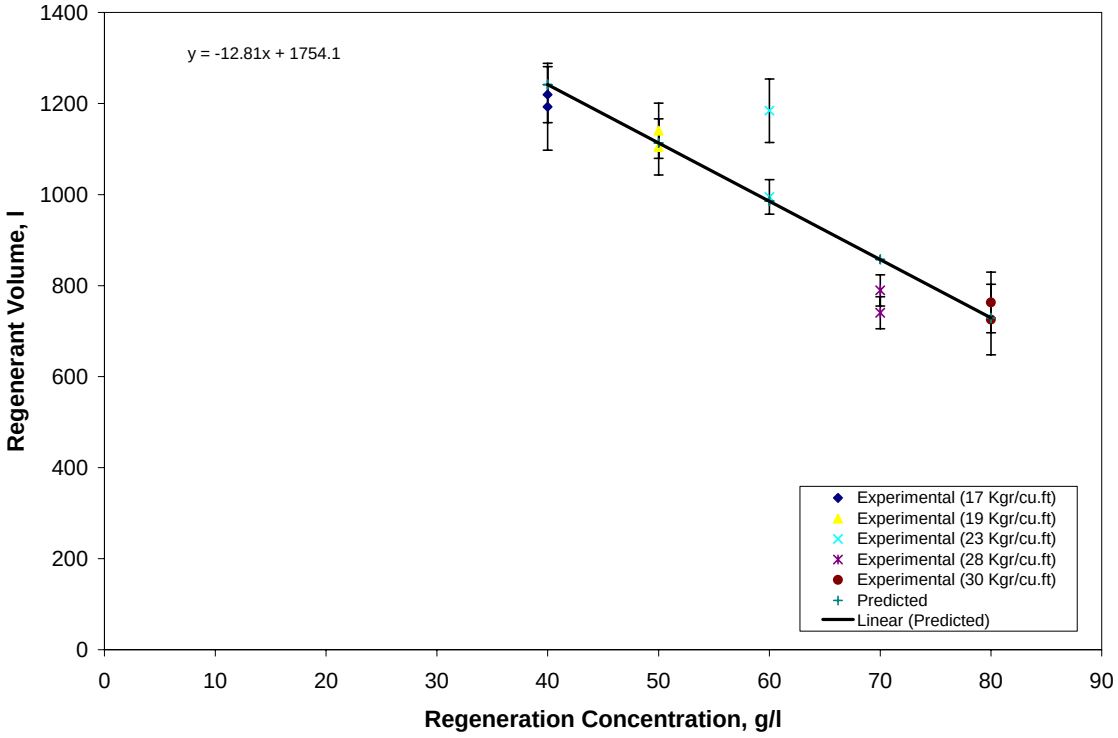

Figure 5.8: Regenerant volume prediction, Bed volume: 500 l

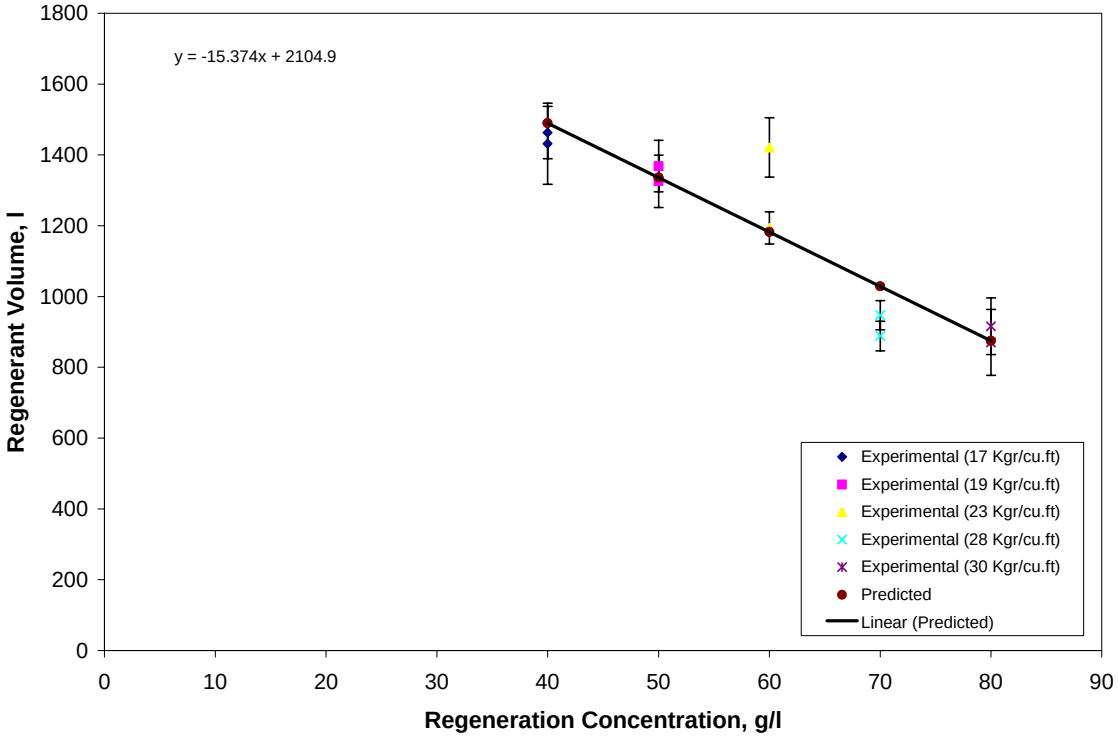

Figure 5.9: Regenerant volume prediction, Bed volume: 600 l

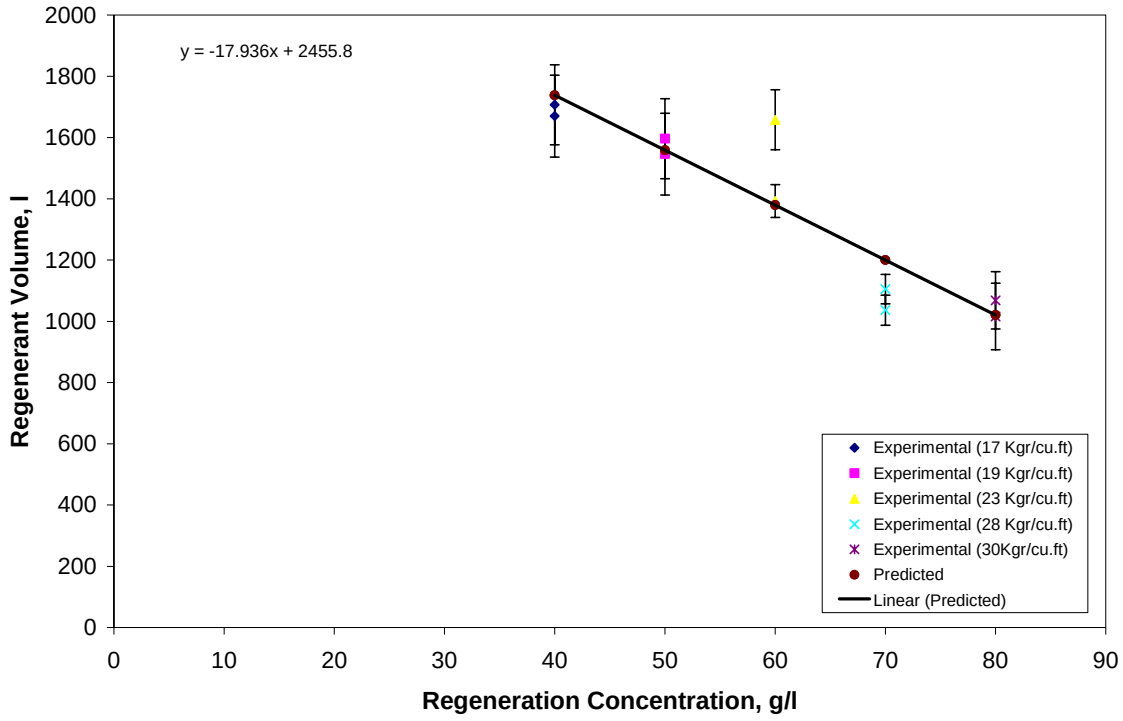

Figure 5.10: Regenerant volume prediction, Bed volume: 700 l

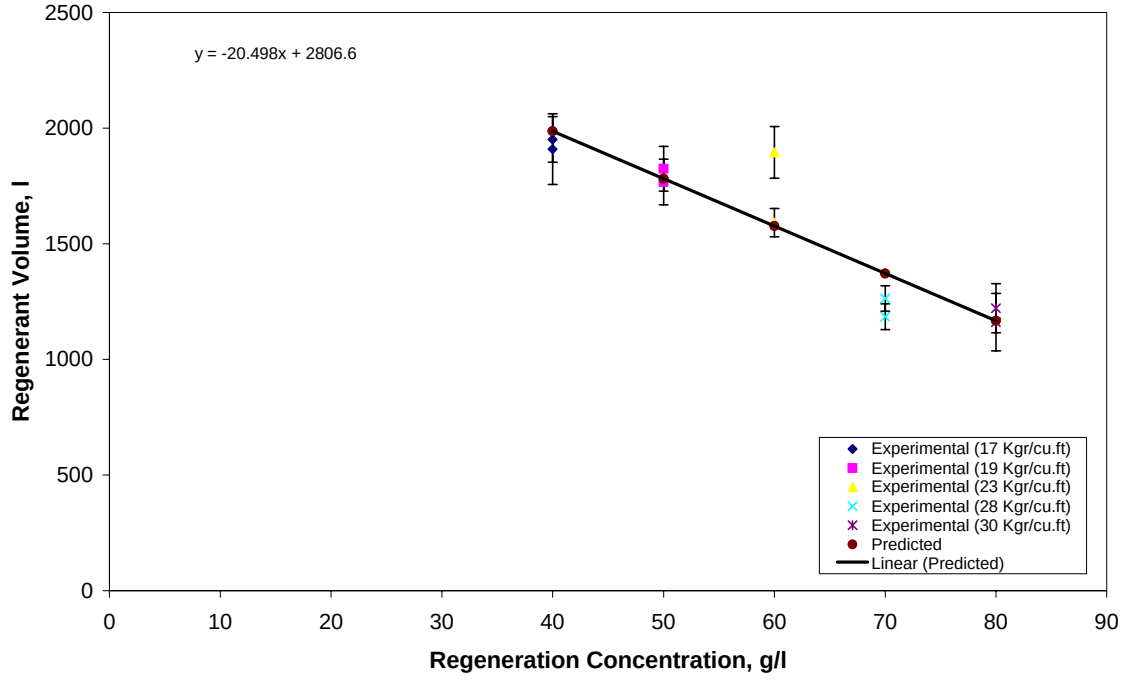

Figure 5.11: Regenerant volume prediction, Bed volume: 800 l

The data from all the figures 5.3 – 5.10 were regressed to a mathematical model. The rinse volume (liters) required to regenerate any volume of resin at any regeneration level can be estimated using the following model

$$y = (m * x + b) * bed\ volume \tag{5.6}$$

x is the concentration of brine in g/l and *bed volume* in Equation (5.6) is expressed in liters. m and b are constants whose optimum values need to be determined by determined using least squares regression technique (LSR). Using the LSR criterion, the objective function that needs to be minimized may be stated as $S = \sum^{n} \left(V_i^{\ m} - V_i^{\ P} \right)^2$

where $V_i^{\ P}$ value of volume as predicted by the model, $V_i^{\ m}$ is the experimental volume processed, n is the total number of readings. The data are tabulated in Appendix D. In this case, n = 80.

The slope and intercept was estimated as

m = -0.03 and b = 3.5

5.4.1.1 How to use Figure 5.4 to Figure 5.11: These figures allow the user to directly read the regenerant volume required for a desired regenerant concentration. These figures are plotted at different bed heights ranging from 100 l to 800 l.

5.5 Correlation of Capacity

The capacity of SAC resin when put to service was measured at different concentrations of test water. The capacity of the resin corresponding to the volume of water treated and the amount of hardness present is tabulated.

Table 5.2: Capacity data obtained from service cycle

Concentration (g/l)	Capacity, Equivalents		Capacity, Kgr/cu.ft.		Volume of water, l	
	Run 1	Run 2	Run 1	Run 2	Run 1	Run 2
50	0.047	0.045	17	16	0.750	0.670
63	0.051	0.053	20	20	0.650	0.660
75	0.062	0.060	24	23	0.510	0.510
88	0.078	0.078	30	30	0.490	0.440
100	0.086	0.084	33	32	0.370	0.330

Capacity of SAC resin was extended to other bed volumes ranging from 100 l to 800 l. Data are tabulated in Appendix D. Capacity of SAC resin was plotted as a function of concentration of hardwater and volume of water 1 liter of bed can treat (Figure 5.12). Capacity was plotted as a function of volume of hard water for different hardness levels. The errors associated with the plot are also mentioned. There is an uncertainty of 7% in reading this plot based on experimental measurements.

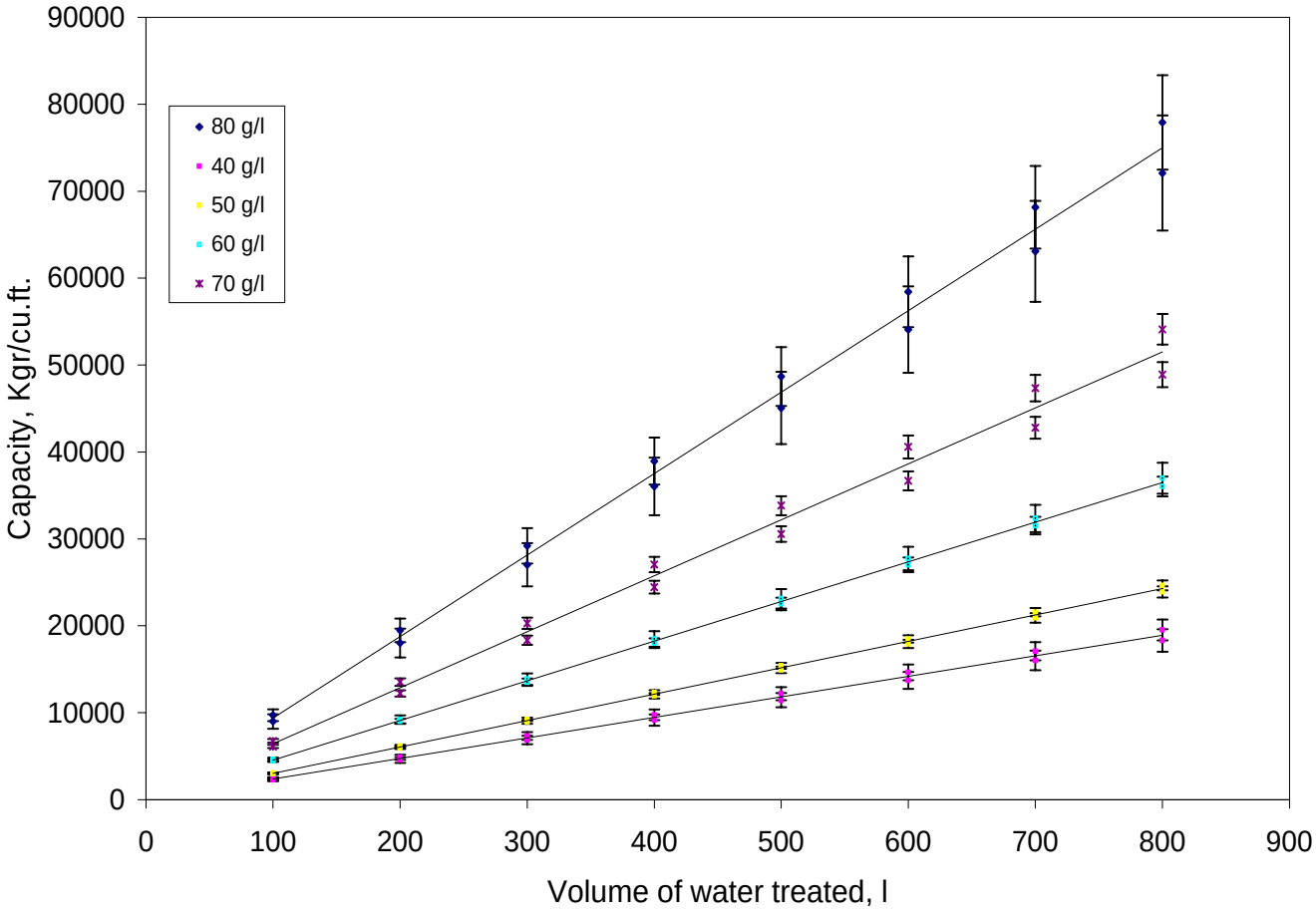

Figure 5.12: Capacity projection as a function of volume of water treated and concentration of 1 liter of bed

(Refer section 5.5.1 for reading plot)

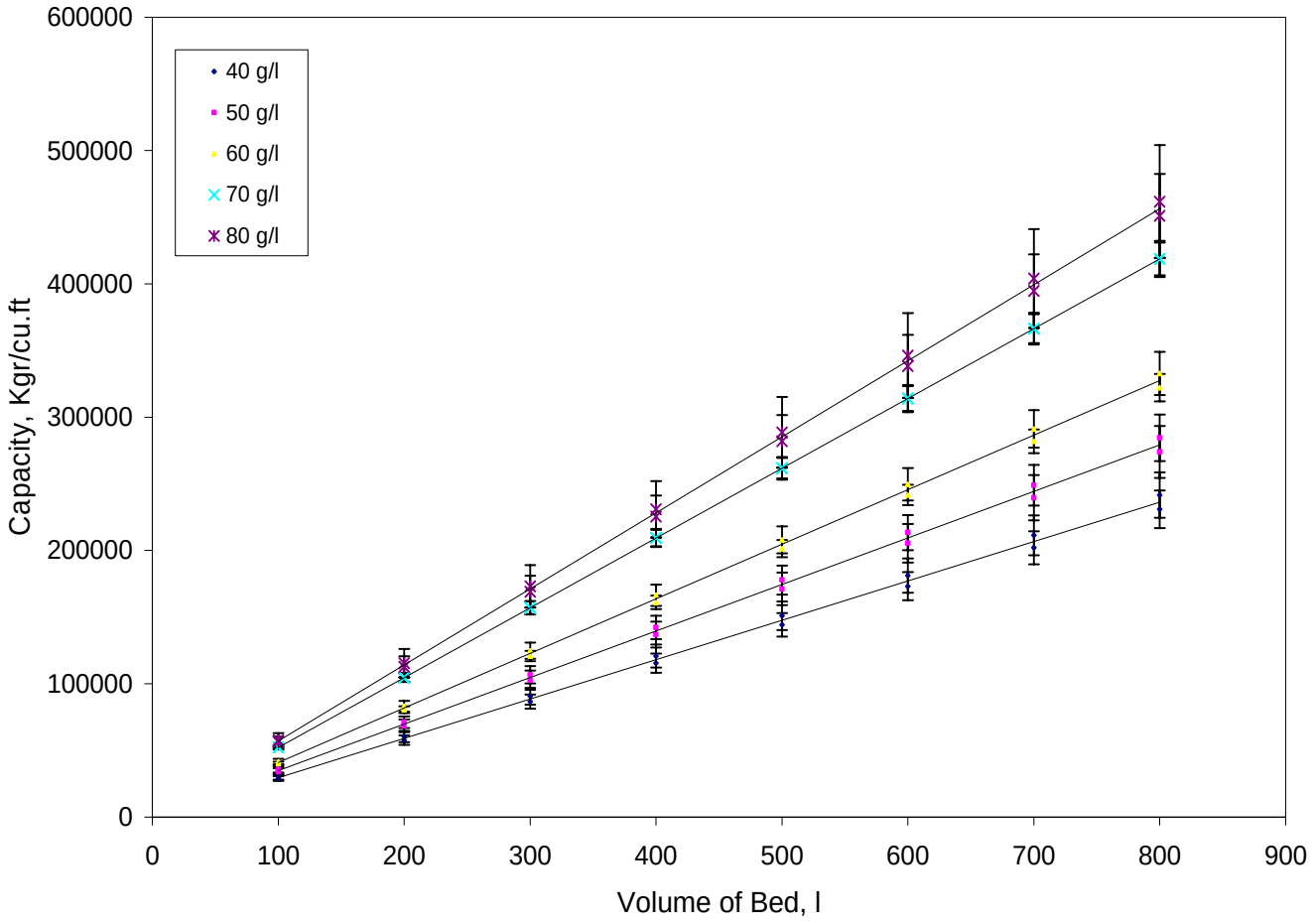

Figure 5.13: Capacity projection as a function of bed volume and concentration of 1 liter of water

(Refer section 5.5.1 for reading plot)

Figure 5.13 shows capacity plotted as a function of volume of bed and hardness of water. The basis for this plot is 1 liter of hard water. The errors associated with this plot are 7% based on uncertainties evaluated from experimental measurements.

5.5.1 How to use Figures 5.12 and 5.13: Figure 5.12 is useful to an operator who wants to know the capacity given the volume of water to be treated and the hardness of water. Figure 5.13 is especially useful to the design engineer who can design the deionizer unit depending on the capacity expected.

CHAPTER 6

CONCLUSIONS AND RECOMMENDATIONS

6.1 Introduction

Based on the results obtained from the experimental determination of capacity of strong acid cation resin, the following conclusions and recommendations can be drawn.

6.2 Conclusions

1. Capacity data obtained for SAC resin, measured in both the service and the regeneration phases were comparable to capacity data available in literature.
2. The capacity projection plots can be used to predict capacity of SAC resin with an average uncertainty of 5%. This model can be used to optimize system performance by assisting in the decision to rebed or institute a regeneration process.
3. The regenerant volumes can be predicted with an average uncertainty of 7%. This model aids in optimizing the regeneration process by reducing regeneration levels without sacrificing quality and minimizing chemical costs.

6.3 Recommendations

1. To account for iron fouling in cation beds, capacities of different samples of resins with different degrees of fouling should be measured. A ‘fouling factor’ should be introduced in the models.
2. Experiments should be conducted with the conductivity detection point at the immediate exit of the column to obtain more precise data. This would eliminate unnecessary spikes and dips in the breakthrough curves which tend to confuse the reader.

REFERENCES

1. *ASTM Book of Standard Test Methods for Operating Performance of Particulate Cation Exchange Materials, D 1782-95,* 2005.

2. Weast, R.C., *Handbook of Chemistry and Physics*, ed.1966: The Chemical Rubber Company.

3. Bergman A., "Membrane softening versus lime softening in Florida: A cost comparison update". Desalination, 1995. **102**: p. 11-24. Article titles are in quotes, book titles are italics.

4. Applebaum, S.B., *Demineralization by Ion Exchange*. 1968, New York: Academic Press Inc.

5. Bruggen, B.V., Vandecasteele, C. "Removal of Pollutants from Surface Water and Groundwater by Nanofiltration: Overview of Possible Applications in the Drinking Water Industry". Environmental Pollution, 2002. **122**: p. 435-445.

6. Bukay, M., "How to Monitor Ion Exchange Efficiency". Ultrapure Water, November/December 1984: p. 35-41.

7. Calmon C., "Recent Developments in Water Treatment by Ion Exchange". Reactive Polymers, 1985. **4**: p. 131-146.

8. Charles, S.A., "Characteristics of Strong -Acid Cation Exchangers 1. Optimization of Regeneration". Desalination, 1984. **51**: p. 313-324.

9. Dardel, D.F., *Ion Exchange - Principles and Applications*. 1989, Reprinted from Encyclopedia of Technical Chemistry, VCH: Weinheim, West Germany.

10. Carlsson, F, Axelsson A., Zacchi G., "Mathematical modelling and parametric studies of affinity chromatography". Computers chem. Engr., 1994. **18**: p. 657-661.

11. Figueroa, R., *Characterization and Comparison of Experimental Methods in the Determination of Capacity and Densities in a Thermally Regenerable Ion-Exchane Resin*, in *Department of Chemical Engineering*. 1988, Ohio State University.

12. Fox, G.T.J., “Hardness of Water and the Reasons and Methods of Softening it”. Water Services, September, 1979. **83**(1003): p. 727-730.

13. Gallant, S.R., “Modeling ion-exchange adsorption of protiens in a spherical particle”. Journal of Chromatography, 2003. **1028**: p. 189-195.

14. Gasem, K.A.M., *Research Methods*, Oklahoma State University, 2002.

15. Gottlieb, M., DeSilva, F. “The relationship between resin operating capacity and static analysis, in Industrial Water Treatment”. 1991.

16. Grantham, J.G., *Ion Exchange in Water Treatment-A Practical Guide for Plant Engineers and Chemists*. 1988: Rohm and Hass Company.

17. Gray, D.M., “Deionization Capacity Monitoring”, Thornton Inc.: Waltham, MA, year unknown.

18. Hoffmann, H., Martonola, F., “Selective Resins and Special Processes for Softening Water and Solutions; A Review”. Reactive Polymers, 1987. **7**: p. 263-272.

19. Harry P. Gregor, J.I.B., Fradelle Gutoff, Robert D.Broadley, David E.Baldwin and C.G. Overberger, “Studies on Ion Exchange Resins. Capacity of Sulfonic Acid Cation-Exchange Resins”. 1950.

20. Helfferich, F., *Ion Exchange*. 1962, New York: McGraw-Hill. Republished by Dover.

21. Desilva, J.F., “Considerations in Portable Exchange Deionization, in Water Technology”. December, 2001. p.1-5.

22. Jonathan, K., “Water Softening Process”. 1992.

23. Kaczmarski, K., Antos, D., Sajonz H., Sajonz, P., Guiochon, G., “Comparative modeling of breakthrough curves of bovine serum albumin in anion-exchange chromatography”. Journal of Chromatography A, 2001. **925**(1-2): p. 1-17.

24. Ho, Y.S., McKay, G., “The sorption of lead (2) ions on peat”. Water Research, 1998. **33**: p. 578-584.

25. Keller, M., “Basic Ion Exchange for Residential Water Treatment”, Sybron Chemical Inc, year unknown.

26. Kunin, R., *Elements of Ion Exchange*. 1960, New York: Reinhold.

27. Kunin, R., *amber-hi-lites*. 1996, Littleton, Colorado: Tall Oaks Publishing.

28. Levenspiel, O., *Chemical Reaction Engineering*. 1999, New York: John Wiley and Sons.

29. McMahon, J.M., “Water Softening Process”. 1992.

30. Mommaerts, G.J., *Softening with WAC Resin*, Ion Exchange Services Inc.: Ontario, Canada. p. 388-393, year unknown.

31. Dowex, *Product Information-Dowex Monosphere 650 (H).*

32. Darwish, N.A., Gasem, K.A.M., Robinson Jr., R.L, *Analysis of errors in adsorption measurements using a volumetric technique*, in *Adsorption studies for optimum production of coalbed methane*. 1992, Oklahoma State Uinvesity: Stillwater.

33. Owens, D.L., *Practical Principles of Ion Exchange*. 1995, Littleton, Colorado: Tall Oaks Publishing.

34. Dankwerts, P.V., “Absorption by simulataneous diffusion and chemical reaction into particles of various shapes and into falling drops”. Transactions of the faraday society, 1951. **47**: p. 1014-1023.

35. Canepa, P.C.G., Szpyrkowicz L., Zilio-Grandi F., “Comparison between ion exchange and nanofiltration for softening of industrial water”. Filtration and Separation, 1996: p. 131-5.

36. Taylor, R., “Simple examples of correlations in error propagation”. American Association of Physics Teachers, 1984. **53**(7): p. 663-666.

37. Riggs, J.B., *An Introduction to Numerical Methods for Chemical Engineers*, Lubbock, Texas: Texas Tech University Press, 1994.

38. Rivero, M., Primo O., Ortiz, M.I., “Modelling of Cr(VI) removal from polluted groundwaters by ion exchange”. Journal of Chemical Technology and Biotechnology, 2004. **79**(8): p. 822-829.

39. Sanks, R.L., “Improving the Efficiency of Cation Exchange”. Proceedings of the American Power Conference, 1967: p. 808-814.

40. Shah, H.A., Bafna, S.L, “Studies in Ion Exchange. Part 1. Studies of Three Synthetic Cation Exchange Resin”. Journal of Indian Chemical Society, 1952. **29**(3): p. 187-192.

41. Shah, H.A., Govindan, K.P, “Ion Exchangers. 4. Operating Characteristics of Some Cation Exchange Resins”. Journal of Scientific and Industrial Research, 1955. **14 B**: p. 222-9.

42. Thomas, H.C., “Chromatography: A problem in kinetics”. Annals of the New York Academy of science, 1948. **49**: p. 161-182.

43. Wiesel, A., Schmidt-Traub, H., Lenz, J., Strube, J., “Modelling gradient elution of bioactive multicomponent systems in non-linear ion-exchange chromatography”. Journal of Chromatography A, 2003. **1006**(1-2): p. 101-120.

44. Sag, Y., Aktay, Y., “Application of equilibrium and mass transfer models to dynamic removal of Cr(6) ions by chitin in packed column reactor”. Process Biochemistry, 2001. **36**: p. 1187-1197.

APPENDIX A

PROPAGATION OF ERRORS

A.1 Introduction

All physical measurements are subject to uncertainties. In order to make meaningful conclusions from the measurements, it is important to indicate the associated error. The result of any physical measurement would thus contain (1) the numerical value and (2) the uncertainty associated with the measurement. Most often, the result of an experiment is not measured directly but is calculated from several measured variables. The error in the final result of the experiment is as a result of propagation of all the individual errors from the measured variables.

A.2 Uncertainty in Capacity Evaluation

Uncertainties in the measurements involved in the procedure to estimate capacity were recorded. Data corresponding to a concentration of 50.3 g/l of test water is used as an example to illustrate the calculations.

A.2.1 Concentration – Solution Preparation

The test water used in the service run contained a measured quantity of $CaCl_2.2H_2O$.

The concentration, *c* of calcium chloride solution is $c = \frac{Weight\ of\ salt, G\ (g)}{Volume\ of\ solution, L\ (l)}$

The accuracy of reading weights of the salt on the electronic balance was noted to be ±0.0003 g. If 50.3 g of salt is to be weighed, the error would be 50.3±0.0003 g. The standard error associated with measuring pure water in a 1 liter carboy is ±5 %, i.e., 1± 0.01 l.

The uncertainties in G and L are uncorrelated and the error in c, produced by errors in G and L, are usually added according to the Pythagorean theorem.

Error in c is expressed as $\Delta c = c \cdot \sqrt{\left(\frac{\Delta G}{G}\right)^2 + \left(\frac{\Delta L}{L}\right)^2}$ (A.1)

$G = 50.3g$
$\Delta G = \pm 0.0003g$
$L = 1l$
$\Delta L = 0.01l$

Substituting the above values in equation (A.1), the error in C was calculated as 1.3 %.

A.2.1 Concentration-Calibration

Calibration equations are of the form $Y = mX + b$

Where *Y* represents the conductivity, '*k*' and *X* represents concentration, '*c*'. *m* and *b* are constants; *m* is slope of the calibration curve and *b* is the *Y* intercept. The errors associated with the fit were evaluated using a linear regression technique in MS Excel. This tool calculates the predicted conductivity using the calibration equation and compares it with the experimentally measured quantity. The difference between the experimental and predicted values was reported as residuals in concentration. The residuals from all the measurements were averaged and reported as $\Delta c = 0.03 eq/l$

The concentration c, of a solution in eq/l is calculated using the formula

$$c\,(eq/l) = \frac{Weight\ of\ \ salt\ \ per\ l}{Equivalent\ \ \ weight\ CaCl_2 \cdot 2H_2O}$$

The feed concentration $= \frac{50.3}{73.5}$

$= 0.68 eq/l$

Error in the concentration $= \frac{0.03}{0.68} \cdot 100$

$\approx 4\,\%$

The total error in the concentration is a sum of errors from solution preparation and calibration which is 5.5 %.

A.2.2 Volume of Solution Consumed

The volume of solution consumed at any time t is calculated using the formula

$v = F\,(l/\sec) \times t\,(\sec)$

A constant rate of flow was maintained using a flowmeter and the flowrate was recorded in ml/min. The errors in F and t are uncorrelated and the error in measuring the volume is expressed as $\Delta v = v \cdot \sqrt{\left(\frac{\Delta F}{F}\right)^2 + \left(\frac{\Delta t}{t}\right)^2}$ (A.2)

$\Delta t = 2\sec$

$t = 500\sec$

$\Delta F = 0$

$F = 0.002\, l/\sec$

The error in volume calculation, $\Delta v = \pm 0.003 l$

A.1.3 Number of Equivalents

The error in determining the capacity by evaluating the area under the curve is based on the theory of multi variate error propagation. The quantity under consideration is expressed as an analytical function of the measured variables. Analysis of error propagation facilitates the prediction of uncertainty that is associated with experimentally measured variables. The scatter in the experimental measurements is expressed in terms of their standard deviations, σ. If Y is calculated from a set of input data (x_1, x_2, x_3,..., x_n), the uncertainty in Y is expressed as follows:

$$\sigma_Y{}^2 = \sum_{i=1}^{N} [(\partial Y/\partial x_i)^2 \, \sigma_{x_i}{}^2] \qquad \text{(A.3)}$$

where the summation is over all the input variables x_i. This equation is valid only when the errors in the input variables are uncorrelated. The uncertainty in Y depends upon the rate of change of Y with respect to the measured variables.

The trapezoidal rule was used to calculate the area under the curve with the concentration in eq/l on the vertical axis and the volume in l on the horizontal axis. This procedure has been explained in Chapter 4.

The total number of equivalents as evaluated from the trapezoidal rule is expressed as

$$e = \left(\frac{c_1 + c_2}{2}\right) \cdot (v_2 - v_1) + \left(\frac{c_2 + c_3}{2}\right) \cdot (v_3 - v_2) + \ldots \qquad \text{(A.4)}$$

In general, $$e = \left(\frac{c_i + c_{i-1}}{2}\right) \cdot (v_i - v_{i-1}) + \left(\frac{c_{i+1} + c_i}{2}\right) \cdot (v_{i+1} - v_i) \qquad \text{(A.5)}$$

If $$e = f(v_1, c_1, v_2, c_2, v_3, c_3, \ldots) \qquad \text{(A.6)}$$

Using Equation (A.3), variance in e can be written as

$$\sigma^2{}_e = \left(\frac{\partial e}{\partial v_1}\right)^2 \cdot \sigma^2{}_{v_1} + \left(\frac{\partial e}{\partial c_1}\right) \cdot \sigma^2{}_{c_1} + \left(\frac{\partial e}{\partial v_2}\right)^2 \cdot \sigma^2{}_{v_2} + \left(\frac{\partial e}{\partial c_2}\right) \cdot \sigma^2{}_{c_2} + \ldots \quad \text{(A.7)}$$

The derivatives of e with respect to v and c are evaluated as follows;

$$\left(\frac{\partial e}{\partial v_i}\right) = \frac{c_i + c_{i-1}}{2} - \frac{c_{i+1} + c_i}{2} = \frac{c_{i-1} - c_{i+1}}{2}$$
$$\left(\frac{\partial e}{\partial c_i}\right) = \frac{v_i - v_{i-1}}{2} + \frac{v_{i+1} - v_i}{2} = \frac{v_{i+1} - v_{i-1}}{2} \quad \text{(A.8)}$$

$$\Delta v = \pm\, 0.003 l$$

$$\sigma^2{}_v = \left(\frac{\Delta v}{2.5}\right)^2$$

Error in concentration is 5.5 %. From the breakthrough plot, the errors associated with all the concentrations $c_1, c_2, c_3, \ldots$ were calculated and averaged as Δc.

$$\Delta c = 0.002\ eq/l$$
$$\sigma^2{}_c = \left(\frac{\Delta c}{2.5}\right)^2$$

Substituting the above values in Equation (A.7),

$$\sigma^2{}_e = 2 \times 10^{-7}$$
$$\sigma_e = 4 \times 10^{-4}$$
$$error = \sigma_e \cdot 2.5 = 0.003\ eq$$

The total number of equivalents as calculated from the plot is 0.045 *eq*.

A.2.3 Volume of Resin Bed

The volume of the resin column V = $\pi \cdot r^2 \cdot h$

Where *r* is the radius of the column

Height of the column = 50 mm

$\Delta h = \pm 3\ mm$

Error in measuring the height of the resin bed $= \frac{3}{50} \cdot 100$

$= 0.06\%$

The inner diameter of the column is 38.1 *mm*

$$V = \pi \cdot \left(\frac{38.1}{2} \right)^2 \cdot 50$$

$= 0.057\ l$

The error in volume measurement is 0.06 %, i.e. $\Delta V = 0.06\,\%\,(V) = 0.03 \times 10^{-3}\ l$

A.2.4 Capacity (Kgr/cu.ft.)

The capacity in units of Kgr/cu.ft is obtained using the formula $C = \frac{e}{V_B} \cdot 21.8$

Where e is the total number of equivalents in the bed and V_B is the volume of the resin bed.

Error in Capacity $\Delta C = C \cdot \sqrt{\left(\frac{\Delta e}{e} \right)^2 + \left(\frac{\Delta V_B}{V_B} \right)^2}$

Substituting the values of $V, e, \Delta e, \Delta V$ in the above equation, $\Delta C = 1.2$ Kgr/cu.ft

A.3 Uncertainty in Measuring Brine Volume

A.3.1 Concentration of Brine

The concentration, c of brine $c = \frac{Weight\ \ of\ \ salt, G\ (g)}{Volume\ of\ \ solution, L\ (l)}$

The accuracy of reading weights of the salt on the electronic balance is ±0.0003 g. The standard error associated with measuring pure water in a 1 liter carboy is ±5 %, i.e., 1± 0.01 ml.

Error in c is expressed as $\Delta c = c \cdot \sqrt{\left(\frac{\Delta G}{G}\right)^2 + \left(\frac{\Delta L}{L}\right)^2}$ (A.9)

and

$G = 50.3g$
$\Delta G = \pm 0.0003g$
$L = 1\,l$
$\Delta L = 0.01l$

Substituting the above values in equation (A.9), the error in c was calculated as 1.3 %.

A.3.2 Calibration

The errors associated with calibration were evaluated using a linear regression technique in MS Excel. The difference between the actual and predicted values was reported as residuals in concentration and the average error in concentration $\Delta c = 0.03\,eq/l$

$$c\,(eq/l) = \frac{Weight\ of\ \ salt\ \ per\ l}{Equivalent\ \ weight\ of\ \ NaCl}$$

The feed concentration $= \frac{40}{58.5}$
$= 0.68\,eq/l$

Error in concentration $= \frac{0.031}{0.68} \cdot 100$
$= 4.6\,\%$

The error in concentration is the sum of errors from solution preparation and calibration, which is 5.9 %. From the breakthrough plot, the errors associated with all the concentrations $c_1, c_2, c_3, \ldots$ were calculated and averaged as Δc.

$\Delta c = 0.03\ eq/l$

A.3.3 Brine Volume

The total number of equivalents to be treated with brine is obtained from the softening cycle, $e = 0.045\ eq$ and the error associated with this calculation $\Delta e = 0.003\ eq$

$$Brine\ Volume = \frac{Total\ number\ of\ equivalents\ (eq)}{Concentration\ of\ \ feed\ (eq/l)}$$

Measured volume of brine = 0.14 l

$$\text{Error in Volume measurement} = V \cdot \sqrt{\left(\frac{\Delta e}{e}\right)^2 + \left(\frac{\Delta c}{c}\right)^2} \qquad \text{(A.10)}$$

$$= \pm 0.03\ l$$

This analysis was performed on all sets of data and is tabulated below. Uncertainties in capacity measurement are presented in Table A.1 and Uncertainties in volume measurement are presented in Table A.2. Tables A.3 – A.12 contain data corresponding to uncertainty in capacity evaluation.

Table A.1: Uncertainty in capacity measurement

Concentration, C (g/l)	50.3	50.3	62.8	62.8	75.4	75.4	88	88	100.5	100.5
Weight of Salt, G (g)	50.3	50.3	62.8	62.8	75.4	75.4	88	88	100.5	100.5
ΔG	0.0003	0.0003	0.0003	0.0003	0.0003	0.0003	0.0003	0.0003	0.0003	0.0003
Volume of solution, L (l)	1	1	1	1	1	1	1	1	1	1
ΔL	0.01	0.01	0.01	0.01	0.01	0.01	0.01	0.01	0.01	0.01
%Error in C	1.3	1.3	1.3	1.3	1.3	1.3	1.3	1.3	1.3	1.3
Flow rate, F (l/s)	0.002	0.001	0.001	0.002	0.0015	0.002	0.002	0.002	0.002	0.002
ΔF	0	0.00	E-05	0.0	0.0	0.0	0.0	0.0	E-05	0.0
Time t, (s)	500	512	493	414	342	312	326	294	226	206
Δt	2	2	2	2	2	2	2	2	2	2
Volume Consumed, V (l)	0.75	0.67	0.65	0.66	0.5	0.51	0.49	0.44	0.37	0.33

%Error in V	0.4	0.4	1.4	0.5	0.6	0.6	0.6	0.7	1.4	1.0
ΔV	0.003	0.003	0.009	0.003	0.003	0.003	0.003	0.003	0.005	0.003
C (eq/l)	0.68	0.68	0.85	0.85	1.03	1.03	1.20	1.20	1.37	1.37
%Error in C-1	1.3	1.3	1.3	1.3	1.3	1.3	1.3	1.3	1.3	1.3
Residual C (eq/l, from calibration)	0.03	0.03	0.01	0.01	0.03	0.03	0.02	0.02	0.10	0.10
%Error in C-2	3.7	3.7	1.1	1.1	2.5	2.5	1.8	1.8	7.5	7.5
Total error in C (eq/l)	0.004	0.003	0.002	0.002	0.005	0.003	0.004	0.005	0.02	0.02
ΔE	0.003	0.003	0.001	0.001	0.003	0.002	0.002	0.003	0.008	0.006
Total Equivalents, E	0.045	0.043	0.051	0.053	0.062	0.06	0.078	0.078	0.086	0.084
Resin volume, V_R (l)	0.057	0.057	0.057	0.057	0.057	0.057	0.057	0.057	0.057	0.057
ΔV_R	E-06	E-06	E-06	E-06	0E-06	E-06	E-06	E-06	E-06	E-06

%Error in Capacity	7.1	6.1	2.6	2.3	4.8	3.2	2.9	3.2	9.2	7.0
Capacity (Kgr/cu.ft.)	17.0	16.0	20.0	20.0	24.0	23.0	30.0	30.0	33.0	32.0
ΔCapacity	1.2	1.0	0.5	0.5	1.2	0.7	0.8	1.0	3.0	2.2

Table A.2: Uncertainty in volume measurement

Concentration, C (g/l)	40	40	50	50	60	60	70	70	80	80
Weight of Salt, G (g)	40	40	50	50	60	60	70	70	80	80
ΔG	0.0003	0.0003	0.0003	0.0003	0.0003	0.0003	0.0003	0.0003	0.0003	0.0003
Volume of solution, L (l)	1	1	1	1	1	1	1	1	1	1
ΔL	0.01	0.01	0.01	0.01	0.01	0.01	0.01	0.01	0.01	0.01
%Error in C	1.3	1.3	1.3	1.3	1.3	1.3	1.3	1.3	1.3	1.3
Concentration C, (eq/l)	0.68	0.68	0.86	0.86	1.03	1.03	1.2	1.2	1.4	1.4
%Error in C-1	1.3	1.3	1.3	1.3	1.3	1.3	1.3	1.3	1.3	1.3
Residual C (eq/l, from calibration)	0.03	0.03	0.08	0.08	0.03	0.03	0.05	0.05	0.08	0.08
%Error in C-2	4.6	4.6	9.3	9.3	3.4	3.4	4.0	4.0	6.0	6.0
Total error in C (eq/l)	0.03	0.03	0.04	0.04	0.04	0.02	0.04	0.04	0.07	0.07

ΔE	0.003	0.003	0.001	0.001	0.003	0.002	0.002	0.003	0.008	0.006
Total Equivalents, E	0.045	0.043	0.051	0.053	0.062	0.06	0.078	0.078	0.086	0.084
Rinse volume, V (l)	0.140	0.140	0.130	0.130	0.140	0.110	0.08	0.1	0.08	0.09
%Error in V	8.0	7.65	5.6	5.3	5.9	3.8	4.7	4.4	10.7	8.7
ΔV	0.03	0.03	0.03	0.03	0.03	0.01	0.02	0.02	0.02	0.02

Table A.3: Error in evaluating Capacity- 4% (run 1)

v	c	σ_e^2
0.00	0.07	1E-08
0.05	0.24	3E-08
0.07	0.12	2E-07
0.12	0.07	4E-07
0.33	0.05	5E-07
0.51	0.05	5E-07
0.66	0.05	
0.75	0.01	

Δv	0.003
Δc	0.004
σ_e^2	2E-06
σ_e	1E-03
Error	0.003

Table A.4: Error in evaluating Capacity- 4% (run 2)

v	C	σ_e^2
0.00	0.18	9E-08
0.13	0.09	3E-07
0.24	0.09	3E-07
0.50	0.02	3E-07
0.60	0.01	
0.67	0.01	

Δv	0.003
Δc	0.003
σ_e^2	1E-06
σ_e	1E-03
Error	0.003

Table A.5: Error in evaluating Capacity- 5% (run 1)

v	C	σ_e^2
0.06	0.15	3E-08
0.09	0.11	3E-08
0.17	0.08	3E-08
0.24	0.06	3E-08
0.32	0.05	8E-08
0.41	0.05	8E-08
0.59	0.04	
0.65	0.04	

Δv	0.014
Δc	0.002
σ_e^2	3E-07
σ_e	5E-04
Error	0.001

Table A.6: Error in evaluating Capacity- 5% (run 2)

v	C	σ_e^2
0.12	0.11	2E-07
0.18	0.08	8E-09
0.66	0.07	
0.65	0.04	

Δv	0.003
Δc	0.002
σ_e^2	2E-07
σ_e	5E-04
Error	0.001

Table A.7: Error in evaluating Capacity- 6% (run 1)

v	C	σ_e^2
0.07	0.28	8E-08
0.18	0.18	2E-07
0.23	0.15	3E-07
0.38	0.01	
0.51	0.00	

Δv	0.003
Δc	0.003
σ_e^2	6E-07
σ_e	7E-04
Error	0.002

Table A.8: Error in evaluating Capacity- 6% (run 2)

v	c	σ_e^2
0.06	0.24	4E-07
0.26	0.09	3E-07
0.36	0.08	3E-07
0.45	0.07	2E-07
0.49	0.03	
0.51	0.03	

Δv	0.003
Δc	0.005
σ_e^2	1E-06
σ_e	1E-03
Error	0.003

Table A.9: Error in evaluating Capacity- 7% (run 1)

v	c	σ_e^2
0.09	0.40	2E-07
0.15	0.20	5E-07
0.28	0.11	
0.49	0.01	

Δv	0.003
Δc	0.004
σ_e^2	8E-07
σ_e	9E-04
Error	0.002

Table A.10 Error in evaluating Capacity- 7% (run 2)

v	c	σ_e^2
0.09	0.23	1E-07
0.12	0.21	4E-07
0.23	0.17	4E-07
0.36	0.13	
0.44	0.13	

Δv	0.003
Δc	0.005
σ_e^2	1E-06
σ_e	1E-03
Error	0.003

Table A.11: Error in evaluating Capacity- 8% (run 1)

v	C	σ_e^2
0.00	0.30	2E-06
0.06	0.26	8E-06
0.16	0.22	
0.36	0.21	

Δv	0.005
Δc	0.02
σ_e^2	1E-05
σ_e	3E-03
Error	0.008

Table A.12: Error in evaluating Capacity- 8% (run 2)

v	c	σ_e^2
0.13	0.31	5E-06
0.14	0.25	
0.33	0.21	

Δv	0.003
Δc	0.02
σ_e^2	5E-06
σ_e	2E-03
Error	0.006

The uncertainties in capacity estimation are presented in the following plot. The average error in capacity estimation is 5 %.

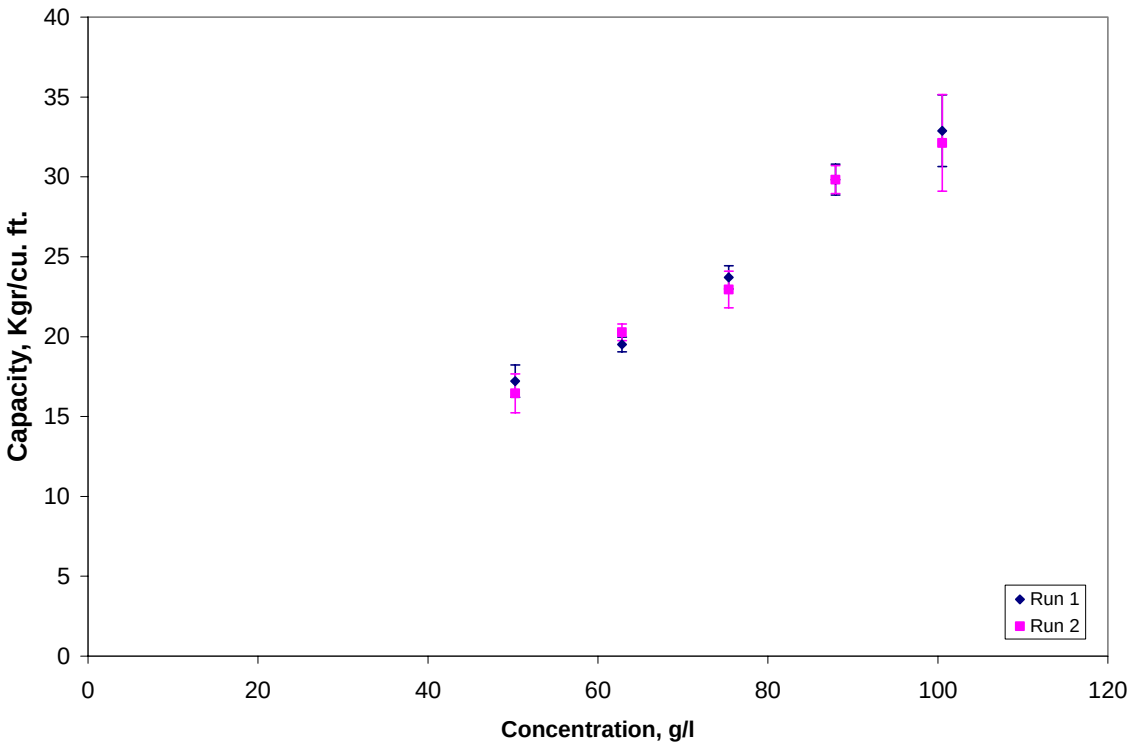

Figure A.1: Uncertainty in capacity measurement

The following plot presents the uncertainties associated with volume determination. The average error in volume estimation is 7 %. The two points determined experimentally are plotted for each of the regeneration levels along with their individual error bars.

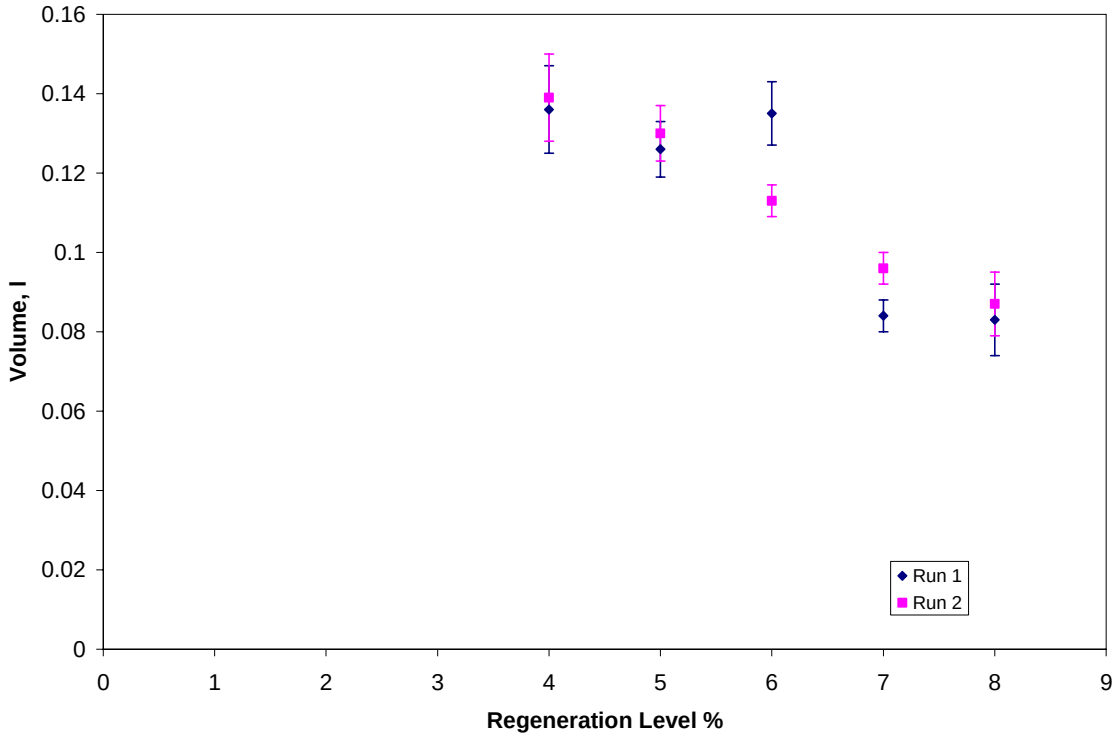

Figure A.2: Uncertainty in volume estimation

APPENDIX B

CALIBRATION

B.1 Calibration Curves

Appendix B contains calibration plots for regeneration levels: 40 g/l – 70 g/l. The calibration curve consists of two sections; the lower conductivity region or the region where the service cycle operates and the higher conductivity region or the region where the regeneration cycle operates. These two sections have been fitted with two separate trendlines to accommodate both cycles. These lines overlap at the center. The trendlines

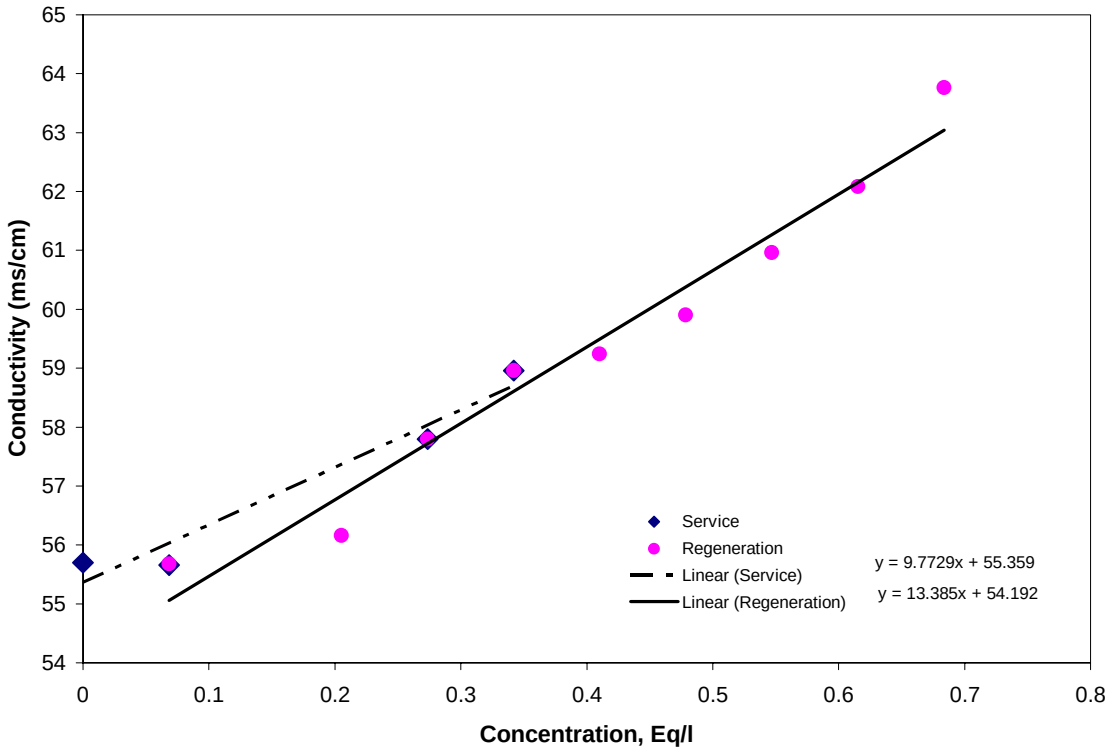

Figure B.1: Calibration curve, regeneration level 40 g/L

were fitted separately for the two cycles because they operate in different ranges. For experiments conducted at 4 % regeneration level the conductivity measurements in the service cycle would lie between 55.0 ms/cm and 60 ms/cm. In the regeneration cycle, the measurements would lie in the range of 60 ms/cm – 65 ms/cm. Using only that range of points to fit the trendline gives a more accurate trend.

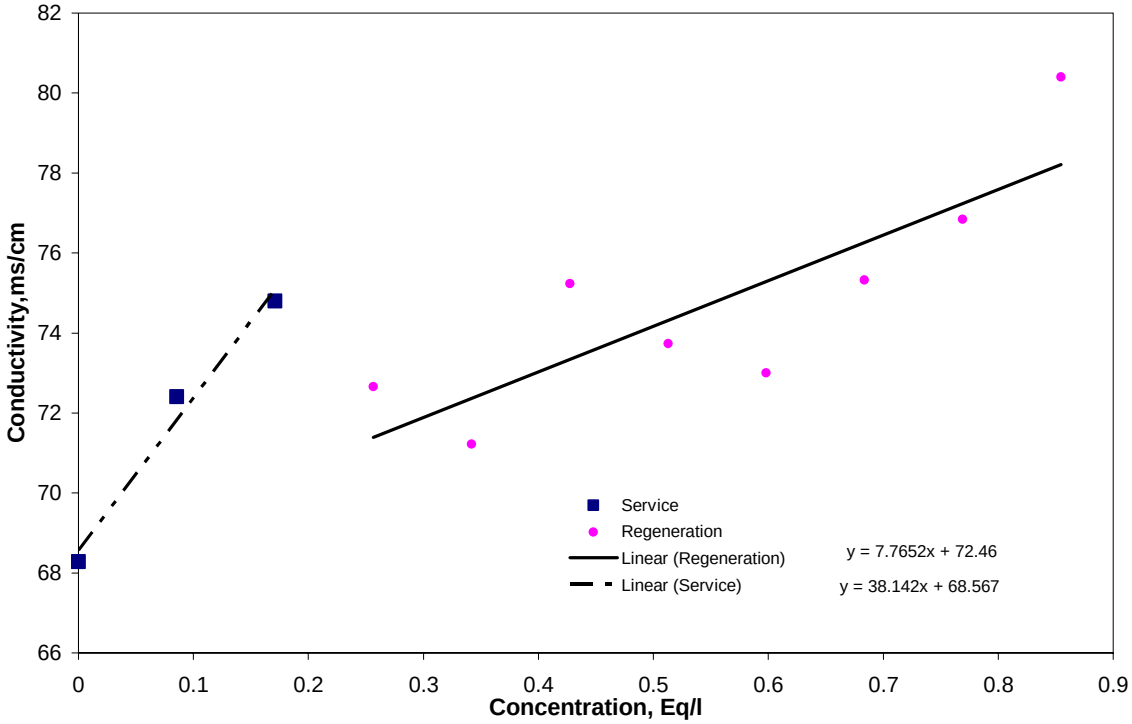

Figure B.2: Calibration curve, regeneration level of 50g/L

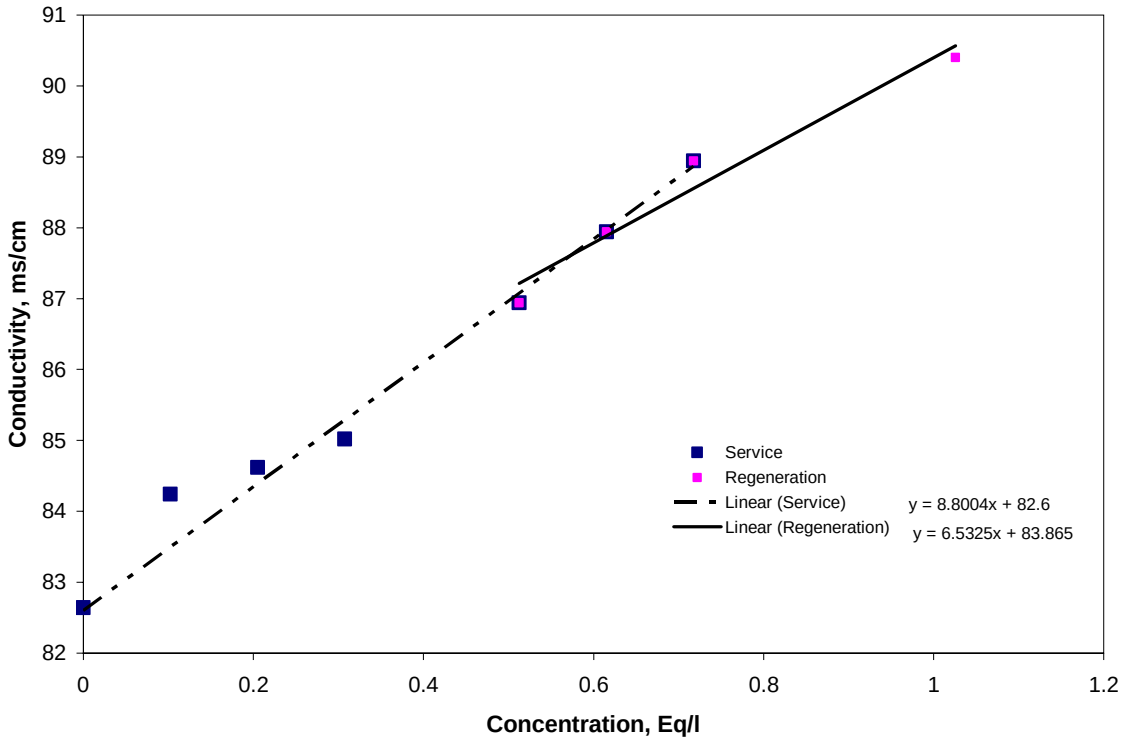

Figure B.3: Calibration curve, regeneration level of 60g/L

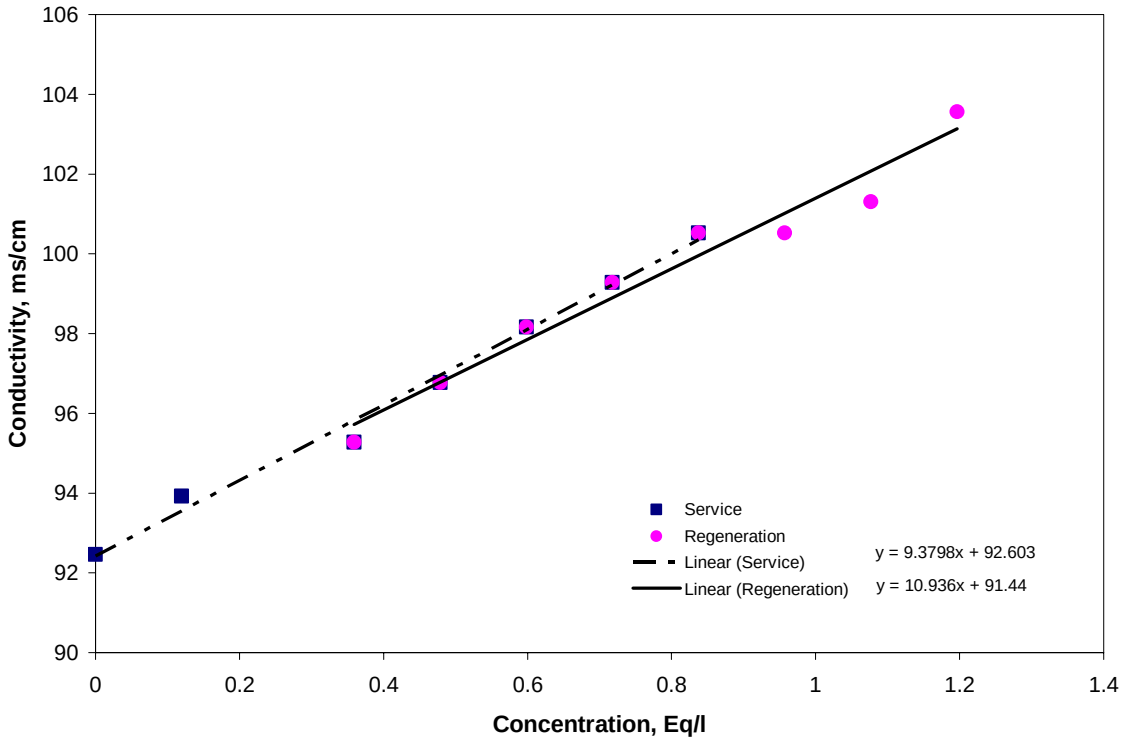

Figure B.4: Calibration curve, regeneration level of 70 g/l

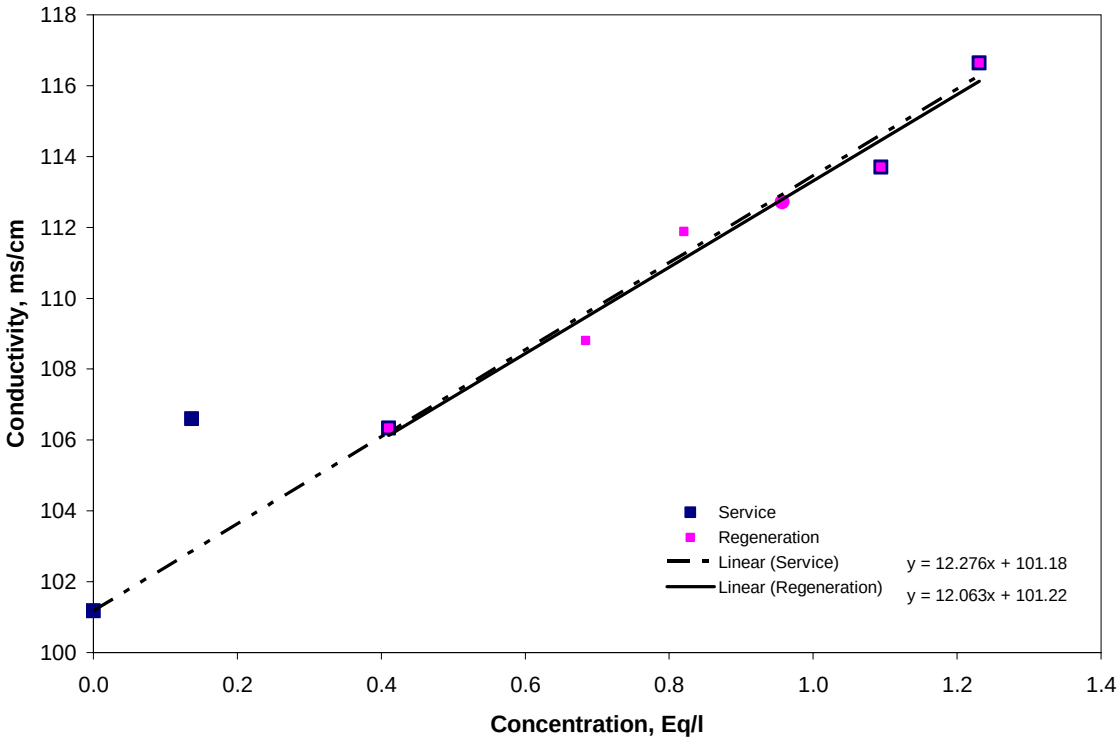

Figure B.5: Calibration curve, regeneration level of 80 g/l

B.2 Calibration Error

Calibration curves for service and regeneration cycles were generated for all regeneration levels. Calibration was repeated several times and the average of the readings were used in calculations. Figures B.6 – B.10 show the errors in calibration for regeneration levels of 40 g/l to 80 g/l. Each of the data point represents sodium chloride and calcium chloride salts in a definite ratio. The calibration procedure has been explained in Chapter 4.

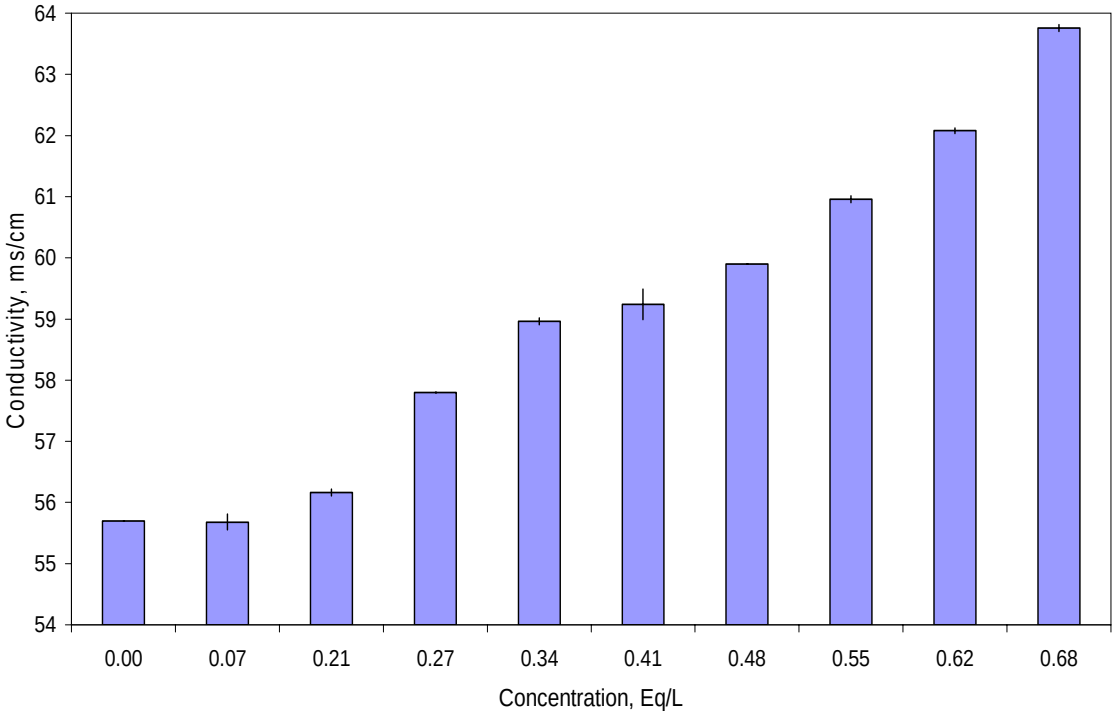

Figure B.6: Errors in calibration, regeneration level of 40 g/l

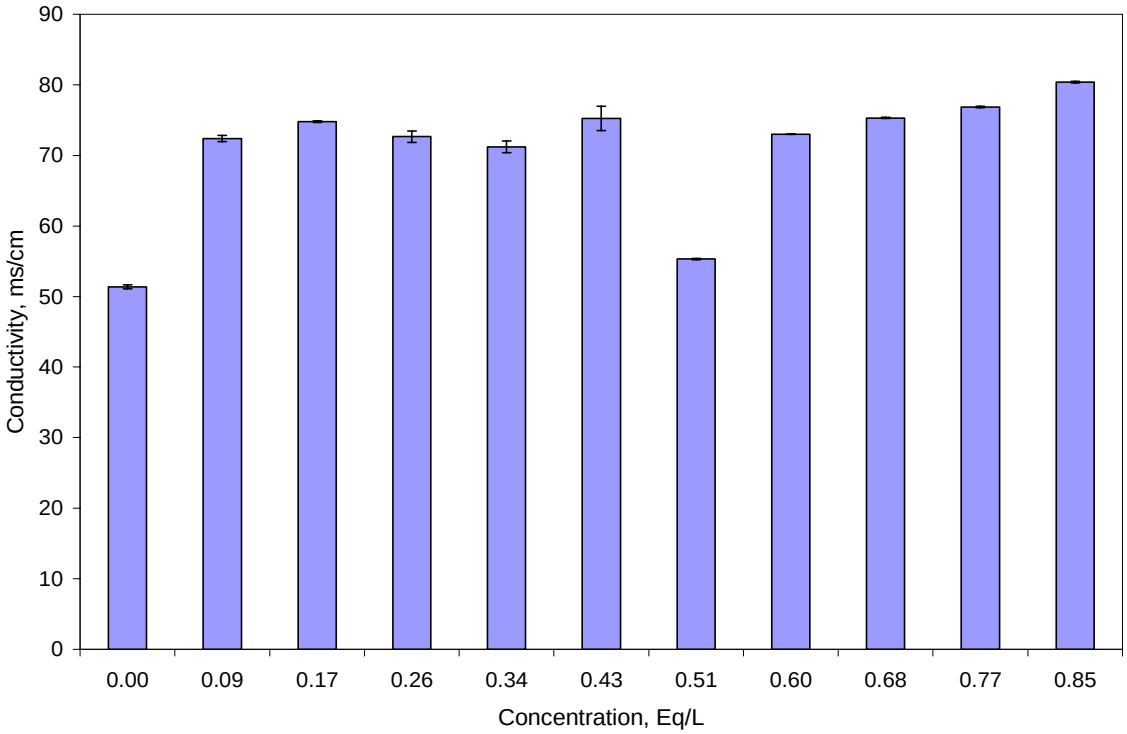

Figure B.7: Errors in calibration, regeneration level of 50 g/l

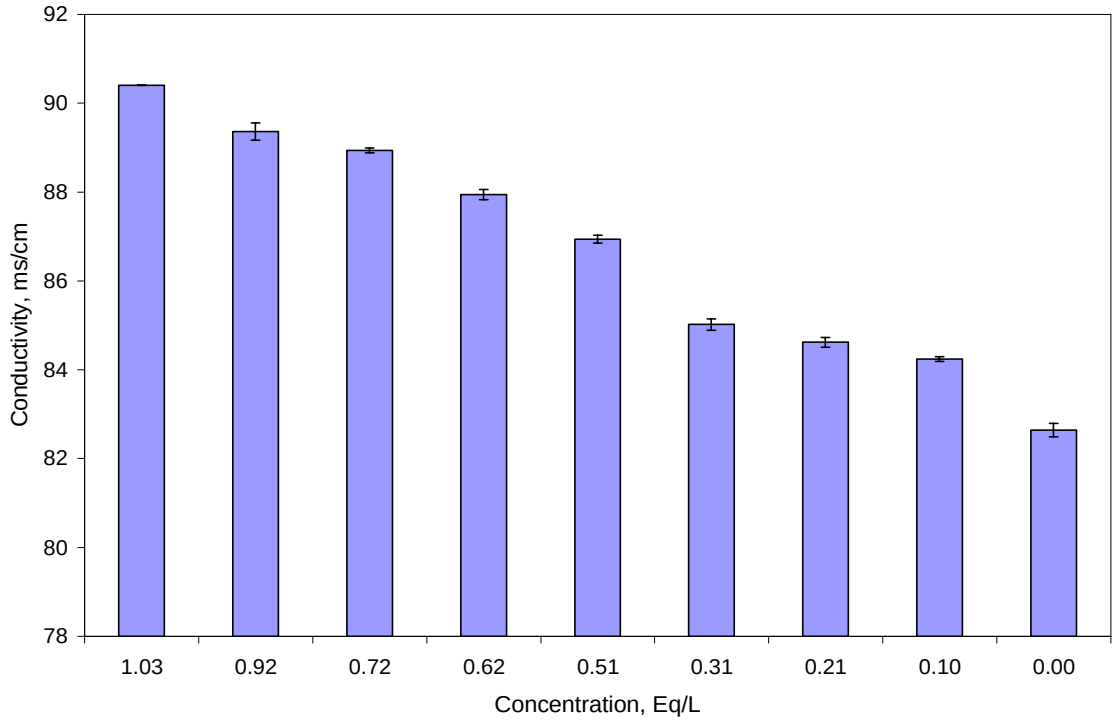

Figure B.8: Error in calibration, regeneration level of 60 g/l

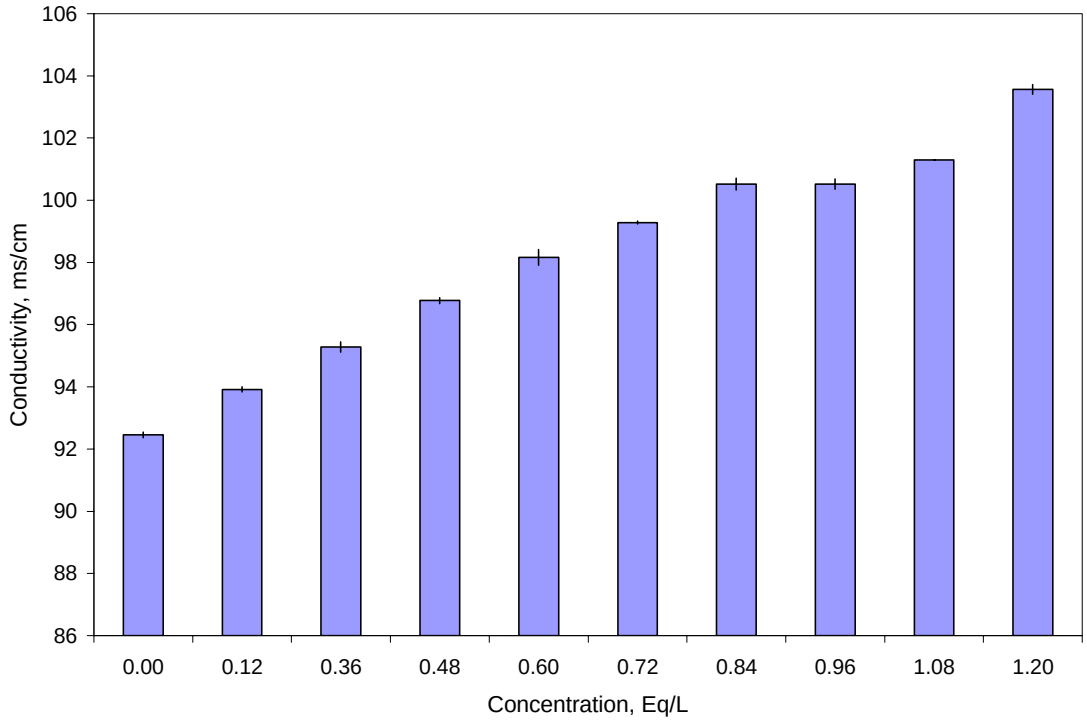

Figure B.9: Errors in calibration, regeneration level of 70 g/l

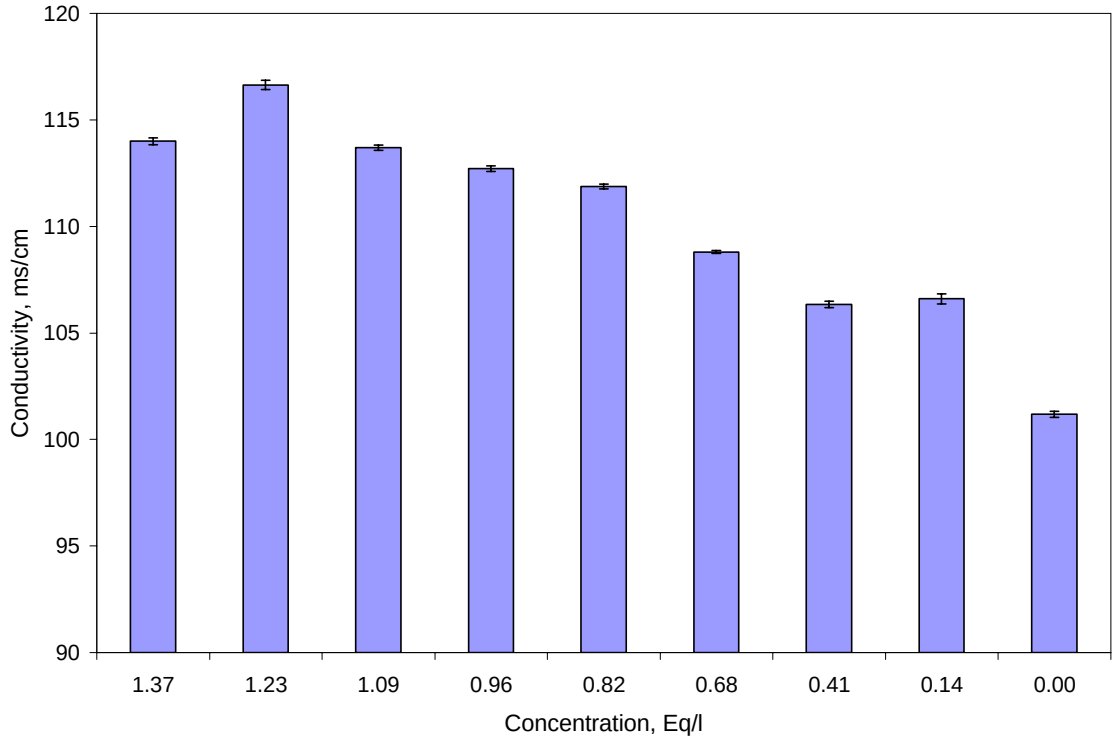

Figure B.10: Errors in calibration, regeneration level of 80 g/l

APPENDIX C

BREAKTHROUGH CURVES

C.1 Introduction

Appendix C consists of breakthrough curves for calcium and sodium for regeneration levels from 50 g/l to 80 g/l. Curves for experiments with 40 g/l regeneration level have already been discussed in detain in Chapter 4. These plots indicate the volume consumed per cycle. This is the volume at the point on the horizontal axis where the curve levels off. The volume data is shown in Table 5.1. The area below the curve would indicate the capacity of the resin sample (total number of equivalents). This is the area of integration used in equation (4.1). When this capacity is converted to represent one liter of bed, the operating capacity in units of eq/l is obtained.

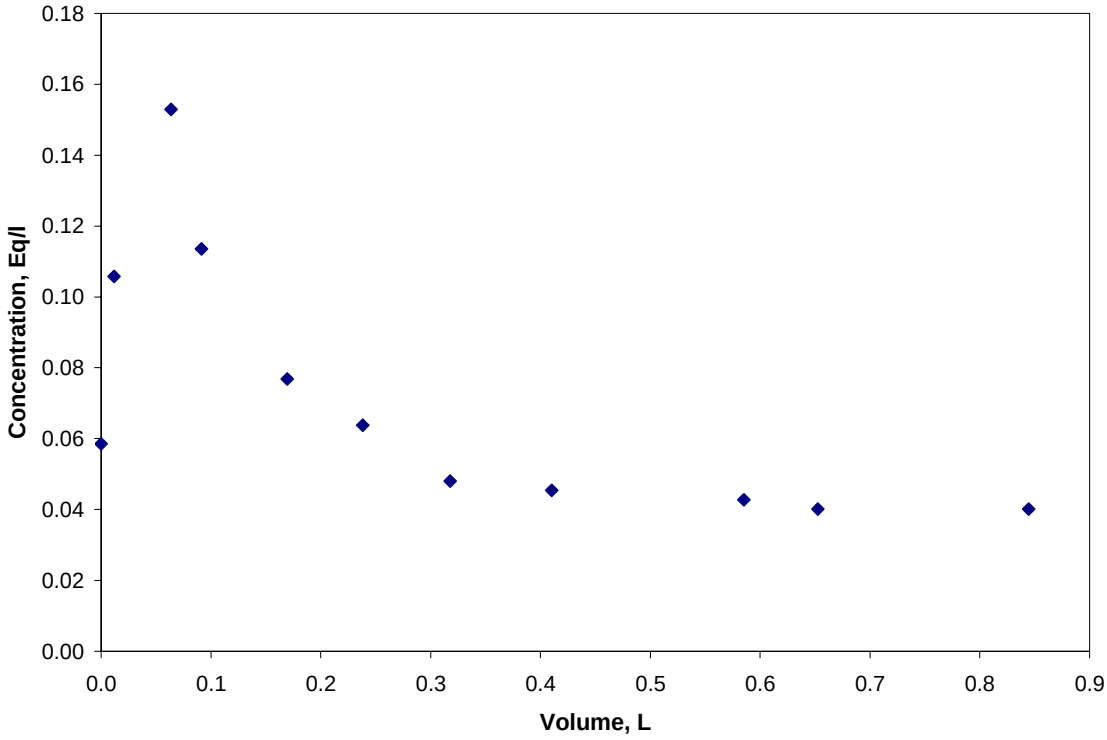

Figure C.1: Breakthrough curve for Ca^{2+} at regeneration level of 50g/L, run 1

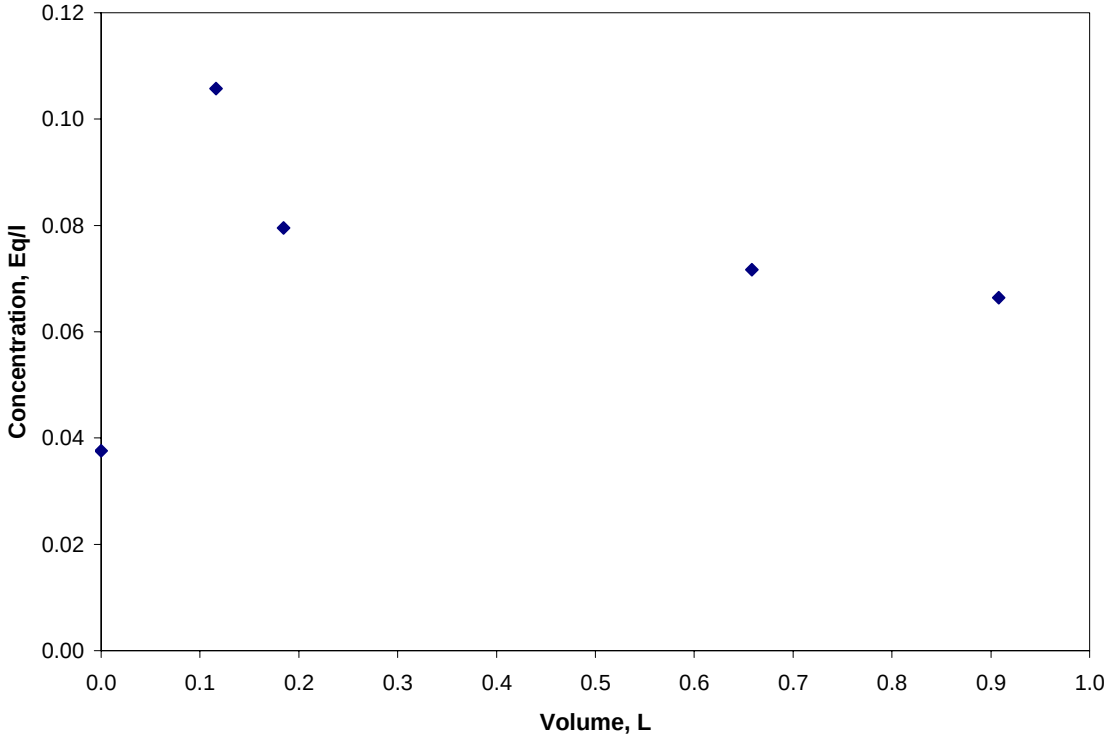

Figure C.2: Breakthrough curve for Ca^{2+} at regeneration level of 50g/L, run 2

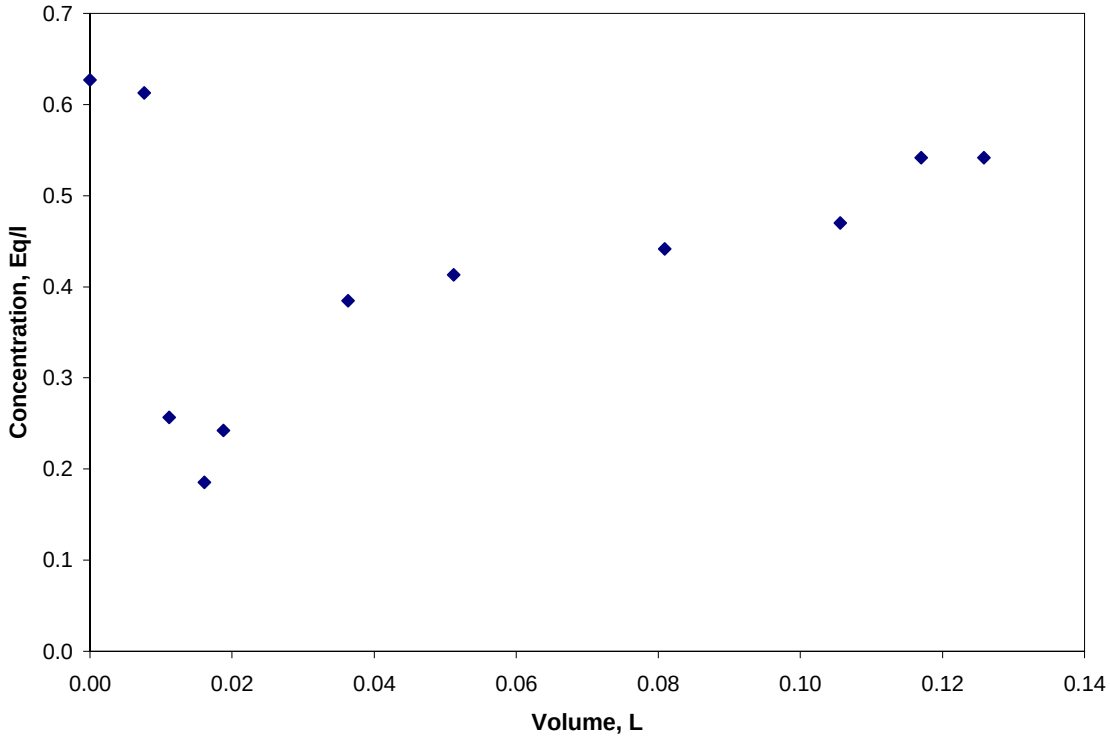

Figure C.3: Breakthrough curve for Na^+ at regeneration level of 50 g/L, run 1

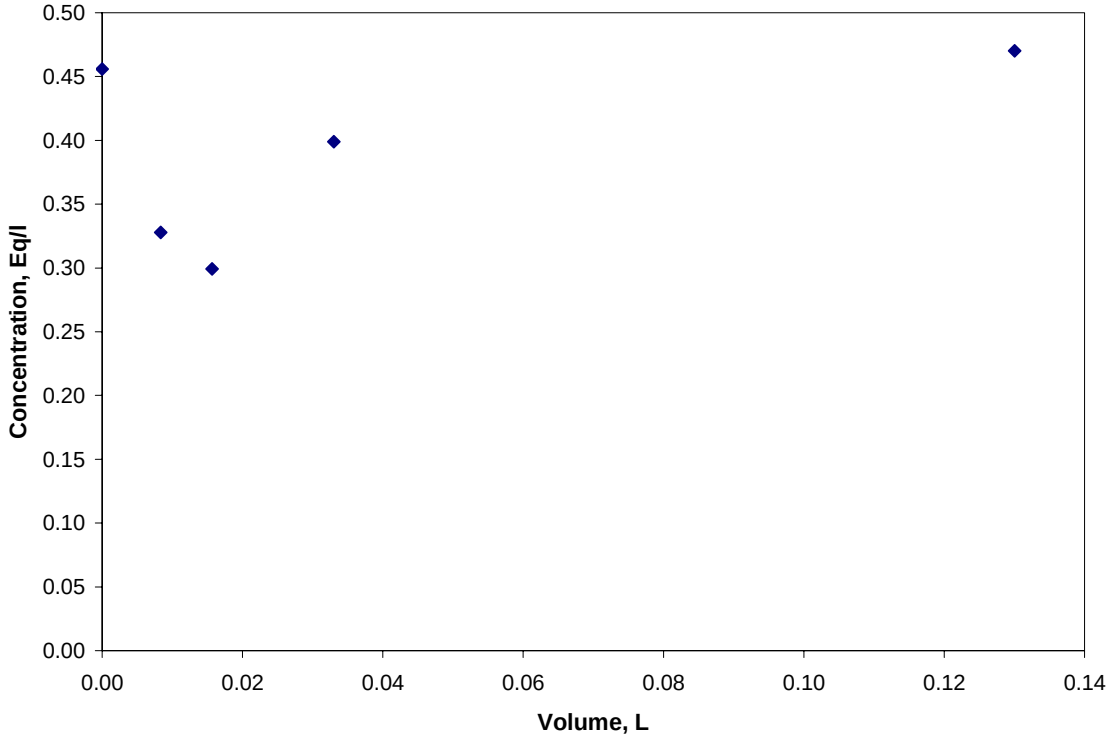

Figure C.4: Breakthrough curve for Na^+ at regeneration level of 50 g/L, run 2

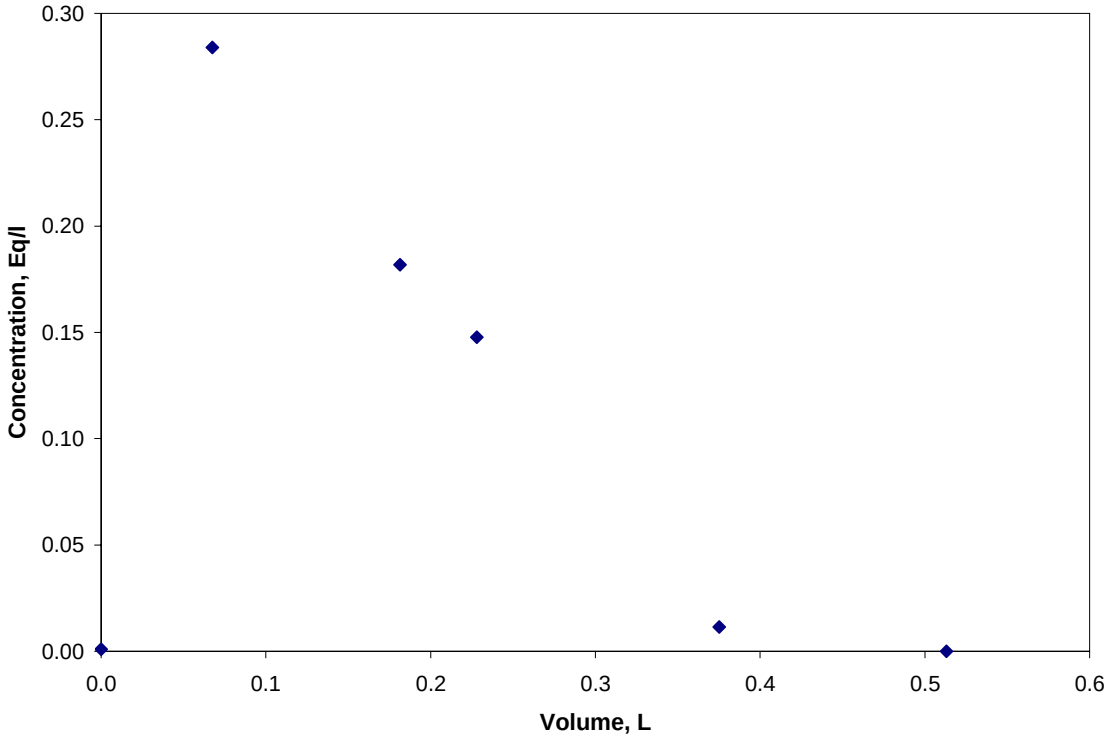

Figure C.5: Breakthrough curve for Ca^{2+} at regeneration level of 60 g/L, run 1

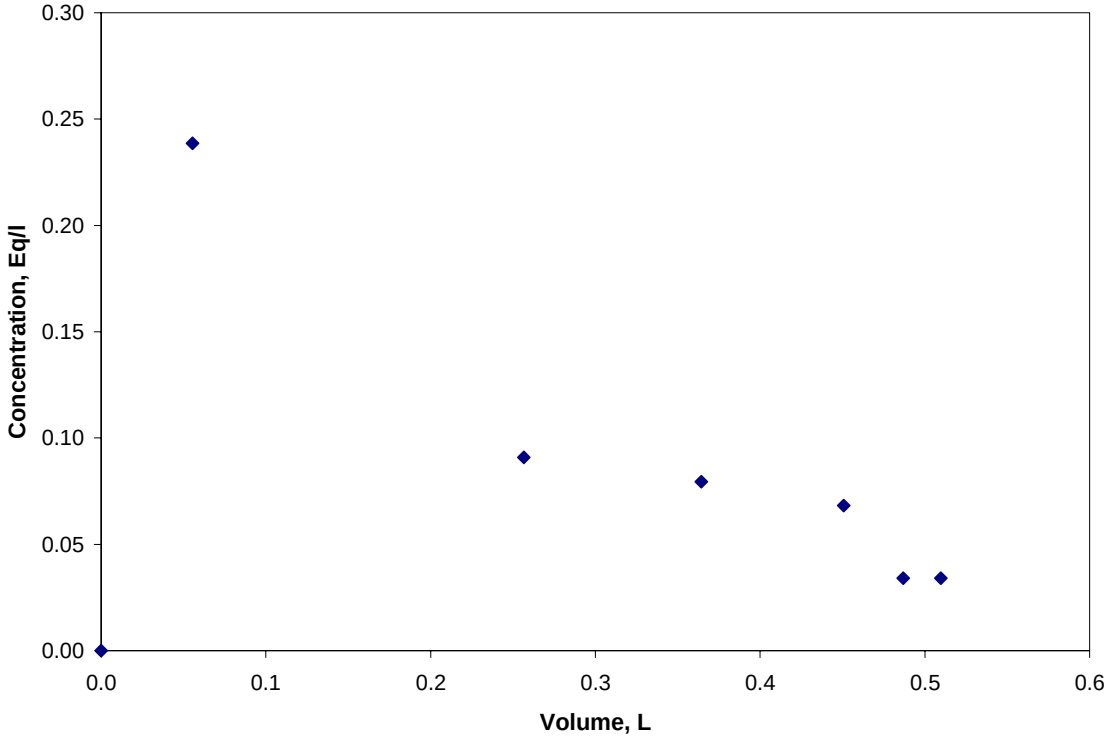

Figure C.5: Breakthrough curve for Ca^{2+} at regeneration level of 60 g/L, run 2

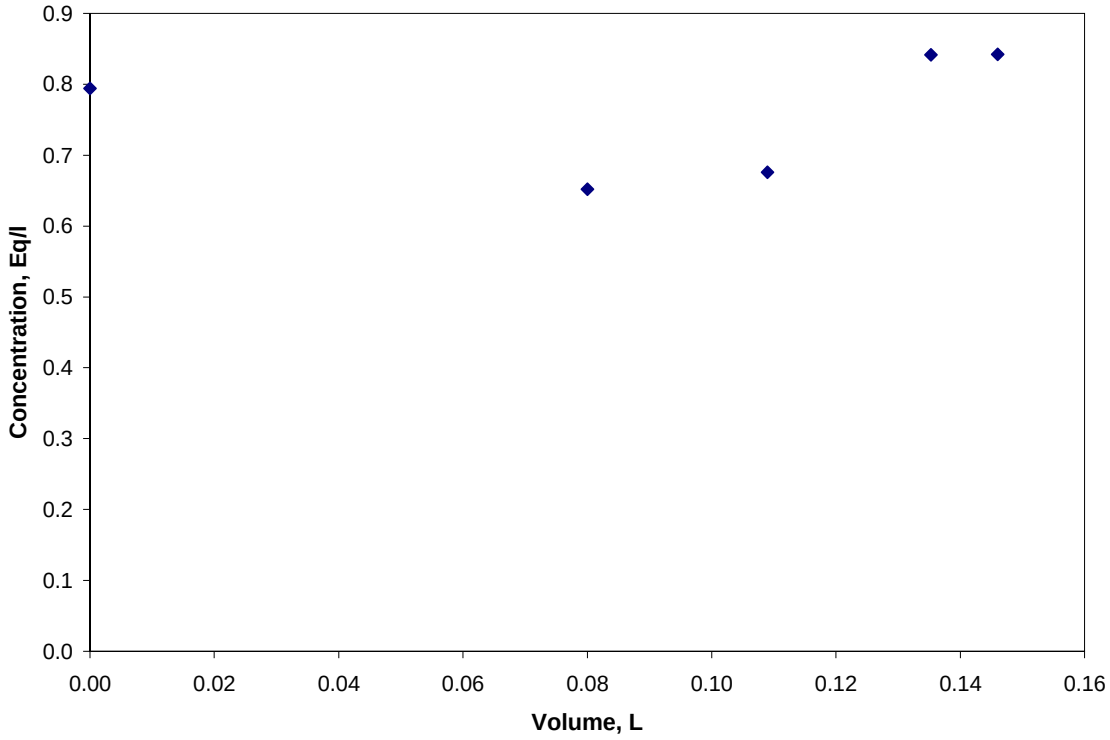

Figure C.6: Breakthrough curve for Na^+ at regeneration level of 60 g/L, run 1

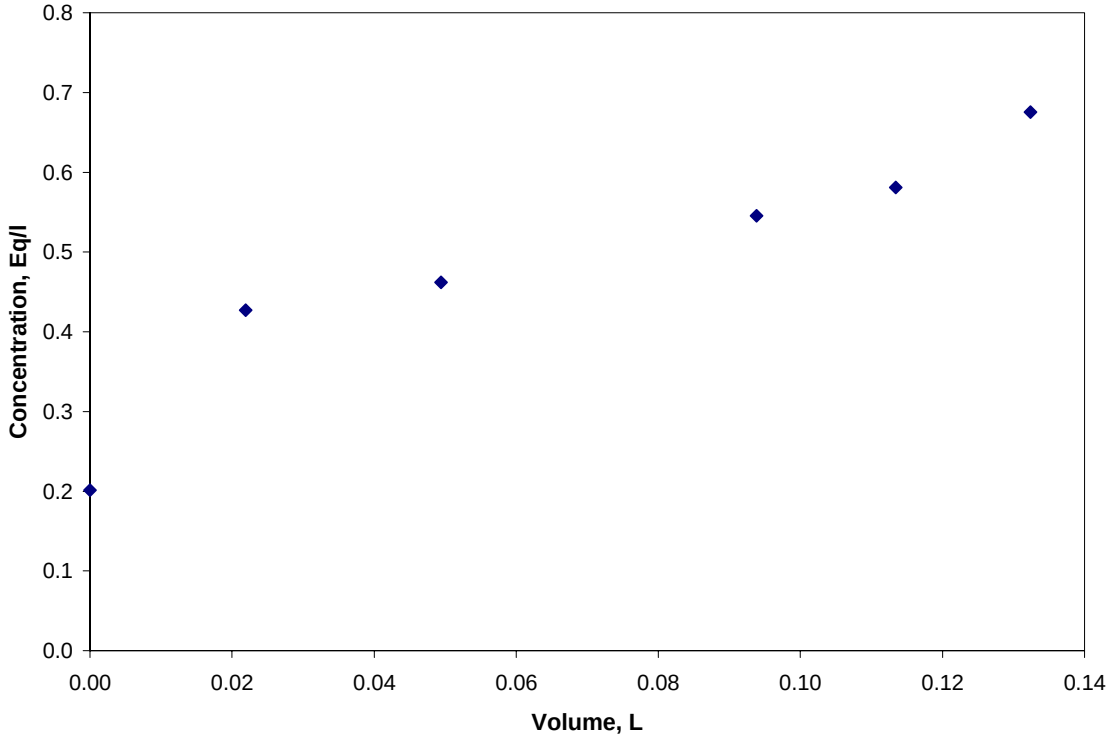

Figure C.7: Breakthrough curve for Na^+ at regeneration level of 60 g/L, run 2

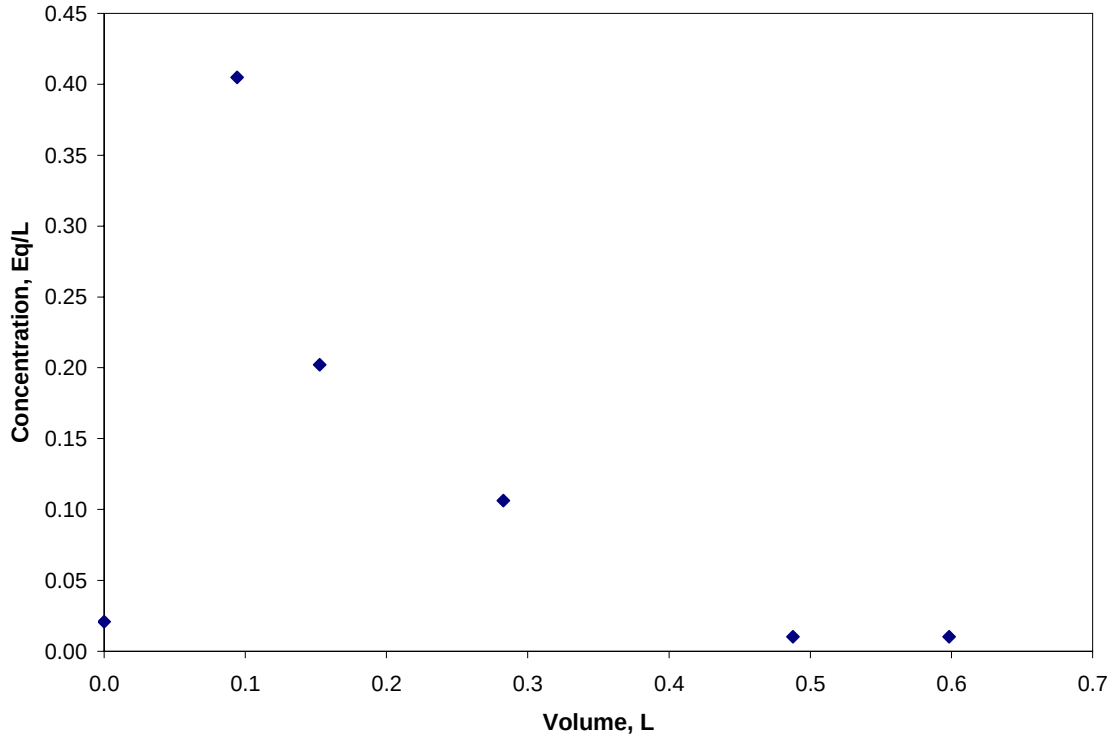

Figure C.8: Breakthrough curve for Ca^{2+} at regeneration level of 70 g/L, run 1

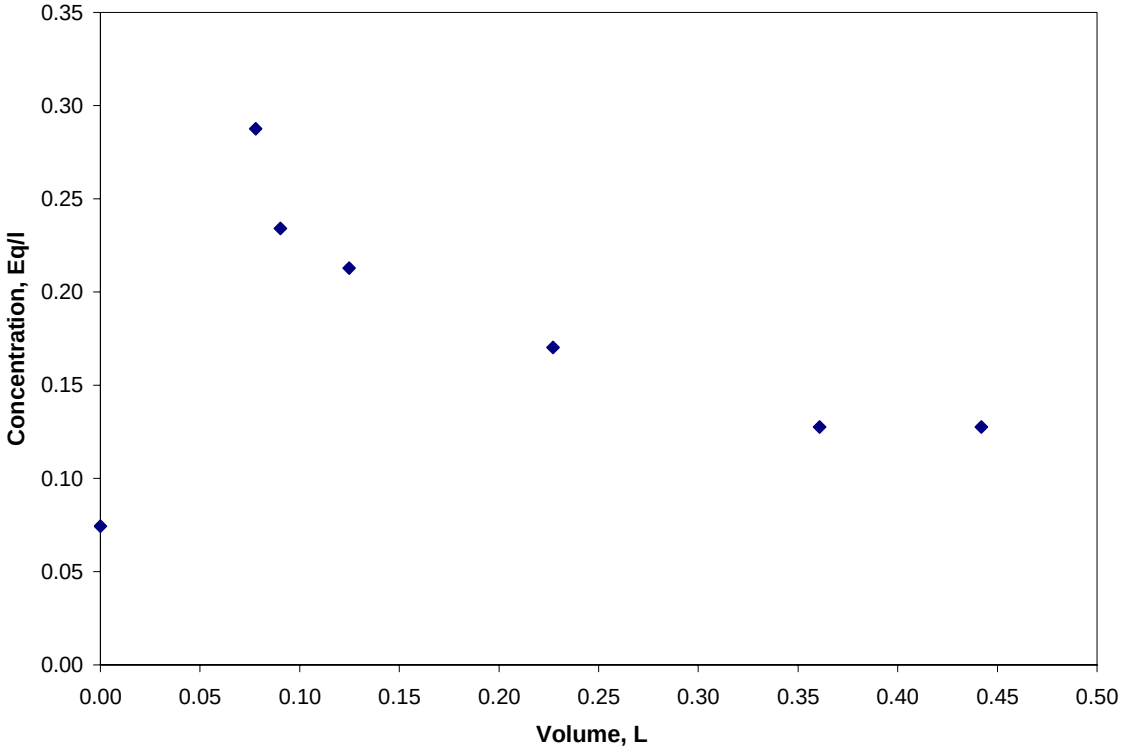

Figure C.9: Breakthrough curve for Ca^{2+} at regeneration level of 70 g/L, run 2

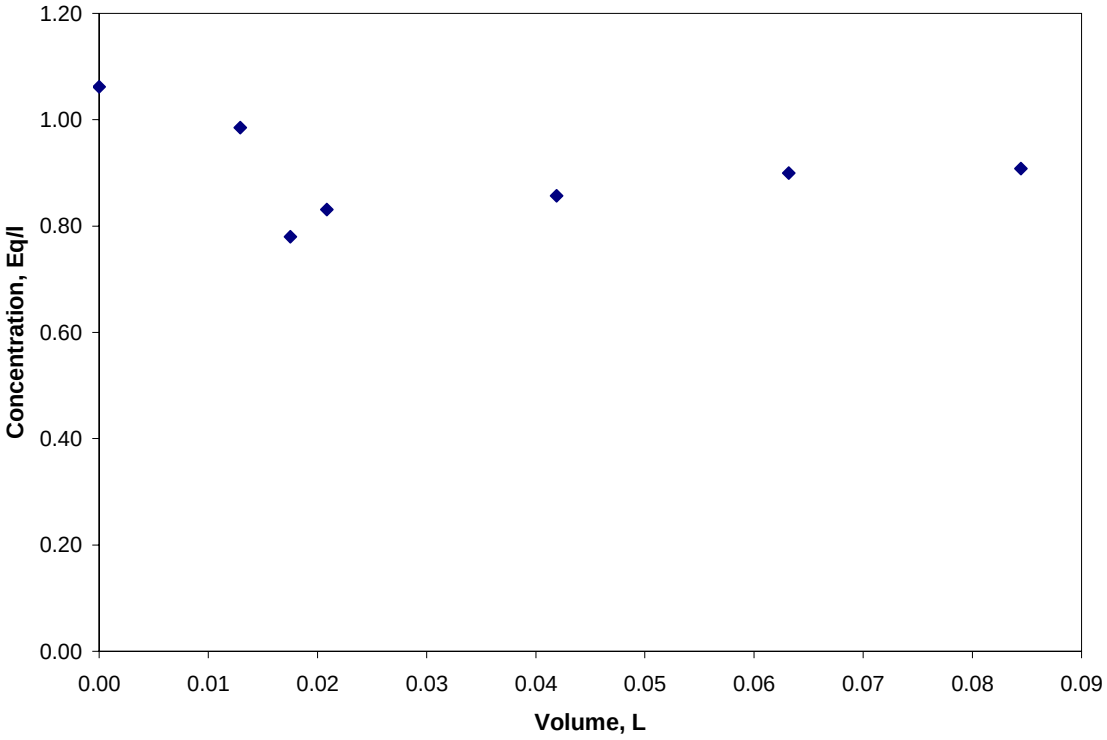

Figure C.10: Breakthrough curve for Na^+ at regeneration level of 70 g/L, run 1

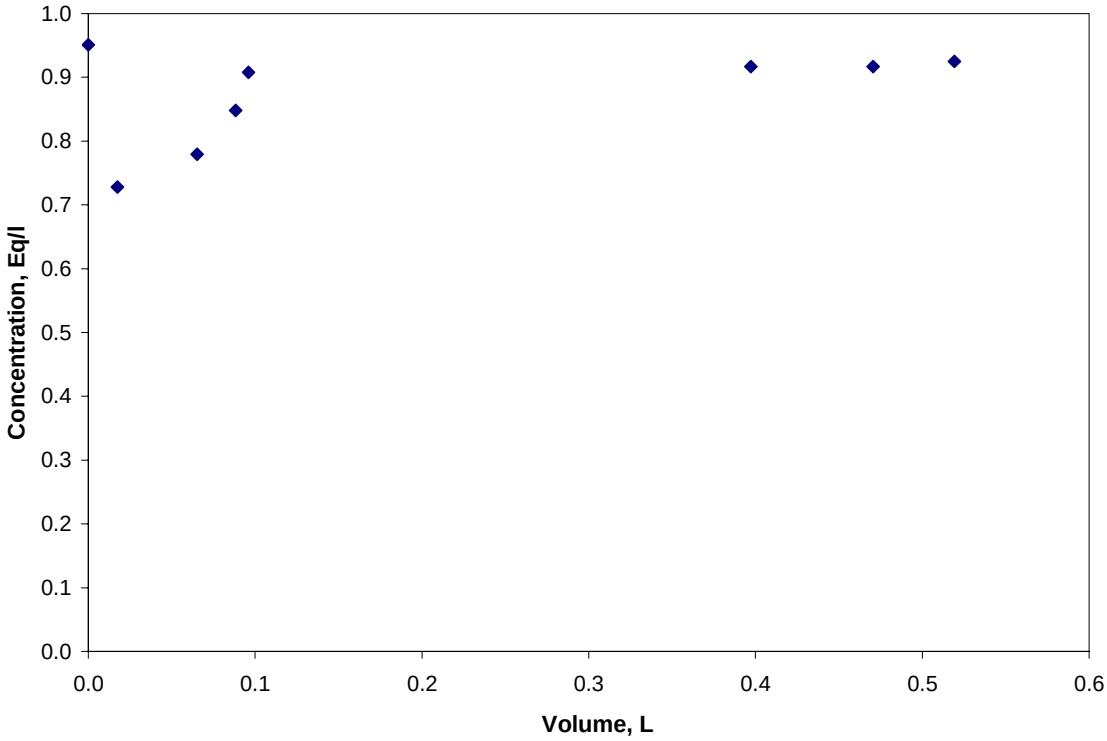

Figure C.11: Breakthrough curve for Na^+ at regeneration level of 70 g/L, run 2

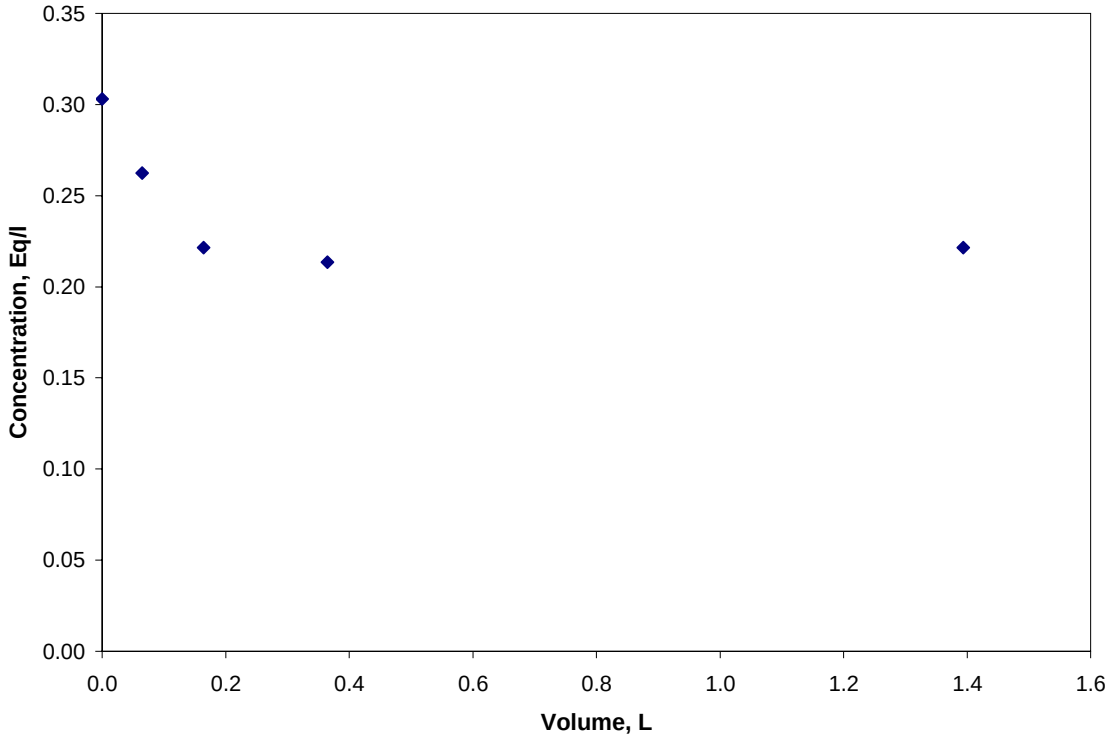

Figure C.12: Breakthrough curve for Ca^{2+} at regeneration level of 80 g/L, run 1

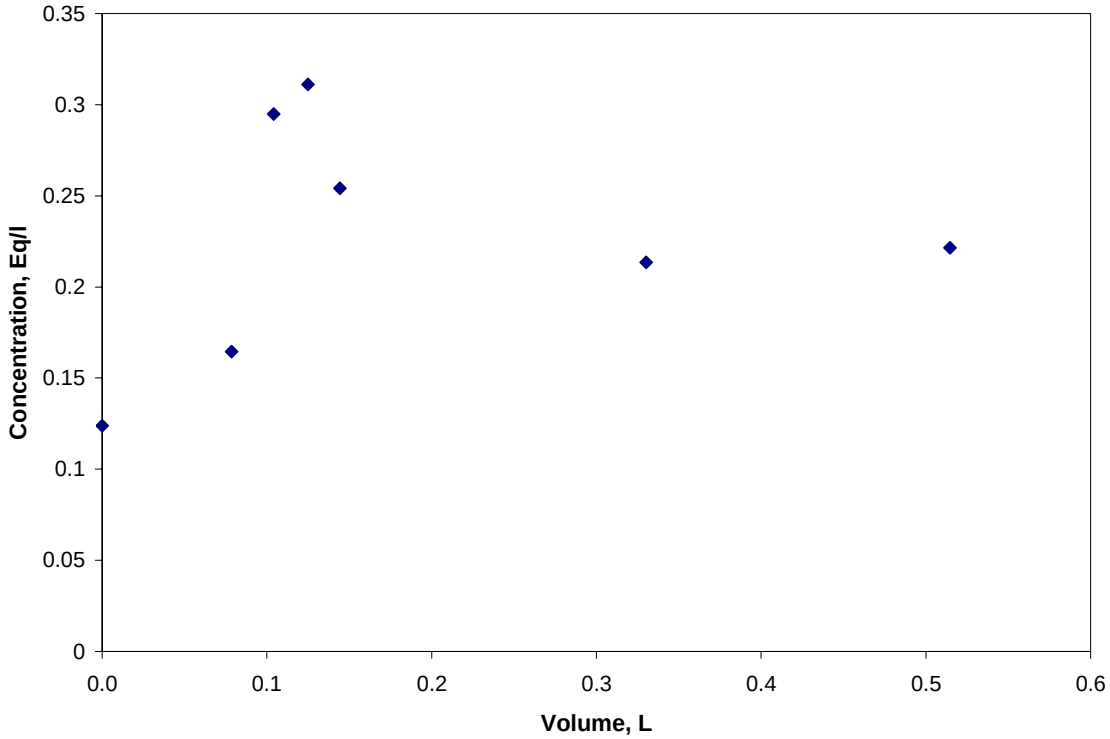

Figure C 13: Breakthrough curve for Ca^{2+} at regeneration level of 80 g/L, run 2

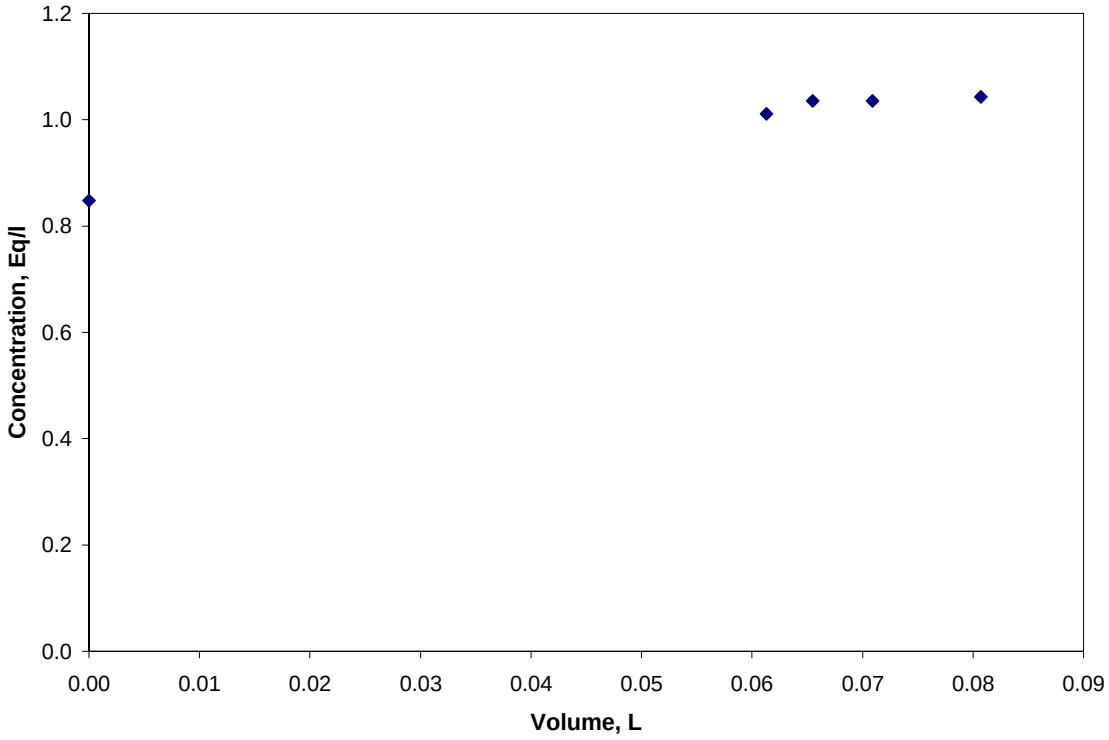

Figure C.14: Breakthrough curve for Na^+ at regeneration level of 80 g/L, run 1

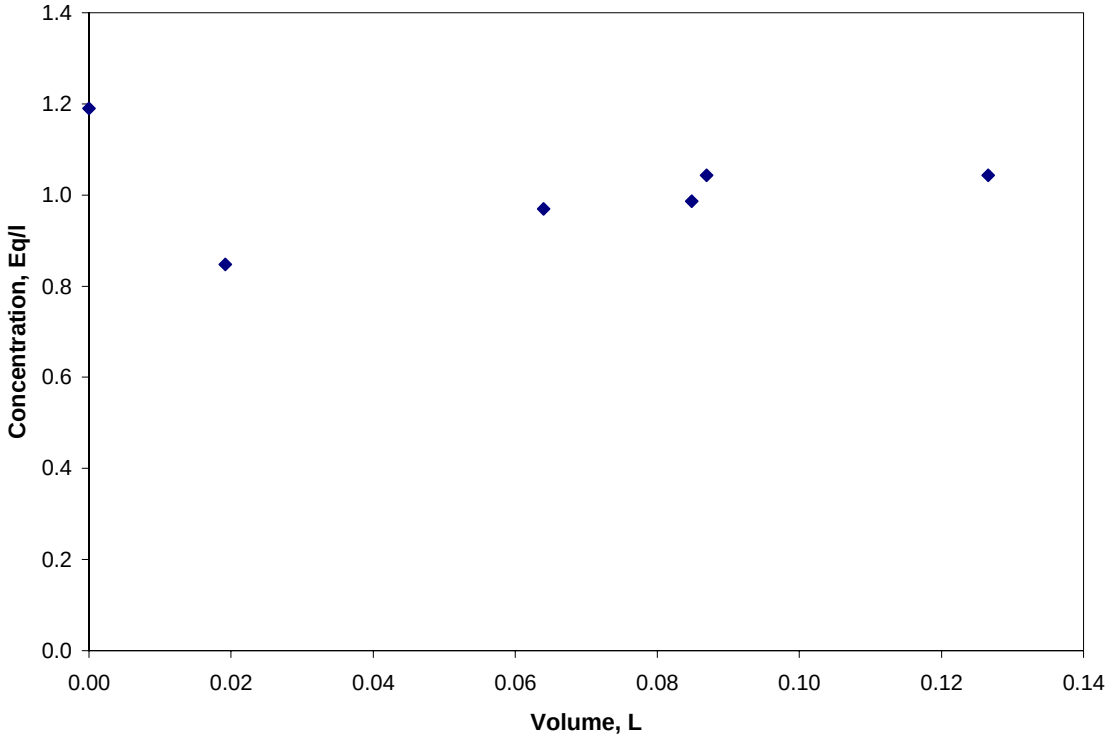

Figure C.15: Breakthrough curve for Na^+ at regeneration level of 80 g/L, run 2

APPENDIX D

DATA USED IN CORRELATION

Appendix contains data that have been used in the correlations obtained in Chapter 5. All data have been extended for bed volumes ranging from 100l – 800 l from experimental data. Experimental data corresponds to 0.057 l of resin. Table D.1 shows the experimental capacities measured along with the error in capacity due to uncertainties from experimental measurement. Table D.2 shows data for capacity as a function of volume of hard water treated at different concentrations. Table D.3 to Table D.7 show data for extended bed volumes at individual concentrations.

Table D.1: Experimentally measured capacity at different regeneration levels

S.No	Regeneration Level, g/l	Volume (l) Run 1	Capacity Kgr/cu.ft.	Error	Volume (l) Run 2	Capacity Kgr/cu.ft	Error
1	4	0.750	17.0	1.2	0.670	16.0	1.0
2	5	0.650	20.0	0.5	0.660	20.0	0.5
3	6	0.510	24.0	1.1	0.510	23.0	0.7
4	7	0.490	30.0	0.9	0.440	30.0	1.0
5	8	0.370	33.0	3.0	0.330	32.0	2.2

Table D.2: Capacity as a function of volume of hardwater treated: 1 liter of resin bed

S.No	Regeneration Level, g/l	Volume (l) Run 1	Capacity Kgr/cu.ft.	Error	Volume (l) Run 2	Capacity Kgr/cu.ft	Error
1	40	13.2	300	21	11.8	290	18
2	50	11.5	340	9	11.5	360	8
3	60	9.0	420	20	8.9	400	13
4	70	8.6	520	15	7.7	520	17
5	80	6.4	580	53	5.8	560	39

Table D.3: Capacity as a function of volume of hardwater treated: Concentration of 40g/l

Volume of Water treated (l) Run 1	Capacity Kgr/cu.ft.	Error	Volume of Water treated (l) Run 2	Capacity Kgr/cu.ft	Error
100	2300	160	100	2400	150
200	4600	320	200	4900	300
300	6900	490	300	7300	450
400	9200	650	400	9800	600
500	11000	810	500	12000	750
600	14000	970	600	15000	900
700	16000	1100	700	17000	1000
800	18000	1300	800	20000	1200

Table D.4: Capacity as a function of volume of hardwater treated: Concentration of 50g/l

Volume of Water treated (l) Run 1	Capacity Kgr/cu.ft.	Error	Volume of Water treated (l) Run 2	Capacity Kgr/cu.ft	Error
100.00	3000	79	100.00	3100	70
200.00	6000	160	200.00	6200	140
300.00	9000	240	300.00	9200	210
400.00	12000	310	400.00	12000	280
500.00	15000	390	500.00	15000	350
600.00	18000	470	600.00	18000	420
700.00	21000	550	700.00	22000	490
800.00	24000	630	800.00	25000	560

Table D.5: Capacity as a function of volume of hardwater treated: Concentration of 60g/l

Volume of Water treated (l) Run 1	Capacity Kgr/cu.ft.	Error	Volume of Water treated (l) Run 2	Capacity Kgr/cu.ft	Error
100	4600	220	100	4500	140
200	9200	450	200	9000	290
300	14000	670	300	14000	430
400	18000	890	400	18000	570
500	23000	1100	500	23000	710
600	28000	1300	600	27000	860
700	32000	1600	700	32000	1000
800	37000	1800	800	36000	1100

Table D.6: Capacity as a function of volume of hardwater treated: Concentration of 70g/l

Volume of Water treated (l) Run 1	Capacity Kgr/cu.ft.	Error	Volume of Water treated (l) Run 2	Capacity Kgr/cu.ft	Error
100	6100	180	100	6800	220
200	12000	360	200	14000	440
300	18000	540	300	20000	660
400	24000	720	400	27000	880
500	31000	900	500	34000	1100
600	37000	1100	600	41000	1300
700	43000	1300	700	47000	1500
800	49000	1400	800	54000	1800

Table D.7: Capacity as a function of volume of hardwater treated: Concentration of 80g/l

Volume of Water treated (l) Run 1	Capacity Kgr/cu.ft.	Error	Volume of Water treated (l) Run 2	Capacity Kgr/cu.ft	Error
100	9000	830	100	9700	680
200	18000	1700	200	19000	1400
300	27000	2500	300	29000	2000
400	36000	3300	400	39000	2700
500	45000	4100	500	49000	3400
600	54000	5000	600	58000	4100
700	63000	5800	700	68000	4700
800	72000	6600	800	78000	5400

Table D.8 shows Capacity as a function of volume of bed processed for different concentrations of hard water. Table D.9 to Table D.13 shows extended data for other bed volumes.

Table D.8: Capacity as a function of volume of bed volume: For 1 liter of water to be processed

Regeneration Level, %	Volume of bed (l) Run 1	Capacity Kgr/cu.ft.	Error	Volume of bed(l) Run 2	Capacity Kgr/cu.ft	Error
4	0.080	23.0	1.6	0.080	24.0	1.5
5	0.090	30.0	0.8	0.090	31.0	0.7
6	0.110	46.0	2.2	0.110	45.0	1.4
7	0.120	61.0	1.8	0.130	68.0	2.2
8	0.160	90.0	8.3	0.170	97.0	6.8

Table D.9: Capacity as a function of volume of bed volume treated: Concentration of 40g/l

Volume of Bed (l)	Capacity Kgr/cu.ft.	Error	Capacity Kgr/cu.ft	Error
100	30200	2140	28900	1770
200	60400	4280	57700	3540
300	90600	6420	86600	5310
400	121000	8560	115000	7080
500	151000	10700	144000	8850
600	181000	12800	173000	10600
700	211000	15000	202000	12400
800	242000	17100	231000	14200

Table D.10: Capacity as a function of volume of bed volume treated: Concentration of 50g/l

Volume of Bed (l)	Capacity Kgr/cu.ft.	Error	Capacity Kgr/cu.ft	Error
100	34200	2430	35600	2180
200	68500	4850	71100	4360
300	103000	7280	107000	6540
400	137000	9710	142000	8720
500	171000	12100	178000	10900
600	205000	14600	213000	13100
700	240000	17000	249000	15300
800	274000	19400	284000	17400

Table D.11: Capacity as a function of volume of bed volume treated: Concentration of 60g/l

Volume of Bed (l)	Capacity Kgr/cu.ft.	Error	Capacity Kgr/cu.ft	Error
100	41600	2010	40300	1280
200	83200	4020	80500	2550
300	125000	6040	121000	3830
400	166000	8050	161000	5100
500	208000	10100	201000	6380
600	250000	12100	242000	7650
700	291000	14100	282000	8930
800	333000	16100	322000	10200

Table D.12: Capacity as a function of volume of bed volume treated: Concentration of 70g/l

Volume of Bed (l)	Capacity Kgr/cu.ft.	Error	Capacity Kgr/cu.ft	Error
100	52300	1540	52300	1700
200	105000	3090	105000	3400
300	157000	4630	157000	5090
400	209000	6180	209000	6790
500	262000	7720	262000	8490
600	314000	9260	314000	10200
700	366000	10800	366000	11900
800	419000	12400	419000	13600

Table D.13: Capacity as a function of volume of bed volume treated: Concentration of 80g/l

Volume of Bed (l)	Capacity Kgr/cu.ft.	Error	Capacity Kgr/cu.ft	Error
100	57700	5310	56400	3930
200	115000	10600	113000	7860
300	173000	15900	169000	11800
400	231000	21200	225000	15700
500	289000	26500	282000	19600
600	346000	31900	338000	23600
700	404000	37200	395000	27500
800	462000	42500	451000	31400

Table D.14 shows the experimentally measured regenerant volumes at different regeneration levels. Table D.15 to Table D.19 are extended data for other bed volumes.

Table D.14: Experimentally measured regenerant volumes at different regenerant concentrations

S.No	Regeneration Level,%	Volume, l Run 1	Error	Volume, l Run 2	Error
1	4	0.136	0.028	0.139	0.031
2	5	0.126	0.028	0.130	0.029
3	6	0.135	0.026	0.113	0.017
4	7	0.084	0.016	0.090	0.017
5	8	0.083	0.021	0.087	0.021

Table D.15: Regenerant volume required as a function of bed volume at a regenerant concentration of 40g/l

S.No	Volume of bed (l)	Volume, l Run 1	Error	Volume, l Run 2	Error
1	100	240	49	240	55
2	200	480	97	490	110
3	300	720	150	730	160
4	400	950	190	980	220
5	500	1200	240	1200	270
6	600	1400	290	1500	330
7	700	1700	340	1700	380
8	800	1900	390	2000	440

Table D.16: Regenerant volume required as a function of bed volume at a regenerant concentration of 50g/l

S.No	Volume of bed (l)	Volume, l Run 1	Error	Volume, l Run 2	Error
1	100	220	50	230	50
2	200	440	99	460	100
3	300	660	150	680	150
4	400	880	200	910	200
5	500	1100	250	1100	250
6	600	1300	300	1400	300
7	700	1500	350	1600	350
8	800	1800	400	1800	400

Table D.17: Regenerant volume required as a function of bed volume at a regenerant concentration of 60g/l

S.No	Volume of bed (l)	Volume, l Run 1	Error	Volume, l Run 2	Error
1	100	240	45	200	30
2	200	470	90	400	60
3	300	710	140	600	90
4	400	950	180	800	120
5	500	1200	230	990	150
6	600	1400	270	1200	180
7	700	1700	320	1400	210
8	800	1900	360	1600	240

Table D.18: Regenerant volume required as a function of bed volume at a regenerant concentration of 70g/l

S.No	Volume of bed (l)	Volume, l Run 1	Error	Volume, l Run 2	Error
1	100	150	29	160	27
2	200	300	58	320	55
3	300	440	86	470	82
4	400	590	120	630	110
5	500	740	140	790	140
6	600	890	170	950	160
7	700	1000	200	1100	190
8	800	1200	230	1300	220

Table D.19: Regenerant volume required as a function of bed volume at a regenerant concentration of 80g/l

S.No	Volume of bed (l)	Volume, l Run 1	Error	Volume, l Run 2	Error
1	100	150	36	150	37
2	200	290	73	310	73
3	300	440	110	460	110
4	400	580	150	610	150
5	500	730	180	760	180
6	600	870	220	920	220
7	700	1000	250	1100	260
8	800	1200	290	1200	290

VITA

Anupama Balachandran

Candidate for the Degree of

Master of Science

Thesis: CORRELATION OF OPERATING CAPACITY OF STRONG ACID CATION EXCHANGE RESIN

Major Field: Chemical Engineering

Biographical Information:

Personal Data: Born in Villupuram, India, on the 23th of September, 1979, the daughter of Karpagam Balachandran and B.N.Balachandran

Education: Graduated from Sri Venkateswara College of Engineering, Pennalur, India, with a Bachelor of Technology degree in Chemical Engineering in June 2001. Completed the requirements for the Master of Science degree in Chemical Engineering at Oklahoma State University, Stillwater, Oklahoma, in December 2005.

Experience: Employed by Oklahoma State University, Department of Chemical Engineering as a Research Assistant, July 2003 to August 2005; Teaching Assistant, August 2004 to December 2004.

Name: Anupama Balachandran Date of Degree: December, 2005

Institution: Oklahoma State University Location: Stillwater, Oklahoma

Title of Study: CORRELATION OF OPERATING CAPACITY OF STRONG ACID CATION EXCHANGE RESIN

Pages in Study: 98 Candidate for the Degree of Master of Science

Major Field: Chemical Engineering

Scope and Method of Study: The purpose of this study was to generate performance data for Strong Acid Cation (SAC) exchange resins and develop models to predict the regenerant volumes and capacity under different operating conditions. To meet this objective, experiments were conducted using Dowex Monosphere 650 (H) resins to measure the capacity in both service and regeneration cycles.

Finding and Conclusions: Experimental data obtained were correlated to develop mathematical models to predict capacity as a function of volume of hardwater treated, amount of hardness and bed volume. Models to predict regenerant volumes at different bed depths were also developed. The capacity models could be used for prediction with an average uncertainty of 5% and the model to predict the regenerant volume can be used with an average uncertainty of 7%.

ADVISER'S APPROVAL: Gary L. Foutch